NTNU – Trondheim
Norwegian University of
Science and Technology

Ice-induced vibrations under continuous brittle crushing for an offshore wind turbine

Qi Wang

Coastal and Marine Engineering and Management
Submission date: June 2015
Supervisor: Michael Muskulus, BAT

Norwegian University of Science and Technology
Department of Civil and Transport Engineering

Abstract

Offshore wind structures located in ice infested waters are subjected to actions from moving ice and forces are generated when a drifting ice crushes against the structure. The main purpose of this Master's thesis is to implement numerical ice loading models on an offshore wind turbine monopile structure, analyze ice induced vibrations and assess the importance of ice loads on offshore wind turbines.

A model of offshore wind turbine monopile structure for time domain simulation will be established on FEDEM and ice loading spectral model will be implemented first. Ice force spectrum will be calculated from empirical formulas and ice loading time series will be generated and applied on structure model directly.

In order to assess the performance of the spectral model, another ice-structure interaction model, Määttänen-Blenkarn model, is also applied on the offshore wind turbine monopile structure. The time domain simulation results from two models are analyzed and compared. The feasibility of both models for different ice speeds are investigated.

The complex ice properties define the difficulty in ice load calculation. The relative speed between structure and ice will influence ice crushing strength. The existing spectral model is only feasible for continuous brittle crushing regime where structure response have little influence. But Määttänen-Blenkarn model considers structure response through stress rate dependent ice crushing strength and is also applicable for low to intermediate ice speeds. Simulation results also illustrate that different ice crushing modes of different ice speeds can be obtained from Määttänen-Blenkarn model and the results of spectral model for different ice speeds have similar characteristics.

To better evaluate the impact of ice loads on offshore wind turbine structure, the coupling model of wind and ice loads will be applied in time domain simulation to investigate the joint effect of wind and ice loading. Fatigue damage assessment is also performed to see the structure damage induced by ice loads. The results illustrate that based on current model and data, ice loads are larger than wind loads and the fatigue damage caused by ice loads should be considered.

Preface

This Master's thesis has been written at Norwegian University of Science and Technology (NTNU) as the final evaluation of the master's degree for Erasmus Mundus master program Coastal and Marine Engineering and Management. The amount of work is equal to 30 credits.

This work aims at the implementation of ice models on offshore wind turbine monopile structure and investigates ice induced vibrations. The task requires a solid study of the available literature on ice mechanics and offshore wind turbine design technology. Two kinds of numerical models are used on the same structure and the results are compared in detail. The limitations of two models are described and possible improvements of the spectral model are recommended. At last, the coupling effect of ice and wind loads and fatigue analysis are performed.

I would like to thank my supervisor Michael Muskulus who shared valuable innovative ideas on this topic and Wojciech Popko who sacrificed lots of private time to answer my questions and offered me significant guidance in thesis writing.

I would also like to deliver my thank Sebastian Schafhirt for the considerable assistance in the numerical work. A thank also goes to Knut V. Høyland regarding my questions on simulation results of Määttänen-Blenkarn model.

Trondheim, June 25, 2015

Abby Qi Wang

Content

List of Figures

List of Tables

Notation

h	Ice thickness
$F_l(t)$	Time varying component of ice force
F_l^{mean}	Mean ice load
F_l^{max}	Maximum ice load
σ_l	Standard deviation of ice force time varying component
k	Probability of exceedance
I_l	Ice crushing intensity
$G_{nn}(f)$	Auto-spectral density functions
$G_{mn}(f)$	Cross-spectral density functions
$F_n(t)$	Normal force
$\widetilde{\mathrm{G}}_{\mathrm{nn}}(\mathrm{f})$	Non-dimensional spectral functions
f	Frequency
v	Ice velocity
k_s	Parameter for non-dimensional spectral functions
a	Experimental parameter for non-dimensional spectral functions
b	Experimental parameter for non-dimensional spectral functions
$\boldsymbol{G_{ff}(f)}$	Spectral matrix
γ_{mn}	Coherence functions
ξ_{nm}	Non dimensional distance
ρ	Experimental coefficient for coherence functions
α	Experimental coefficient for coherence functions
β	Experimental coefficient for coherence functions
θ	Angle of incidence
μ	Friction coefficient

$G_F(f)$	Global ice load spectrum
φ_f	Random phase
ϑ_A	Ice temperature
S_B	Bulk salinity
ϕ_B	Ice porosity
σ_c	Ice crushing strength
$\dot{\varepsilon}$	Strain rate
F_m	Mean ice load
$\dot{\sigma}$	Stress rate
A	Contact area
A_0	Reference area
r	Structure radius
P	Contact force
$\dot{u}$	Structure velocity
D	Structure diameter
M	Structure mass
C	Damping coefficient
K	Structure stiffness
σ_0	Reference ice crushing strength
N	Number of cycles
S	Damage of one stress range
K	Material factor
D	Fatigue damage
EFL	Equivalent fatigue load
I	Moment of inertia
t_{ref}	Reference thickness

Chapter 1
Introduction

This work is aimed to contribute to knowledge on numerical modelling of ice induced vibrations for offshore wind turbine monopile structure. In the thesis, a stucture model will be established and time domain simulation will be performed based on spectral model first. In order to check the performance of spectral model, another process-based model will be applied and results of two models will be compared. At last, joint wind-ice effect is investigated and fatigue analysis is performed to see the damage induced by ice loads.

This introductory chapter presents a brief introduction of arctic issue in offshore wind industry. A short recapitulation of ice theories and numerical models for ice induced vibrations analysis is given. The tools for numerical simulation will be introduced. Finally, the formulation of project and scope of the work is addressed.

1.1 Background

1.1.1 Offshore wind development in temperate and arctic regions

Offshore wind energy has been one of the most promising environmental-friendly renewable energy resources nowadays around the world, which will help to reduce environmental problems. As with the development in offshore wind industry, OWT (Offshore Wind Turbine) design technology has getting mature and the increasing number of offshore wind farms in northern cold climate area indicates the trends of exploration of wind power in temperate and artic regions. Even though some arctic region might offer better wind resources, the harsh environment might also introduce extra difficulties for offshore wind projects. The installation operation in these highly remote area has induced additional challenge. The functionality of OWT in arctic region

should be tested due to ice problems like sea ice loading, ice accretion on the structure, blade icing. Thus, ice forces calculation on offshore wind turbines has come to the eyes of researchers.

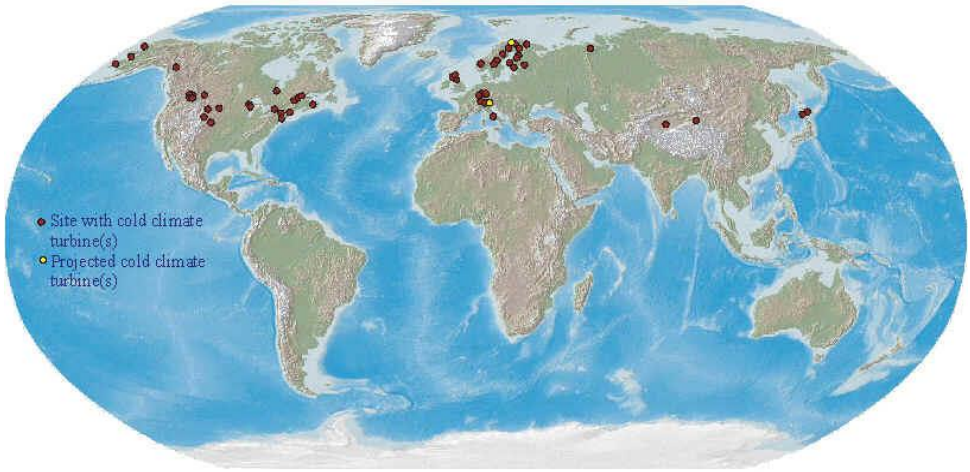

Figure 1-1 Wind Energy in Cold Climates (T. Laakso, 2003)

1.1.2 Sea ice crushing loads characteristics

Due to the increased human activity in Arctic regions, interaction between ice and offshore structures occurs more frequently. Some investigations on ice loads and ice induced vibrations have been promoted and laid foundation for numerical simulations of structural response due to ice.

Since early 1960s, the ice induced vibration phenomenon has been noticed on the drilling platform in Cook inlet (Blenkarn, 1970; H.R.Peyton, 1968), after which similar phenomenon on other structures were analyzed such as lighthouses (Engelbrektson, 1977) , bridge piers (Sodhi, 1988) and offshore jacket oil platforms (Q. Yue, 2001)

The complex features of ice define the difficulty of precise prediction of ice loads. The ice breaking strength is influenced by ice physical properties like temperature, porosity, salinity, crystallography and etc. These properties might vary from different regions and rather difficult to consider. There are some field measurement lighthouses which provide convincing data on regional differences of ice physical properties.

It was also found that ice strength during ice-structure interaction depends on strain rate (Blenkarn, 1970; H.R.Peyton, 1968). And the failure of ice can be ascribed to 3 regimes, namely ductile regime, transitional regime and brittle regime.

For low strain rate, ice floes will subject to ductile failure, which allows more time for deformation and crack propagation before ice failure. When ice is loaded with a relatively slow strain rate cracks do not propagate. In such situation creep allows stresses to relax – grain boundaries can slide with respect to each other after crossing the yield point. This can be described as a ductile behavior.

When the strain rate is very large, the brittle crushing might happen with only small elastic deformation followed by crack propagation. The brittle behavior is characterized by elastic deformation followed by a sudden failure of the material without yielding process. The instantaneous elastic deformation happens due to the elastic response of the crystal lattice due to the applied stress. Then the maximum threshold stress level is reached the strain energy is released resulting movement of dislocations in crystals on the deformation of the entire body.

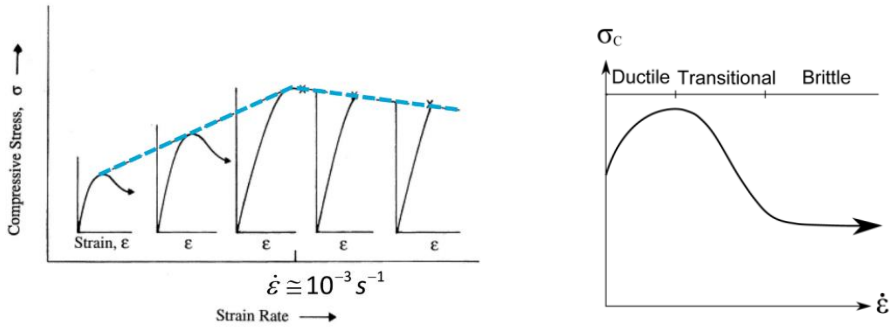

Figure 1-2 Ice crushing capacity and stain rate (Schulson, 2001)

The ice physical properties and approaching speed might influence ice floe failure mechanism. Figure 1-3 illustrates possible failure modes for the interaction of ice sheets and vertical structures under different aspect ratio, ice speed and deformation development.

Bending failure mode is main failure type for conical shape structures. When ice approaches structure, ice sheet has the tendency to climb up the slope of structure and the ice failure mode will be bending. For vertical structure, crushing failure mode has the largest possibility.

Thus, for offshore wind turbine support structures with vertical wall, crushing type of failure dominates, which is also the main failure mechanism considered in this thesis.

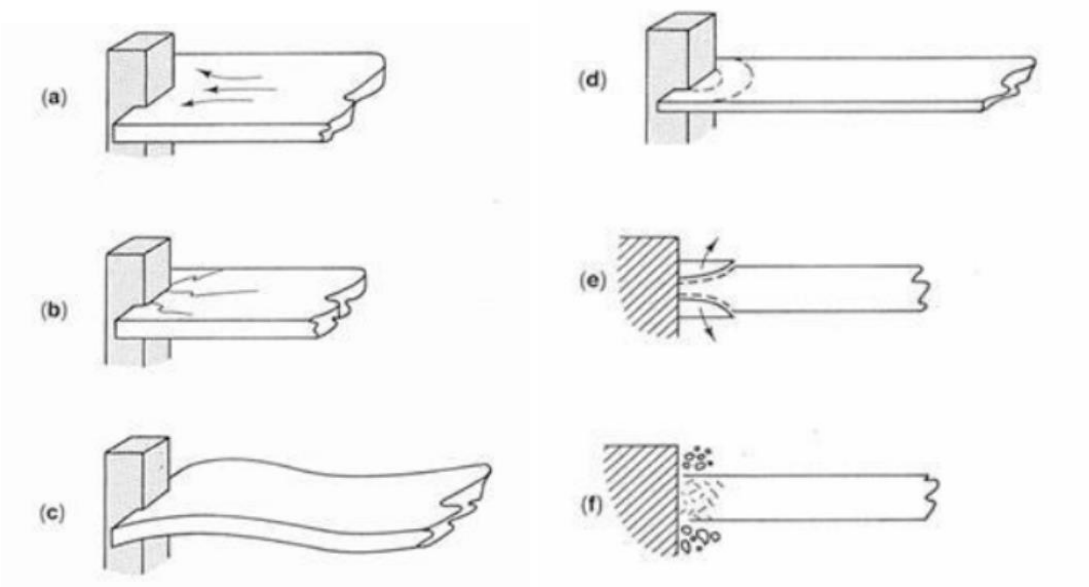

Figure 1-3 Ice failure modes (a) creep (b) radial cracking (c) buckling (d) circumferential cracking (e) spalling (f) crushing (Løset, 2006)

Based on the speed of ice sheet, ice crushing characteristics during ice-structure interaction can be categorized into 3 regimes. As can be seen in Figure 1-4, the ice force and structure response development over time under different speed range are illustrated. For low ice speed, the response of structure has saw-tooth feature which is defined as quasi-static response. Ice load will climb up to ice loading capacity then drop and another cycle will commence. For high speed ice, the crushing is continuous and results in a random stationary response. Frequency lock-in phenomenon may happen within the regime between intermittent crushing and continuous brittle crushing, in which natural frequency of structure is within the ice loading frequency range and resonance might occur.

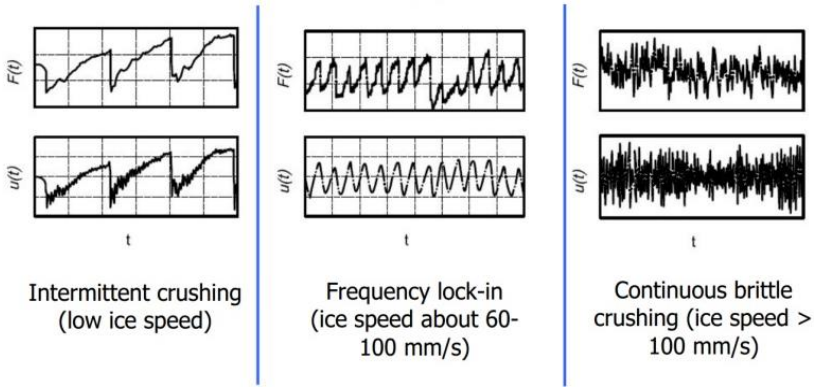

Figure 1-4 Crushing failure regimes (International Organization of Standarisation, 2010)

1.1.3 Time domain numerical models for ice action analysis

The ice action problems initiated theoretical studies on ice induced vibrations. Based on these theoretical approaches and experimental results, numerical models have been developed for ice-structure interaction analysis.

According to the observations from a drilling platform in Cook Inlet, Peyton(1968) put forward rate dependency of ice crushing strength theory. Based on this theory, Blenkarn(1970) and Määttänen(1978) proposed the concepts of negative damping and self- excited vibration. A mathematical model to describe negative damping and self-excited vibration was established by Määttänen through combining equation of motion and stain rate-dependent ice crushing strength. This model was further developed by Xu and Wang (1986) and Vershinin and Iliadi (1990).

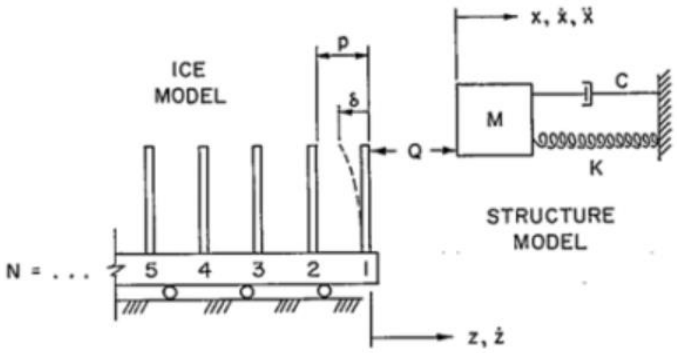

Figure 1-5 Dynamic Ice-Structure Interaction Model (Matlock, 1969)

A simple mechanism is proposed by Matlock(1971). The moving ice is simplified as a sequence of brittle cantilevers crushing with structure. Under the Matlock model, ice load can be simplified as saw-tooth shape load. Admittedly, the use of Matlock model greatly simplifies the ice structure interaction analysis. But, the model fails in predicting load level, which is a significant drawback in the analysis of the load effects for OWTs, where proper assessment of load levels is crucial for calculation of the ultimate loads in the design process of every OWT.

Saw-tooth ice force was also recommended in ISO (2010) as design ice load to model ice induced vibrations. The peak load can be determined through maximum ice crushing stress and contact area and load period equals to structure natural frequency. In this way, the complex changing ice crushing stress is avoided.

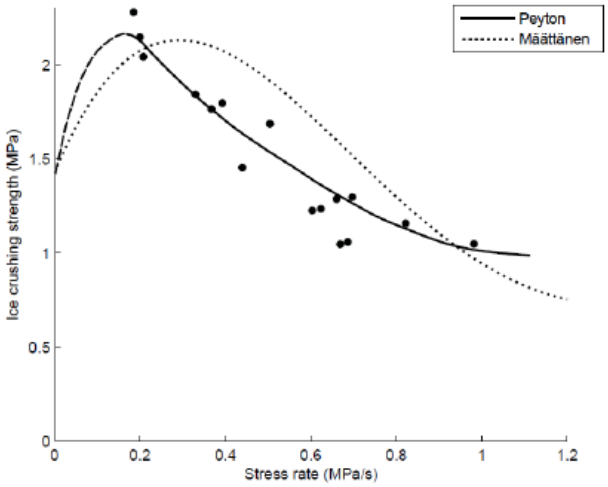

Figure 1-6 Stress rate dependency after Peyton(1986) and Määttänen(1998)

Sodhi (1988) suggested another approach relying on the concepts of crushing strength and characteristic failure frequency. He argued that ice breaking process determines characteristic failure frequency which is related to ice velocity and ice thickness. (Michel,1978) (Sodhi, 1988).

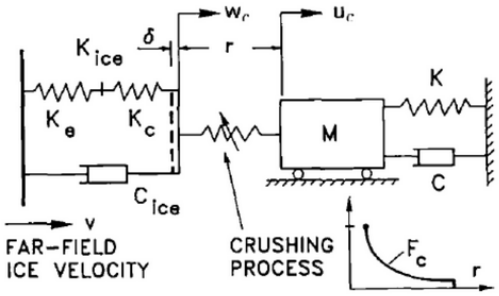

Figure 1-7 Empirical model for time domain analysis (Kana and Turunen ,1989)

Kärnä also developed comprehensive numerical model by looking at detail ice failure process (Kärnä T. a., 1989).A kind of zonal approach by dividing ice body into several zones with different contact possibility is employed for wide offshore structures (Eranti, 1992; Kärnä T. a., 1989). Considering foundation influence, a soil-structure- ice interaction numerical model was also established (Kärnä T. , 1992)

In order to consider ice material properties, phenomenon based model was suggested by Shkhinek at al (2000) and Kolary (2004) by paying special attention to 3 dimensional ice failure

development. The phenomenon based models focus on modeling details of ice crushing process such as crack propagation, unloading features and failure envelope.

The complex ice properties determine the difficulty of numerical simulation. It is seems that the phenomenon based models and Kärna's comprehensive numerical model would give more realistic results due to the consideration of details during ice crushing process. And Määttänen model would offer simplified method to estimate ice loads with acceptable accuracy.

1.1.4 Frequency domain analysis and response spectrum method

The frequency domain analysis was first initiated by Sundarajan and Reddy (1973) based on stochastic analysis theory for ice-structure interaction. It was argued that the ice loads can be assumed to be ergodic and stationary based on the field data of Cook Inlet and the structure can be simplified as a damped single-degree-of-freedom elastic system. Based on this frequency domain method, Reddy et al. (1975,1977) further established response spectrum method. It was found that ice force records and earth quake records look similar and the response spectrum method for earth quakes was used on ice loading analysis for a multi-DOF offshore tower. Both the response spectrum method and stochastic approach frequency domain analysis were applied on lighthouse in the Gulf of Bothnia for ice-structure interaction analysis by Määttänen et al(1977). Assuming non-stationary ice loading process due to irregular, the application of spectral model was discussed by Reddy et al (1979), in which the ice force excitation was calculated through evolutionary white noise approach which will capture gradual growth of excitation.

Generally, the response spectrum method is much simpler than direct frequency domain analysis and time integration technique. At the same time, the response is expressed in a brief way which can save the long and tedious time history response record. After the research on formulation of ice load spectrum and structure response spectrum was initiated by Reddy et al, more field data were analyzed and empirical equations for spectrum calculation were proposed. The auto-spectral density function calculation was describe by Ou and Duan (1996) based on measurements in Bohai area and Tuomo Kärnä el al (2007) summarized the experimental data from light house Norströmsgrund and mooring pole JZ9-3MDP2 in Bohai Bay and derived equation for cross spectrum density functions and total ice force spectrum.

As is introduced, the spectral analysis and frequency domain analysis are mainly based on in field data measurements. Seeing that the ice properties will change over different regions and the structures are also not necessarily of the same scale and type, it is difficult to validate the parameters existing models1. But it is promising that theoretically, these models could be applied on OWT structures if the parameters are carefully calibrated.

1.1.5 Simulation tools for OWT

Considering the complex operating environment of offshore wind turbines, the coupled simulation tools which take into account an interaction of various environmental conditions and the entire structural assembly of the turbine with its control system will be deployed. Offshore wind turbines analysis will be performed in the time domain through aero-hydro-servo-elastic simulation tools, through which both the transient events and non-linear dynamic effects could be considered. The aero-hydro-servo-elastic simulation tools consist of several sub modules including: aerodynamics (aero), control systems (servo), hydrodynamics (hydro) and structural-dynamics of a wind turbine and its offshore support structure (elastic). The interaction between different modules should be considered for the potential loss of accuracy and the coupled approach is required by design standards and guidelines for an accurate prediction of the system dynamic response and fatigue loads of offshore wind turbines. (Popko, et al., 2012; Vorpahl, Schwarze, Fischer, & Seidel, 2013)

1.2 Project formulation

The thesis focuses on the implementation of the state-of-the-art ice force spectral mode on offshore wind turbines, comparison of spectral model and Määttänen-Blenkarn model and analyzing ice induced vibrations.

The time series for ice loading will be generated from spectral model through Matlab and time domain simulation will be performed on FEDEM.

Seeing that the spectrum calculation equations are derived from field data, the spectral model is considered to be feasible for ice velocities from 0.04 m/s to 0.35 m/s (Kärnä T. a., 2004). It has been acknowledged that even though the spectral model is much simpler compared with time domain simulation, the ice force time series obtained for moderate and low ice speeds might not be accurate enough because the influence of structure response is not considered. According to

past experience, for high ice speeds in continuous brittle crushing regime, the structure response feedback effect can be ignored and the spectral model can be valid.

In order to investigate the performance of spectral model for moderate and low ice speeds, Määttänen-Blenkarn model will also be applied on the same OWT monopile structure. As is known that Määttänen-Blenkarn model is processed based model based on stress rate- crushing strength relation, it considers structure response from old time step for estimation of ice load at new time step. The results of two models will be compared to see the possible improvements on spectral model in moderate to low ice speed regime.

To have a better view of the significance of ice loads for OWT structure design, the joint effect of ice and wind loads will be tested and fatigue analysis will be performed to see the possible damage induced by ice loads.

1.3 Scope of work

This work aims at the implementation and comparison of ice load spectral model and Määttänen-Blenkarn model and check the fatigue damage induced by ice loads. The total process could be divided into several phases.

First, a monopile wind turbine structure model based on parameters offered by OC3 will be defined and built on software FEDEM. (Musial, 2010).

Spectral model will be implemented on structure model. Global ice force spectrum calculation will be performed based on empirical equations and ice loads time series will be generated through inverse Fourier transform. (Kärnä T. Q. Y., 2007) . The ice loading time series will be applied on the structure model directly.

In order to assess the performance of spectral model, Määttänen-Blenkarn model will be studied and implemented on the structure model. (Määttänen M. , 1978; Määttänen M. , 1998).The results for both models will be compared and the feasibility of two models on different ice speed regime will be discussed. Possible improvements on spectral model will be provided.

Wind and ice coupling effect will be tested and analyzed based on M-B model and fatigue damage caused by ice loads and constant wind will be studied and calculated.

1.3 Project delimitation

This thesis work focuses on the implementation of spectral model and Määttänen-Blenkarn model on an OWT monopile structure. Therefore, no new ice models will be introduced and attention will be paid on improving and comparing existing models.

The parameters for OWT monopile structure, including turbine top and substructure, will be directly obtained from recommendations of OC3 Offshore Code Comparison Collaboration (OC3) (Musial, 2010). And all the study will be based on this monopile structure only. Some predictions and analysis will be made on structure with different diameters and of other type, like jacket structure, but not verified.

The structure will be established on software FEDEM and time domain simulation will be run through FEDEM. The simulation will concentrate on ice induced vibration of stand-by mode OWT and joint effect of constant wind and ice loads only at this stage. The influence of other environmental loads will be not investigated within this work.

Chapter 2

Description of structure model in FEDEM

The structure model will be built on software FEDEM. In this chapter, brief introduction of FDEM will be given. Benchmark models of OC3 will be introduced and structure dimensions will be described. A comparison of parameters from OC3 report and the built models will be performed and structural properties of established model will be analyzed.

2.1 FEDEM Windpower

2.1.1 Software introduction

FEDEM Windpower is commercial software created by technology company FEDEM Technology AS. FEDEM Technology is specialized in engineering, dynamic simulations and lifetime calculations of structures and mechanical systems, FEDEM Windpower is a simulation software for dynamic analysis of offshore wind turbines and consists of wind field module, hydro module, structural model, soil descriptions and complete control system.

2.1.2 FEM analysis on FEDEM

In FEDEM, a beam is assumed as flexible body, represented by a standard two-noded beam finite element. Its stiffness matrix is based on Euler – Bernoulli beam theory, quadratic interpolation functions and continuous rotations at the nodal points. The deformations in such elements account for bending, axial compression and elongation, and St. Venants torsion. The cross section properties are assumed constant along the beam element.

2.2 Building of structure model

The structure model for simulation is defined referring to the benchmark models proposed by Offshore Code Comparison Collaboration (OC3). In the model, a NREL offshore 5-MW wind turbine was installed on a monopile with a rigid foundation in 20 m of water.

2.2.1 Wind turbine selection

NREL 5MW wind turbine is selected for the model and parameters are listed in Table 2-1. NREL offshore 5-MW baseline wind turbine is a representative utility-scale multi megawatt turbine that is defined for concept studies and offshore wind technology assessment by National Renewable Energy Laboratory of U.S. (J. Jonkman, February 2009) This wind turbine is a conventional three-bladed upwind variable-speed variable blade-pitch-to-feather-controlled turbine which is also accepted as the reference model for the integrated European Union (EU) UpWind research program. (T. Fischer, 2010)

Table 2-1 Summary of properties for the NREL 5-MW baseline wind turbine (J. Jonkman, February 2009)

Rating	5 MW
Rotor orientation , configuration	Upwind, 3 blades
Control	Variable speed , collective pitch
Drivetrain	High speed, multiple-stage gearbox
Rotor, hub diameter	126 m , 3m
Hub height	90 m
Cut-in, rated, cut-out wind speed	3 m/s, 11.4 m/s, 25 m/s
Cut-in, rated rotor speed	6.9 rpm, 21.1 rpm
Rated tip speed	80 m/s
Overhang, shaft tilt, precone	5m, 5o, 2.5o
Rotor mass	110000 kg
Nacelle mass	240000 kg

2.2.2 Support structure

The dimensions of tower (Figure 2-1) are based on the base diameter (6m) and thickness (0.027m), top diameter (3.87m) and thickness (0.019m). The radius and thickness of tower are assumed to be linearly tapered for top to base. The height of the tower is designed to be 87.6 m and connected to a monopile with constant diameter of 6 m and constant thickness of 0.06 m.

The monopile extends from the end of tower (10 m above mean sea level) to sea bed (20 m below mean sea level) with total length 30m. (Musial, 2010)

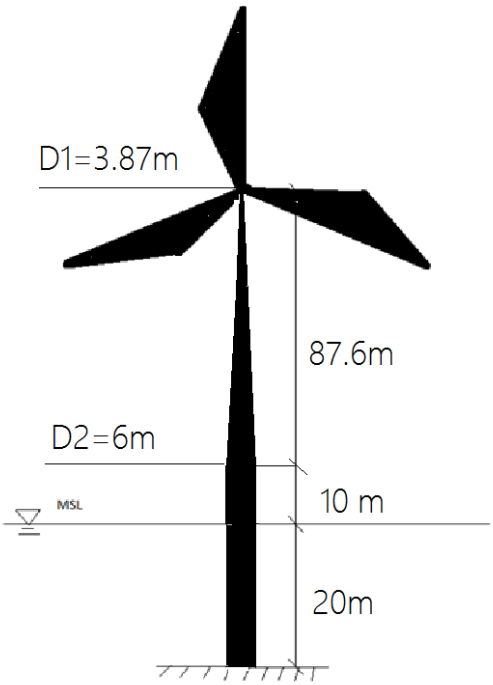

Figure 2-1 Dimensions of structure

The standard mechanical steel properties are taken as effective material parameters. The Young's Modulus, shear modulus and effective density of steel are taken to be 210 GPa, 80.8 GPa and 8500 kg/m^3 respectively. The use of increased steel density 8500 kg/m^3 instead of 7850 kg/m^3 will account for bolts, welds and flanges which are not included in steel thickness.

Table 2-2 Support structure dimensions

Tower-top height above MSL	87.6 m
Tower-base height above MSL	10 m
Water depth (From MSL)	20 m
Monopile diameter and thickness	6 m , 0.06 m
Tower-top diameter and thickness	3.87 m , 0.019 m
Tower-base diameter and thickness	6 m , 0.027 m
Structure mass	522617 kg

2.2.3 Structure model on FEDEM

The simulations of structure-ice interaction are processed on FEDEM Windpower.

The rotor-nacelle assembly (RNA) of the NREL 5MW turbine—including the aerodynamic, structural, and control system properties will be defined on FEDEM Windpower based on parameters in Table 2-1 .

The wind turbine support structure will be modeled as slender beams. As is described in Table 2-2, the support structure consists of a tower with changing diameter and a monopile with constant diameter. The tower structure is divided into 78 segments and monopile 30 segments, so that each beam elements will share length of approximately 1m and weight of elements would not vary a lot.

Ice forces are simplified as concentrated force working on structure at sea surface. Therefore, the ice stress will be integrated over structure first and then the point load will be applied on FEDEM.

After installing the structure, the masses of structure can be obtained in Table 2-3.

Table 2-3 Mass of sturcture segments

		Structure mass(kg)	Mass OC3(kg)
Nacelle	Main shaft	129041	240000
	Secondary shaft	6905	
Rotor		58291	110000
Support structure	Tower	236964	522617
	Monopile	285510	

The structure mechanical properties like Young's modulus and shear modulus were also defined. For structure damping, the concept of stiffness-proportional damping coefficient was used in FEDEM. The default value of stiffness proportional damping coefficient is 0.005.

2.2.4 Natural frequency of structure

In order to avoid the complex soil properties at seabed, the monopile is assumed to be fixed on the bottom. It is notable that this simplified foundation model might introduce inaccuracy by omitting soil- structure interaction. According to previous studies of OC3, compared with fixed foundation, the flexible foundation might reduce 10% of first natural, which could influence the dynamic amplification factor of structure response. (Musial, 2010) The value of first eigen

frequency of the designed fixed structure is reported to be in the range of 0.28 Hz and the support-structure configuration with flexible foundation has an even lower natural frequency of approximately 0.25 Hz.

The natural frequency of the structure has been calculated through FEDEM after the structure model has been established. The first eigen frequency of the monopile turbine is 0.32 Hz which is higher compared with OC3 figures. Eigen simulation was run on FEDEM and first 30 eigen values are listed in Table 2-4.

Table 2-4 First 30 eigen frequencies for designed structure

0.32	0.33	0.62	0.65	0.69	0.91	1.07	1.09	1.68	1.77
1.95	2.32	2.36	3.39	3.60	3.92	4.04	4.27	4.49	4.96
5.14	5.34	5.44	5.57	5.84	7.50	7.74	8.14	8.19	8.49

Chapter 3

Spectral model

In this chapter, theoretical background of spectral model will be introduced in detail. The formulation of global ice load spectrum will be given. Time domain simulation results will be analyzed and frequency domain analysis will be performed. At last, limitations of existing spectral model will be summarized.

3.1 Backgrounds for spectral model

3.1.1 Continuous ice crushing as stochastic process

The ice failure modes can be classified into several domains based on the ice velocity. For high ice speed, continuous ice crushing phenomenon might happen. Figure 3-1 below illustrates the observed phenomenon during continuous ice crushing. After the ice sheet hitting on the structure, some horizontal cracks could be observed at the edge of ice sheet. Flaking could also happen and divide the ice sheet into several layers. Part of the ice sheet might be crushed and pulverized and the rubbles would pile up and slide around ice surface. Compared with low ice velocity, vertical motion at ice-structure interface can be observed. (Kärnä T. a., 1989)

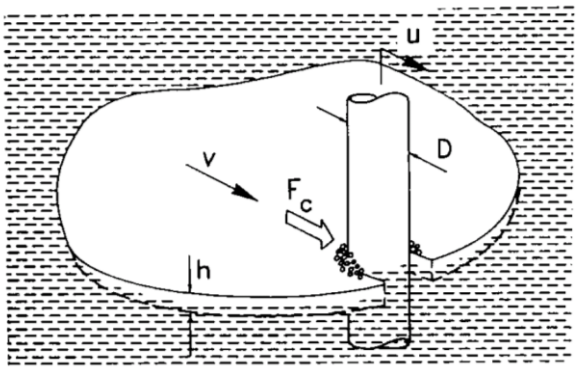

Figure 3-1 Ice crushing against structure (Kärnä T. a., 1989)

The main property of this ice crushing mode lies in the large ice action and small structure response. The ice failure capacity reaches the brittle crushing regime, in which the ice crushing strength could be a constant value with almost no influence of strain rate. In this case, the structure response will have little influence on the ice crushing strength and the structure response induced feedback mechanism could be omitted. Thus, the structure response can be ignored for high ice speed, which makes the spectral model feasible. (Kärnä T. Q. Y., 2007)

3.1.2 Monopod JZ9-3 MDP2 in Bohai Sea

Ice load spectrum will be directly formulated from available measurement data in field. The empirical spectrum formulation equation promoted by Kärnä is mainly based on the field data from mooring pole located at oil field JZ9-3 MDP2 in Bohai Bay. (Kärnä T. Q. Y., 2007)

The MDP2 monopod structure was designed for mooring oil takers for JZ9-3 oil fields located in northern Bohai Bay. The structure is designed for ice thickness 10-50 cm and maximum ice velocity 1 m/s which is controlled by wind and tidal currents.

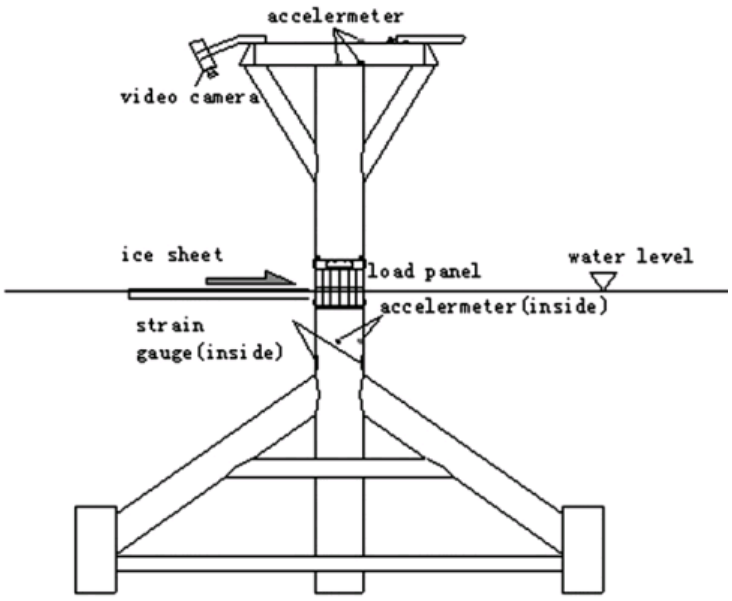

Figure 3-2 Test setup on JZ9-3 MDP2 (Yue, 2000)

Video camera was installed on top of structure to monitor ice failure process, ice speed and ice thickness. Accelerometers, strain gauges and load panels were used to measure responses and ice forces. Altogether 12 individual panels were attached on around waterline covering ice direction around 110^{o}.

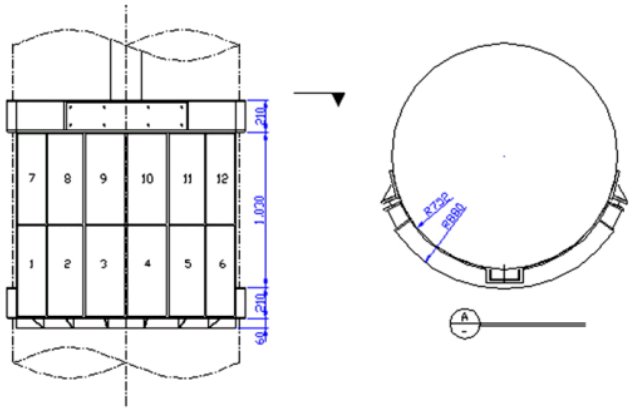

Figure 3-3 Ice load panels for direct ice force measurements (Qianjin Yue X. B., 2002)

An example of measurements for 90 seconds and corresponding spectrum is given inFigure 3-4 An example time signal for ice crushing and the corresponding auto-spectral density function Figure 3-4. The sampling rate is set to be 30 Hz, which could satisfy the requirements of ice

crushing analysis. As can be seen in the spectrum, most of the energy is within low frequency region.

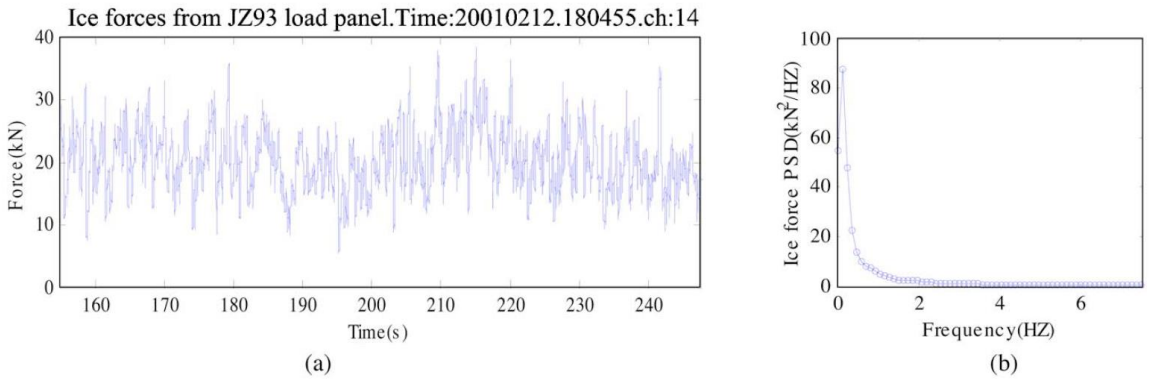

Figure 3-4 An example time signal for ice crushing and the corresponding auto-spectral density function (Kärnä T. Q. Y., 2007)

The observations show that 60% of all loading events occurred in crushing failure mode if ice was thicker than 0.2 m and if the diameter of sheet ice was at least 50 times the structure diameter. Flexural and mixed failure modes were common for thin ice (h<0.3 m) and small ice floes usually failed by splitting. Dynamic buckling and creep buckling were seen occasionally. A variety of ice failure modes were observed when ice ridges were encountered. Ice brittle crushing failure mode is assumed to be the ice crushing mode with the largest probability.

3.1.3 Formulation of global ice spectrum

3.1.3.1 Static and dynamic force component

The total ice loads consist of two components, a quasi-static mean ice load component F_l^{mean} and a time varying component $F_l(t)$. (Kärnä T. a., 2004)

For local ice load measurements, the local compressive loads will fluctuate around a positive mean level. Due to the cylindrical alignment of panels, local mean force and varying force will depend on the angle between ice moving direction and panel direction.

Based on statistical concept, the maximum values of ice loads can be estimated as

$$F_l^{max} = F_l^{mean} + k\sigma_l \qquad \textit{Equation 3.1}$$

Where σ_l corresponds to standard deviation of the fluctuating force component and *k* represents a selected probability of exceedence (Kärnä T. Q., 2006). Maximum ice crushing strength has been studied and could be calculated through ice crushing strength and contact area which are assumed to be known parameters. (Bendat, 2000)

Considering that the spectral model consists of mean part and time varying part, the concept of ice crushing intensity is introduced

$$I_l = \frac{\sigma_l}{F_l^{mean}} \qquad \textit{Equation 3.2}$$

According to field data, the crushing intensity varies from 0.2 to 0.5 with largest possibility at 0.4. In this paper, the crushing intensity will be taken as 0.4. (Stearns, 2003)

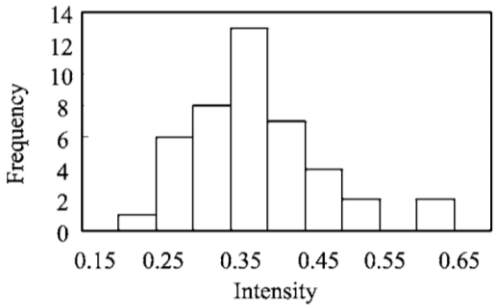

Figure 3-5 Intensity of time-varying ice force due to ice crushing in Bohai Bay (Kärnä T. Q. Y., 2007)

Based on the definition of crushing intensity, the relation between maximum ice loads and standard deviation can be expressed as

$$\sigma_l = \frac{I_l}{1 + kI_l} F_l^{max} \qquad \textit{Equation 3.3}$$

And the mean level of time varying component can be rewritten as

$$F_l^{mean} = \frac{F_l^{max}}{1 + kI_l} \qquad \textit{Equation 3.4}$$

Given above two formulas and the known value of F_l^{max}, mean value of local ice loads and standard deviation of time varying component of ice loads can be obtained. (Lin, 1967)

3.1.3.2 Spectral matrix for time varying component

A spectral matrix will be built for zero-mean time varying ice load component. Information for local ice force at each point and between local points will be contained in this spectral matrix.

Noting that local ice force will change due to the influence of incident angle of approaching ice, the global spectral matrix not only has diagonal term $G_{nn}(f)$, which represents local force $F_n(t)$, but also has off diagonal terms $G_{mn}(f)$, which show the influence of one local force $F_n(t)$ on another local point m.

The diagonal terms $G_{nn}(f)$ are called autospectral density functions and the off diagonal terms $G_{mn}(f)$ are called cross spectral density functions. The recipe for the calculation of diagonal and off diagonal terms will be provided in this chapter. (Newland, 1975)

For the generation of diagonal terms of spectral matrix, attention should be paid on local force measurements at arbitrary point n first.

Based on the physical meaning of spectrum, the relation between spectrum and standard deviation of time domain readings is given by

$$\sigma_n^2 = \int_0^\infty G_{nn}(f)df \qquad \textit{Equation 3.5}$$

Referring to the definition of non-dimensional spectrum for wind gust, non-dimensional auto spectrum function can be defined by

$$\tilde{G}_{nn}(f) = \frac{fG_{nn}(f)}{\sigma_n^2} \qquad \textit{Equation 3.6}$$

The non-dimensional spectrum was summarized by the measurements in Bohai Bay. As is indicated in the distribution of ice crushing intensity over frequency, most of the ice crushing frequency components are within the frequency range from 0 to 15 Hz. Thus, to simplify the model, the spectrum formulation will focus on frequencies below 15 Hz.

After measurement data processing, the formula for non-dimensional auto spectrum function was obtained as

$$\widetilde{G}_{nn}(f) = \frac{af}{1 + k_s a^{1.5} f^2} \qquad \textit{Equation 3.7}$$

$$a = b \times v^{-0.6} \qquad \textit{Equation 3.8}$$

Where v is ice velocity. k_s and b are experimental parameters from curve- fitting routine. The analysis of ice force data of JZ9-3 MDP2 shows that the mean value of parameter k_s is 3.24 and mean value of parameter b is 1.34. These empirical values will be used for establishment of spectral model.

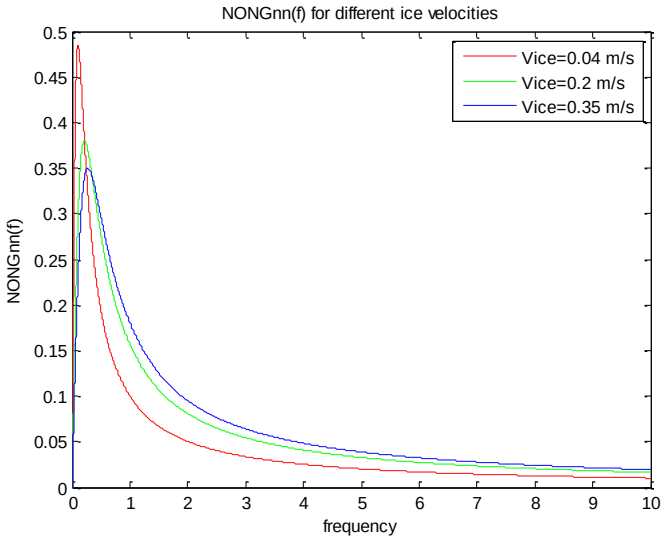

Figure 3-6 Non dimensional spectrum for different velocities

The non-dimensional spectrums for different ice velocities were calculated and compared. As can be seen from Figure 3-6, the peak frequency might shift to the left when ice velocity increases and the peak value will also increase leading to wider and higher spectrum shape.

The off diagonal terms $G_{mn}(f)$ in the spectral matrix $G_{ff}(f)$ are defined as cross spectral density functions. The cross spectral density functions represent the influence on location m induced by force exerted at location n .

In order to clarify the relations between two local points, the coherence function γ_{mn} was investigated first. The coherence function γ_{mn} is used to evaluate two local forces located at a distance of r_{mn} from each other.

In frequency domain, the coherence function γ_{mn} can represent the relation of spectrums in spectral matrix and be expressed by auto spectral density functions and cross spectral density functions as

$$\gamma_{mn}{}^2(f) = \frac{|G_{mn}(f)|^2}{G_{nn}(f)\, G_{mm}(f)} \qquad \textit{Equation 3.9}$$

Thus, if auto spectral density functions $G_{nn}(f)$ have been obtained and the values of the coherence functions γ_{mn} at each frequency between arbitrary two locations are known, it is possible to calculate cross spectral density functions $G_{mn}(f)$.

In reality, the physical meaning of coherence functions in time domain is about the relation of forces at two locations and the value of coherence functions can be estimated through experimental data.

Kärnä & Yan (2007) studied the properties of the coherence function and combined these properties with experimental data. The final expression of the coherence function has been acquired as

$$\gamma_{mn} = \left(\frac{1}{1+\rho+\alpha\xi_{nm}}\right)\left(\rho + e^{-\beta\xi_{nm}f}\right) \qquad \textit{Equation 3.10}$$

$$\xi_{nm} = \frac{r_{nm}}{h} \qquad \textit{Equation 3.11}$$

Where ξ_{nm} is the non dimensional distance, which is distance between two locations r_{mn} divided by ice thickness h. The other parameters ρ , α and β are all experimental coefficients.

An example for coherence function is given in Figure 3-7 for ice thickness h=0.5 m, $= 0.1$, $\alpha = 0.2$ and $\beta = 3$. It is notable that in this thesis work, spectrum of frequency ranging from 0 to

15 Hz will be formulated with step length 0.001 Hz and 12 points distributed along the structure surface due to limited computer storage capacity.

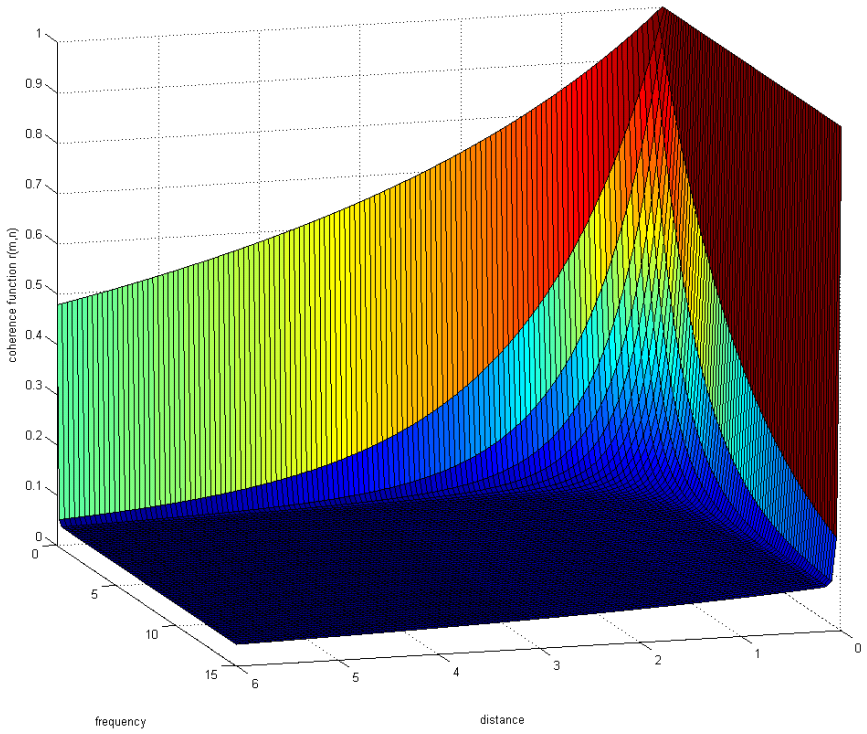

Figure 3-7 Coherence function for h=0.5, ρ=0.1 , α=0.2 and β=3

It is obvious that the coherence function is related to location distance and frequency. As is expected, for two location points near to each other the correlation will be larger. Peak value equals to 1 corresponding to 0 frequency and 0 distance.

3.1.3.3 Global ice spectrum

Based on the above discussion, the diagonal terms and off diagonal terms of the spectral matrix can be obtained. In the numerical modeling of wind turbines, the support structure will be simplified as a slender beam, which means the ice loads will be exerted at sea surface point of the beam. Thus, the ice load input for ice-structure interaction simulation should be a point load. In this session, the spectral matrix will be summed up to be a point load spectrum under the consideration of structure surface geometrical effect.

During the formulation of spectral matrix, it was assumed that the auto spectral density function is valid for every point on the structure, which means the load spectrum on each panel are the same. Therefore, the diagonal terms for existing spectral matrix are all the same because of the same auto spectral density function.

While, due to the cylindrical structure surface, the local forces on panels might be different from each other. The geometrical effect should be considered for curve surface.

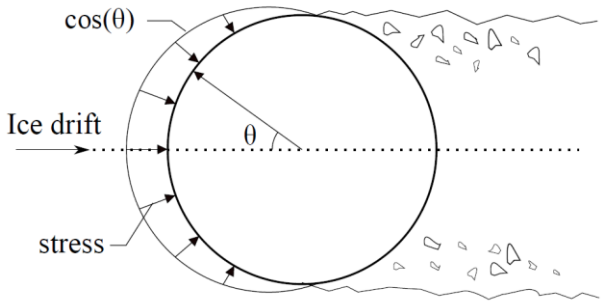

Figure 3-8 Stress distribution on an offshore structure (Sinding-Larsen, 2014)

As is shown in the figure above, the load working on the panel consist of two parts, one is a projection on the angle of incidence and the other is shear force on structure surface. Considering this geometrical effect, the local ice force should be rewritten as

$$F_l(t) = (\cos\theta + \mu \sin\theta)F_f(t) \qquad \textit{Equation 3.12}$$

μ is the friction coefficient which is assumed to be 0.05.

In frequency domain, applying this geometrical effect on auto spectral density functions, the new auto spectral density functions can be described as

$$G_{mm}(f) = G_{nn}(f) \times (\cos\theta^2 + \mu^2 \sin\theta^2) \qquad \textit{Equation 3.13}$$

In order to get concentrated global ice loads, the spectral matrix should be summed up to obtain a total ice force spectrum. Considering the angle of incidence at each local point, the summation can be achieved by

$$G_F(f) = (\mathbf{C} + \mu\,\mathbf{S})^T \mathbf{G_{ff}}(f)(\mathbf{C} + \mu\,\mathbf{S}) \qquad \textit{Equation 3.14}$$

Where $\boldsymbol{C}$ and $\boldsymbol{S}$ are vectors with dimension $n \times 1$ for $cos\theta$ and $sin\theta$ at each local point and $\boldsymbol{G_{ff}}(f)$ is $n \times n$ spectral matrix including auto spectral density functions and cross spectral density functions.

Equation 3.14 includes a geometrical correction process and summation process of local spectrums. The result on left hand side is a spectrum obtained by summing up all the local loads, which equals to total ice force working on structure.

3.2 Generation of time varying ice load time series

The time series for ice loads could be generated based on the physical meaning of spectrum. Spectrum is also called energy spectrum or power spectral density. The value of spectrum *G(f)* represents power content of frequency f . It is possible to see the energy contribution of each frequency component to total ice load through power spectrum distribution.

The concept of Fourier transform shows that time signals are overlap of harmonic functions with different periods and can be decomposed into frequency components. In this way, the time series could be translated from time domain to frequency domain.

Inversely, the power spectrum can also be translated into time domain. First, Time series generated by each frequency component will be formulated. The amplitude could be derived by the relation between energy and force and a random phase will be allocated to each frequency component. The total ice load time series could be obtained by adding all the frequency components together.

The process can be summarized in the formula below

$$\mathrm{F(t)} = \Sigma\sqrt{2 \times \mathrm{G_F(f)} \times \Delta\mathrm{f}}\cos(2\pi\mathrm{ft} + \varphi_\mathrm{f}) \qquad \textit{Equation 3.15}$$

Where $\sqrt{2G_F(f)\Delta f}$ is the amplitude of ice loads variation for frequency *f*, φ_f is the random phases allocated frequencies.

3.3 Mean ice load

The ice load consists of mean ice load component and time varying component. The time varying part can be acquired by ice load spectrum as is described above. For the mean ice load component, ice strength formulas from GL guideline will be deployed as mean ice crushing load. (GL, 2005)

The ice compressive strength could be determined by strain rate and ice porosity， the relation could be shown by

$$\sigma_c = 2700 \times \dot{\varepsilon}^{1/3} \times \phi_B^{-1} \qquad \textit{Equation 3.16}$$

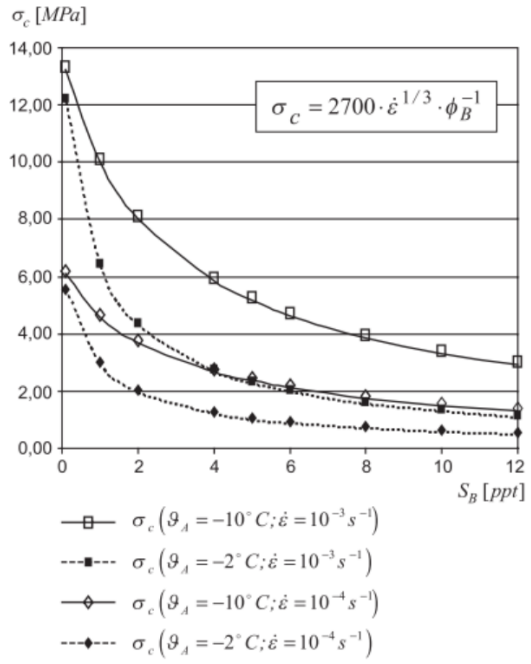

Figure 3-9 Compressive Strength of Sea Ice vs salinity (GL, 2005)

The ice temperature varies from surface to bottom. The freezing temperature for saline water is about -1.9^{o}C. In Bohai Bay average temperature for January will be – 17.8 ^{o}C, which is assumed to be the ice top surface temperature. The average temperature over ice thickness would be -9.85 ^{o}C.

Bulk Salinity S_B is the salinity after ice freezing process, because desalination might happen as sea ice formed from sea water. According to experience, lower boundaries are 4 ppt for first year

ice and 2 ppt for multi-year ice. An average of 3 ppt is chosen because of the existence of both first year ice and multi-year ice in this region.

Ice Porosity can be calculated when bulk salinity and average ice temperature are known

$$\phi_B = 19.37 + 36.18 \times S_B^{0.91} |\vartheta_A|^{-0.69} = 39.66 \quad \textit{Equation 3.17}$$

Typical value for strain rate 10^{-3} s^{-1} is chosen and the compressive strength of sea ice can be approximated to be

$$\sigma_c = 2700 \times c \times \phi_B^{-1} = 6.9 \text{ MPa} \quad \textit{Equation 3.18}$$

An integration over the whole structure surface will lead to a total mean ice load

$$F_m = \int_{-\frac{\pi}{2}}^{\frac{\pi}{2}} \sigma_c \times (\cos\theta + \mu \times \sin\theta) d\theta = 6 \times 6.9 \times 1000000 = 41.4 \times 10^6 N \quad \textit{Equation 3.19}$$

3.4 Time domain simulation on FEDEM

Time domain simulation will be launched on the structure model established in Chapter 2 through FEDEM.

The simulation will sustain for 300 seconds which is assumed to be long enough to avoid initial effect. To simplify the model, only ice loads will be considered with no wind force and hydro force.

The ice load is assumed to act on OWT monopile sub-structure at mean water level. The global ice crushing force will consist of two parts, mean ice load which has been calculated and time varying oscillations which could be generated based on the method introduced above.

Matlab will be used for the spectrum calculation and an input file containing ice loading oscillation time series for FEDEM can also be created. The time varying ice force will be applied on structure through time series input file.

Simulation results at MSL point including ice load, displacement and velocity will be exported separately. Post processing of data will be done through Matlab.

3.5 Analysis of spectral model

Time domain simulations for ice speed 0.04 m/s, 0.13 m/s, 0.2 m/s and 0.3 m/s are performed in FEDEM. Ice loads, structure response and velocities at mean water level are measured. The steady state measurements are exported and attached in Appendix 2. Some descriptive statistical indexes are used to have a preliminary view of simulation results.

Table 3-1 Statistical indexes for results of spectral model

Ice speed (m/s)	Ice loads (MN)			Velocity (m/s)			Displacement (m)		
	Mean	Standard Deviation	max	Mean	Standard Deviation	Max	Mean	Standard deviation	max
0.04	41.13	8.23	66.68	-1.73E-04	0.089	0.312	0.121	0.028	0.216
0.13	39.11	8.12	67.67	-4.03E-04	0.107	0.360	0.121	0.031	0.121
0.2	42.44	7.22	63.59	-5.94E-04	0.113	0.363	0.127	0.034	0.221
0.3	42.25	7.80	68.54	1.99E-04	0.113	0.389	0.127	0.029	0.222

Generally, no much differences can be seen directly from the simulation results for different ice speeds which can be explained by the dominating influence of mean ice loads. Mean values for structure response are almost constant for different ice speeds and larger standard deviation can be observed for high ice speeds. Specifically, for ice speed 0.04 m/s which is very likely to be within the ductile-to-brittle transient region, larger ice loads and structure response are expected which is not reflected in the simulation results.

3.5.1 Input ice force

3.5.1.1 Mean ice loads

The spectral model consists of mean ice loads and time varying ice loads. The time varying ice force time series is obtained by inverse Fourier transform of empirical ice load spectrum. The mean ice loads are calculated from GL guideline, in which strain rate is assumed to be a fixed value $\dot{\varepsilon}=10^{-3}$. Without considering the influence of structure response, the mean ice load will be a constant value for different ice speeds and will not change during ice crushing process. As is shown in Table 3-1, the mean ice force is almost constant regardless of ice speeds.

3.5.1.2 Time varying ice loads

The time varying part of input ice loads can be generated based on the global spectrum obtained from previous instructions. The power spectrums for different ice velocities is plotted in Figure 3-10, from which it is possible to come to the conclusion that the peak of the power spectrum will decrease as ice velocity increases. It is worth mentioning that most of energy are within low frequency range from 0 to 0.5 Hz and the differences of spectrums for different ice speed mainly lies in frequency range smaller than 0.25 Hz. Noticing that the natural frequency of structure is 0.32 Hz, the changing spectrum in low frequency region might not have large influence on structure response.

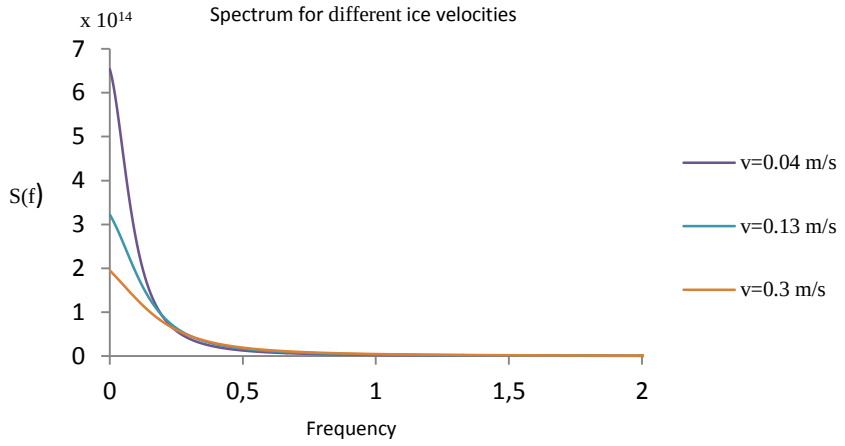

Figure 3-10 Ice load spectrum

As is expected, little differences in ice load amplitude can be observed in Table 3-1, which can be explained by the almost constant values in spectrums around natural frequency.

The small variation of force spectrum for frequency larger than 0.25 Hz explains why time varying components will not change much when ice speed increases, apart from slight rise of amplitude. Compared with time varying components, the value of mean load is rather large and will have dominating effect. It is understandable that the time signals for different ice speeds could be very similar as is shown in Figure 3-11.

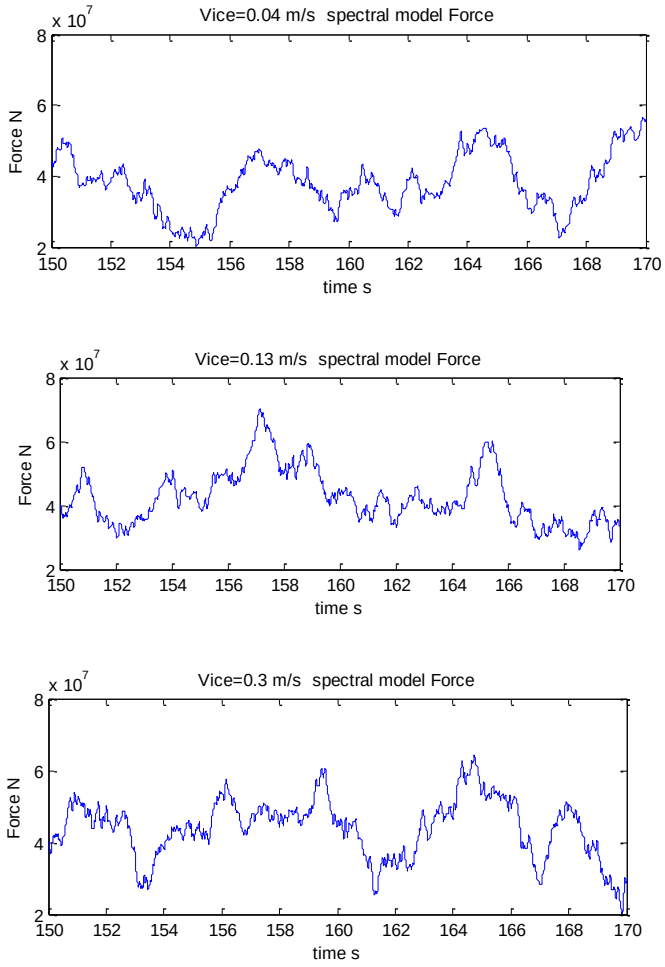

Figure 3-11 Time varying ice loads for ice speed 0.04 m/s 0.13 m/s 0.3 m/s

3.5.2 Structure response

Considering that the spectral model is calibrated by ice speed ranging from 0.04 m/s to 0.35 m/s, simulation tests for ice speeds within this range only will be executed. The time signals for structure displacement of ice velocity 0.04 m/s, 0 .13 m/s and 0.3 m/s are taken out and will be compared in this session.

As is indicated in Table 3-1, the mean values of displacement are almost the same and the standard deviation have the trend to increase with increasing velocity, which is similar to loads signals.

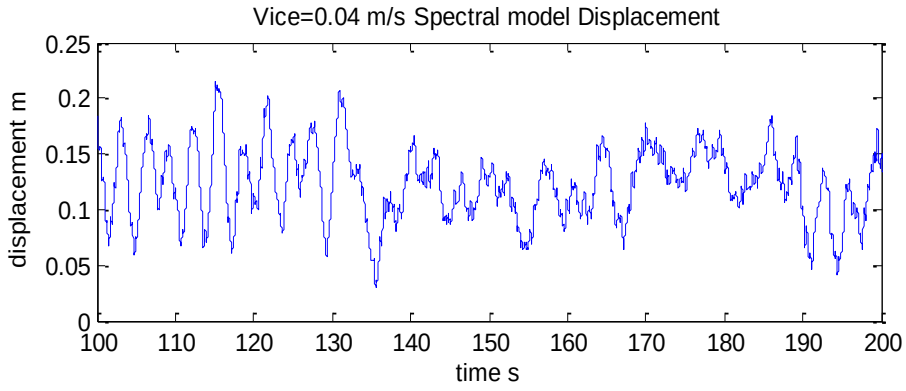

Figure 3-12 Simulation result for ice speed 0.04 m/s

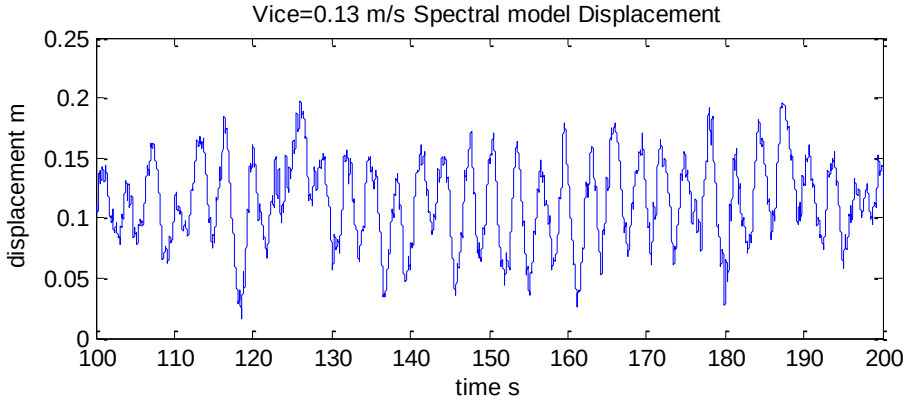

Figure 3-13 simulation result for ice speed 0.13 m/s

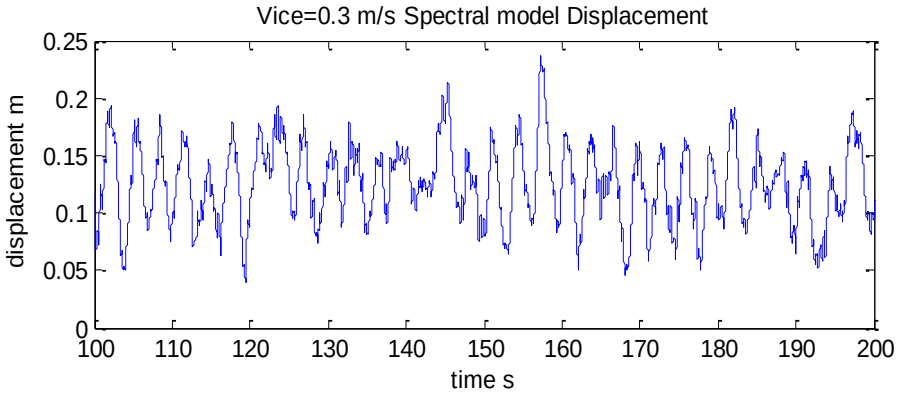

Figure 3-14 Simulation results for 0.3 m/s

It can also be found in Figure 3-12, Figure 3-13 and Figure 3-14 that the ice velocity does not have large influence on structure response, which can be explained by the dominating effect of constant mean ice loads. A close look at structure displacements reveals that, for high ice speed, the amplitudes is getting larger. This can also be explained by the larger time varying component

of ice loads for higher ice velocity. Also, cyclic oscillation with frequency about 3.3 Hz can be observed, and the structure is excited at this frequency.

3.5.3 Response spectrums

The time series for structure response are translated into response spectrum by Fourier transform. As is discussed above, the time series of structure response for 3 ice velocities are quite similar. A detail check of response spectrum shows that structure will be excited at frequency 3.3 Hz for all ice speeds and low frequency components will have dominant influence.

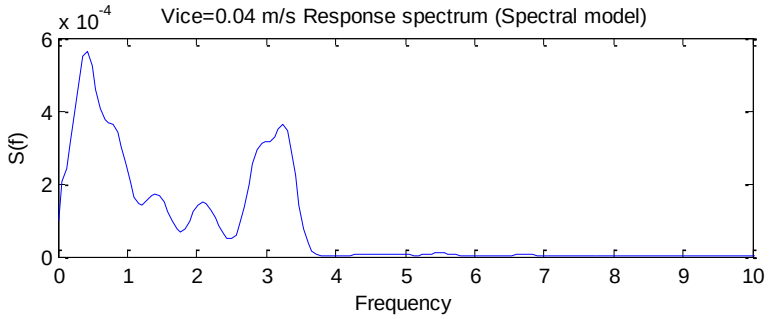

Figure 3-15 Load and response spectrum for Vice=0.04 m/s

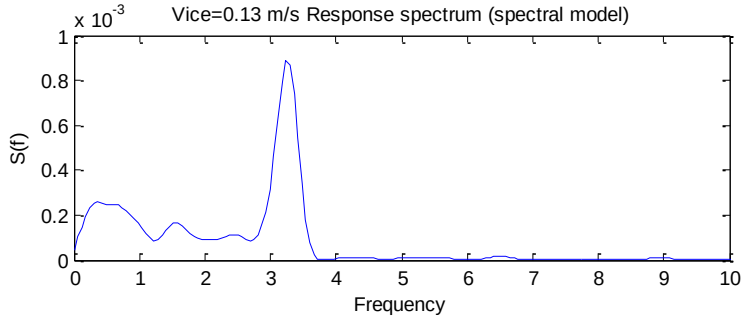

Figure 3-16 Load and response spectrum for Vice=0.13 m/s

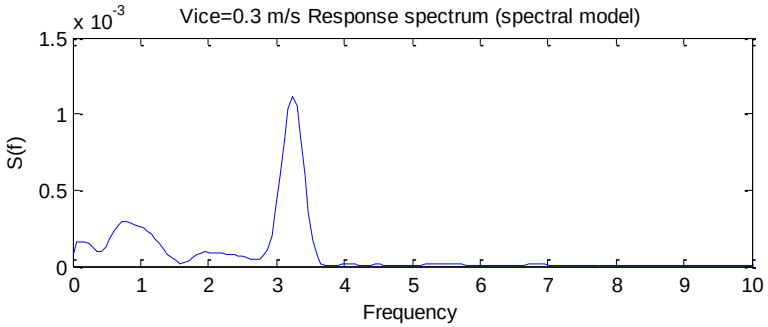

Figure 3-17 Load and response spectrum for Vice=0.3 m/s

Specifically, for low ice speed (Vice=0.04 m/s), the primary peak of response spectrum at structure natural frequency 0.32 Hz can be observed. The value for this frequency component will decrease with growing ice speed and this low frequency component will lose it dominance for intermediate and high ice speeds.

In spite of the excitation at the first eigen frequency for low ice speed, the response is not very larger and resonance is not obvious. This could be explained by the low time varying ice loading values and large mean values for ice loads. Also, a comparison of peak values of response spectrums for different ice speeds shows that peak value for ice speed 0.04 m/s at 0.32 Hz is low compared with high ice speed response spectrum peaks at 3.3 Hz.

3.6 Limitations

3.6.1 Structure feedback effect

In the first chapter, ice crushing characteristics have been introduced in detail. It has been well known that for ice velocities in different regimes, the structure response will illustrate distinct properties. These special phenomena discovered under various ice velocities are attributed to the response of structure, which influences relative velocity between ice and structure. Researches show that ice crushing strength depends on strain rate and will change during ice-structure interaction process. This mechanism is not investigated in current spectral model.

Instead of calculating ice loads through formulas, the ice load spectrum is calibrated by panel data for ice speed rage 0.04 m/s to 0.35 m/s directly. It is notable that this speed range might cover both the ductile-brittle transitional regime and brittle crushing regime. As is known that the ductile-brittle transitional regime and brittle crushing regime have different ice crushing characteristics. For intermediate ice speed, frequency lock in phenomenon might happen which could lead to very large structure displacement amplitude. For high ice velocities, the mean displacement value will increase but fluctuation amplitude could be smaller.

As can be seen from the results, these properties cannot be reflected in spectral model. The input ice loads time series look similar for all ice speeds and the resulting response spectrum also seem to be much alike. It is rather difficult to incorporate the influence of structure response into the

spectral model. In spectral model, predefined ice force time series is created and applied on structure directly and the structure response in not involved in ice load calculation.

For high ice velocity, when structure response is so small and could be ignored, the ice failure will enter into continuous brittle crushing regime and the spectral model could be valid. But it is also worthy of noticing that if the stiffness of structure is very low, it is possible that structure has large response and the feedback effect cannot be omitted anymore.

3.6.2 Regional effect

The ice loads for spectral model consist of two parts, time varying component and mean ice load. The ice load spectrum for time varying component is formulated based on the empirical data in Bohai Bay. And due to different ice properties in different areas, the parameters for ice spectrum might also change. The mean ice loads is obtained through the empirical formula from GL, which includes parameters like temperature, salinity and average strain rate. Obviously, the values of these parameters are very hard to define and will vary a lot from one region to another region. Therefore, existing spectral model is only valid for regional analysis.

3.6.3 Scaling effect

Structure size effect might also have influence on simulation results. The dimension of measurement structure is illustrated in Figure 3-2. As is indicated the diameter of the cylindrical structure is 1.76 m, which might not be comparable with the monopile structure tested in this paper which has diameter of 6 m. The validity of the coherence function might be open to doubt, specifically when considering the inhomogeneous and curved ice sheet surface that the ice and structure might not fully contact each other. Admittedly, the effective contact area is difficult to calculate. (Andrew Palmera, 2010)

Also, the measurements on panels are simplified as point loads without considering the ice stress distribution over ice thickness. Thus, the coherence function is only for force distribution over horizontal direction and the ice aspect ratio effect could not be taken into account.

3.6.4 Mean ice loads with constant strain rate

As is indicated above, the mean ice load is assumed to be a constant value during ice crushing process and will be the same for different ice speeds. Mean ice crushing strength is calculated

based on GL formula, in which strain rate is assumed to be a fixed value $\dot{\varepsilon}=10^{-3}$. But in reality this parameter will change over time due to structure displacement and ice sheet deformation.

As can be seen from Figure 3-9 , ice crushing strength is quite sensitive to the strain rate and salinity, the ice crushing strength might vary from 2 MPa to 12 MPa, which means constant mean crushing load assumption could lead to inaccuracy.

Chapter 4

Määttänen-Blenkarn ice load model

In this chapter, the relation between stress rate and ice crushing strength is described first and the implementation of the Määttänen-Blenkarn in time domain simulation is performed. Both time domain analysis and frequency domain analysis are given and limitation of the model will be discussed at the end of the chapter.

4.1 Background for Määttänen-Blenkarn ice load model

4.1.1 Stress rate dependent ice crushing strength

In 1960s, the study of mechanical and structural properties of sea ice commenced based on the available measurements from Cook Inlet Alaska. In 1968, Peyton published two reports on sea ice force and sea ice strength, in which the concept of dependence of ice strength upon loading rate was first introduced. This concept was adopted and confirmed by Blenkarn in 1970. (H.R.Peyton, 1968; Blenkarn, 1970)

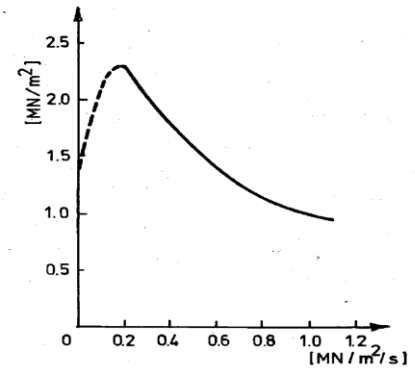

Figure 4-1 Peyton's compressive strength data (Määttänen M. , 1978)

The strain rate could determine the ice crushing mode and ice crushing capacity. For low ice deformation strain rate, the ice crushing mode tends to be ductile crushing failure which allows

more interaction between ice and structure. For high ice velocity, the ice failure might enter into brittle crushing domain in which ice is mainly subject to elastic deformation (Figure 4-2).

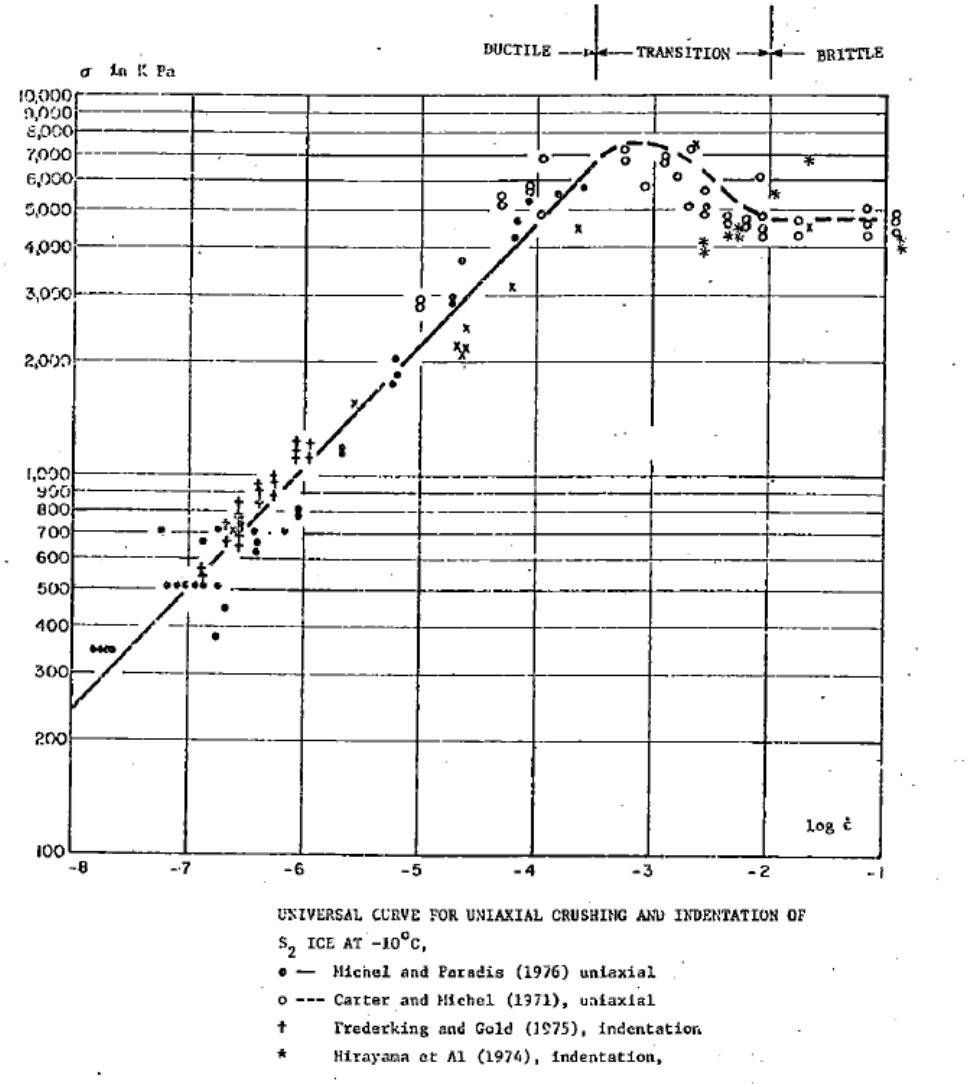

Figure 4-2 Ice crushing capacity and stain rate (Toussain, 1976)

Määttänen calibrated the relation between ice crushing strength and strain rate and empirical relation between ice crushing strength and stress rate was estimated as

$$\sigma_c = \begin{cases} (2 + 7.8\dot{\sigma} - 18.57\dot{\sigma}^2 + 13\dot{\sigma}^3 - 2.91\dot{\sigma}^4)\sqrt{\frac{A_0}{A}} \; for \dot{\sigma} < 1.3Mpa \\ \sqrt{\frac{A_0}{A}} \; for \; \dot{\sigma} > 1.3Mpa \end{cases} \qquad \textit{Equation 4.1}$$

In which, A is the contact area and A_0 is the reference area.

This formula employs a polynomial that is approximated to the stress rate dependency measure by Peyton. The stress rate and strength relation in Määttänen formula is compared with Peyton data in Figure 4-3.

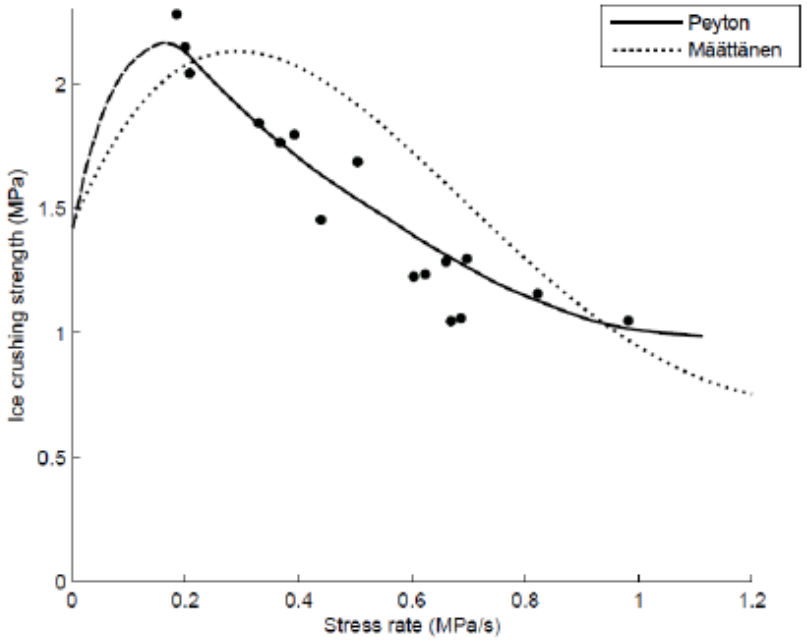

Figure 4-3 Stress rate dependency after Peyton(1986) and Määttänen(1998)

As can be seen from Figure 4-4, the ice – structure interaction can also be ascribed in to 3 regimes. Ductile ice failure for low ice stress rate and brittle crushing failure for high stress rate. When the stress rate is larger than 0.13 MPa/s, the ice crushing strength might become a fixed value independent of stress rate. Specifically, in the regime for ice stress rate between 0.2 MPa/s to 1 MPa/s, frequency lock-in phenomenon could be expected which might lead to stronger structure vibrations.

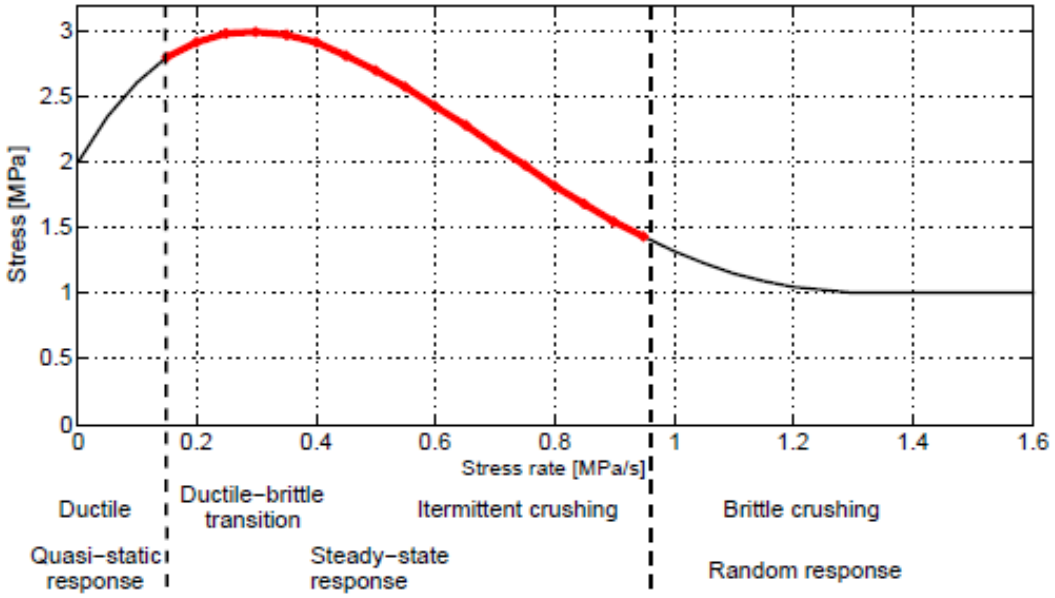

Figure 4-4 Ice crushing stress vs stress rate with different interaction regions (Popko W. , 2014)

4.1.2 Stress rate

The determination of ice crushing strength is described by relation between stress rate and crushing strength. The definition of stress rate was first formulated by Blenkarn(1970) and developed by Maaattanen.

Similar to the radial stress concept promoted by Timoshenko and Goodier(1951), the contact force between ice and cylindrical structure calculation equation was given by Blenkarn. Timoshenko and Goodier characterized the spreading of radial stress as Figure 4-5, the radial stress on a semicircular surface with radius r can be calculated as

$$\sigma = -\frac{2P}{\pi}\frac{cos\theta}{r} \qquad \textit{Equation 4.2}$$

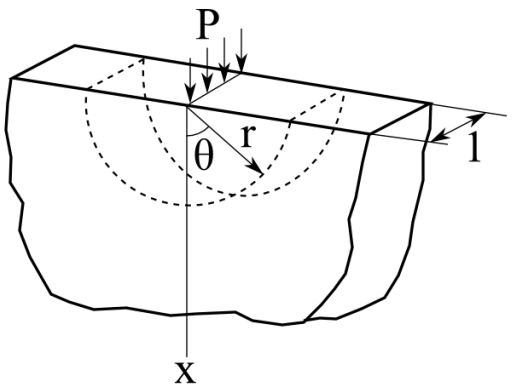

Figure 4-5 Model for calculating radial stress, as described by Timoshenko and Goodier (1951)

Blenkarn(1970) suggested the analogy between the radial stress calculation and the contact force on cylindrical surface. The radial stress equation was modified to calculate contact ice stress on cylindrical structure with radius r

$$\sigma = \frac{4pz}{\pi r}\cos(\theta) \qquad \textit{Equation 4.3}$$

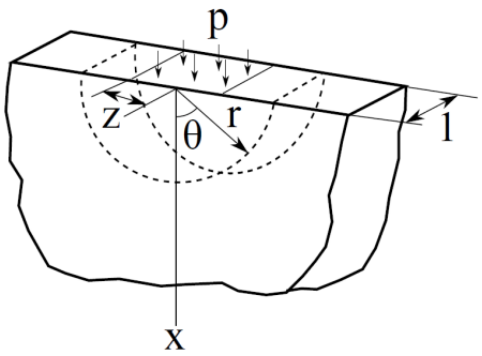

Figure 4-6Model for calculating radial stress, as described by Blenkarn (1970).

It is assumed by Blenkarn that the equivalent ice load works on half length of structure width with constant pressure p .The stress is related to the position on structure edge with angle θ.

For static situation without relative motion between ice and structure, parameter r will equals structure radius. But during the ice –structure interaction process with moving ice and structure, this parameter is changing over time and time varying stress rate can be obtained through time derivation of r ,

$$\dot{\sigma} = \frac{d\sigma}{dt} = \frac{4pzv_{ice}}{\pi r^2} \qquad \textit{Equation 4.4}$$

Where $v_{ice} = \frac{dr}{dt}$ is the ice velocity.

Based on the Blenkarn's theory, another expression for stress rate was also given by Määttänen when calibrating stress rate- ice crushing strength relation

$$\dot{\sigma} = (v - \dot{u})\frac{8\sigma_0}{\pi D} \qquad \textit{Equation 4.5}$$

In which $\dot{\sigma}$ is the stress rate, v is ice speed and $\dot{u}$ represents structure velocity. Parameter σ_0 is defined as reference ice strength. To be conservative, the maximum value in the stress rate-stress curve 3 MPa is chosen.

Noting that the stress rate definition suggested by Blenkarn is based on the assumption that ice and structure fully contact each other, this might work for narrow structure and the contact area is determined by width of structure and thickness of ice sheet. For wide structure, this is not necessarily the case. Due to the irregular shape of ice sheet, the ice load might only work on several scattered contact points at protrusions on ice edge. For the simplicity of calculation, it is assumed that the ice and structure fully contact each other, and parameter D is the diameter of the structure. This thesis aims at analyzing ice problems for monopile structure for OWT and the diameter of the example structure is 6 m.

4.1.3 Negative damping

Based upon the strain rate dependence ice failure characteristics, the theory of negative damping and self-excited vibration was proposed by Määttänen. A mathematical model to describe negative damping and self-excited vibration was established through the combination of equation of motion and stain rate-dependent ice crushing strength.

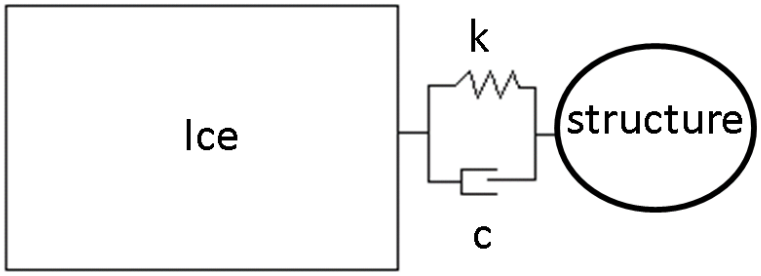

Figure 4-7 The response of structure

The ice-structure interaction model can be simplified to be a single degree of freedom mass-spring system. The equation of motion for the SDOF system can be expressed as

$$M\ddot{u} + C\dot{u} + Ku = F(v_{ice} - \dot{u}) \qquad \textit{Equation 4.6}$$

At the right hand side, stress rate-dependent ice load $F(v_{ice} - \dot{u})$ is used and ice loads will be determined by relative speed between ice and structure. It is noticeable that the damping term at left hand side of equation is dependent of structure velocity $\dot{u}$ and the ice force is also dependent of structure velocity $\dot{u}$. If the structure response related part of the ice force could be extracted and moved to left side of equation, the damping coefficient will change and the remaining ice loads will be ice velocity related only.

This could be achieved by applying first order Taylor expansion at point $\dot{u} = 0$, and the ice load can be modified as

$$\begin{aligned} F(v_{ice} - \dot{u}) &= F(v_{ice} - 0) + \frac{dF(v_{ice} - 0)}{d\dot{u}}((v_{ice} - \dot{u}) - (v_{ice} - 0)) \\ &= F(v_{ice}) + \frac{dF(v_{ice})}{d\dot{u}}(-\dot{u}) \end{aligned} \qquad \textit{Equation 4.7}$$

Moving the second term $\frac{dF(v_{ice})}{d\dot{u}}(-\dot{u})$ to the left, the equation of motion can be rewritten as

$$M\ddot{u} + (C + \frac{dF}{d\dot{u}})\dot{u} + Ku = F(v_{ice}) \qquad \textit{Equation 4.8}$$

In which, the ice loads on right hand side depend on ice velocity only and an extra damping term $\frac{dF(v_{ice})}{d\dot{u}}$ is shown on left hand side. The new damping coefficient will be

$$C_{new} = C + \frac{dF}{d\dot{u}} \qquad \textit{Equation 4.9}$$

Due to the negative sign before structure velocity $\dot{u}$ in the expression of ice force F, $\frac{dF}{d\dot{u}}$ could be a negative term. If the magnitude of this negative term is larger than c, negative damping could happen. Negative damping might induce increasing structure vibration amplitude over time and lead to instability of system.

4.2 Implementation of Määttänen-Blenkarn ice load model

4.2.1 Linearized stress rate and ice crushing strength relation

As is introduced from previous chapters, the polynomial expression of stress rate dependent strength is rather complex. But the shape of polynomial expression can be divided into 3 segments (Figure 4-8).

The peak value for the ice crushing strength can be reached at $\dot{\sigma} = 0.3Mpa$. For $\dot{\sigma} < 0.3Mpa$, the ice failure strength will increase as with increasing stress rate. The ice strength will decrease when stress rate increases between $0.3\ Mpa < \dot{\sigma} < 1.3\ Mpa$. For ice stress rate larger than 1.3 MPa, the ice strength will reach a constant value and be independent of stress rate.

Based on the characteristics of stress rate - strength relation, Määttänen (1978) first introduced the linearization of the formula for simplicity of calculation.

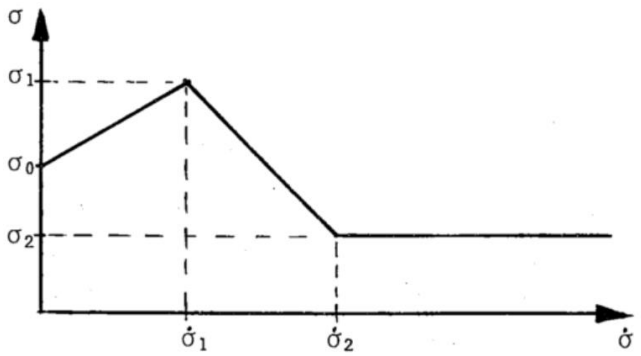

Figure 4-8 Linearized stress rate - strength relation

After the linearization, the stress rate dependent ice failure strength can be approximated to be

$$\sigma_c(\dot{\sigma}) = \begin{cases} (b_{\ 1} + a_1\dot{\sigma})\sqrt{\frac{A_0}{A}} & for\ \dot{\sigma} < 0.3Mpa \\ (b_2 + a_2\dot{\sigma})\sqrt{\frac{A_0}{A}} & for\ 0.3\ Mpa < \dot{\sigma} < 1.3Mpa \\ \sqrt{\frac{A_0}{A}} & for\ \dot{\sigma} > 1.3Mpa \end{cases} \quad \textit{Equation 4.10}$$

Curve fitting tool of Matlab was deployed for determining values for a_1, b_1, a_2 and b_2. By inserting the unknown values, the ice crushing strength can be further elaborated to be

$$\sigma_c(\dot{\sigma}) = \begin{cases} (2.193 + 3.352\dot{\sigma})\sqrt{\frac{A_0}{A}} & for\ \dot{\sigma} < 0.3Mpa \\ (3.783 - 2.8347)\sqrt{\frac{A_0}{A}} & for\ 0.3 < \dot{\sigma} < 1.3\ Mpa \\ \sqrt{\frac{A_0}{A}} & for\ \dot{\sigma} > 1.3\ Mpa \end{cases} \quad \textit{Equation 4.11}$$

4.2.2 Implementation of linearized model on FEDEM

As is discussed above, after the linearization, ice crashing strength can be simplified as

$$\sigma_c = (b + a\dot{\sigma})\sqrt{\frac{A_0}{A}} \quad \textit{Equation 4.12}$$

Where parameters *a* and *b* will have different values in different stress rate range. For flat vertical wall structure, total ice force will be

$$F(v_{ice} - \dot{u}) = \sigma_c \times \sqrt{\frac{A_0}{A}} \times A \quad \textit{Equation 4.13}$$

In which $\sqrt{\frac{A_0}{A}}$ is a scaling term considering the contact area. The model established has cylindrical surface and the contact area can be assumed to cover half of structure. Therefore, instead of using the reference area, the global force can be obtained through an integration of local stresses with angle ranging from $-\frac{\pi}{2}$ to $\frac{\pi}{2}$. The same as spectral model, local stresses should also consist of radial normal stress component and tangential shear stress component. The total ice loads can be estimated as

$$F_G(v_{ice} - \dot{u}) = t \times r \int_{-\frac{\pi}{2}}^{\frac{\pi}{2}} (\sigma(\dot{u}) \times \cos(\theta) + \mu \times \sigma(\dot{u}) \times \sin(\theta)) d\theta = 2hr\sigma(\dot{u}) \quad \textit{Equation 4.14}$$
$$= A_0 \times \sigma(\dot{u})$$

In which *h* is ice thickness, *r* is structure radius. New reference contact area is defined as

$$A_0 = 2th \quad \textit{Equation 4.15}$$

By inserting ice crushing strength, the total ice force could be rewritten as

$$F(v_{ice} - \dot{u}) = A_0 \times \sigma(\dot{u}) = A_0(a \times (v_{ice} - \dot{u})\frac{8\sigma_0}{\pi D} + b) \quad \textit{Equation 4.16}$$
$$= (A_0 \times b + v_{ice} \times A_0 \times a\frac{8\sigma_0}{\pi D}) - \dot{u} \times A_0 \times a\frac{8\sigma_0}{\pi D}$$

The part of ice load independent of structure response is determined by ice velocity only and can be expressed as

$$F(v_{ice}) = (b + v_{ice} \times a\frac{8\sigma_0}{\pi D})A_0 \quad \textit{Equation 4.17}$$

The added damping coefficient can be calculated by $\frac{dF}{d\dot{u}} = -A_0 * a\frac{8\sigma_0}{\pi D}$, together with the original damping coefficient *c*, the new damping coefficient can be obtained as

$$c_{new} = c + \frac{dF}{d\dot{u}} = c - A_0 \times a\frac{8\sigma_0}{\pi D} \quad \textit{Equation 4.18}$$

Structure velocity independent ice load $F(v_{ice})$ is exerted at water level point of structure. For linearized Määttänen model, this ice load could be divided into 3 regimes by stress rate and each part corresponds to a fixed value. A segment function will be built on FEDEM to simulate ice loads as below

$$F(v_{ice}) = \begin{cases} (2.193 + v_{ice} \times 3.352 \times \frac{8\sigma_0}{\pi D})A_0 & for\ \dot{\sigma} < 0.3Mpa \\ (3.783 - v_{ice} \times 2.8347 \times \frac{8\sigma_0}{\pi D})\ A_0 & for\ 0.3 < \dot{\sigma} < 1.3\ Mpa \\ A_0 & for\ \dot{\sigma} > 1.3\ Mpa \end{cases} \quad \textit{Equation 4.19}$$

A damper will also be attached to the structure at water level. The same as ice load $F(v_{ice})$, damping coefficient will also change by varying stress rate and the function can be described as

$$c = \begin{cases} -A_0 \times 3.352 \frac{8\sigma_0}{\pi D} & for\ \dot{\sigma} < 0.3Mpa \\ -A_0 \times 2.8347 \frac{8\sigma_0}{\pi D} & for\ 0.3 < \dot{\sigma} < 1.3\ Mpa \\ 0 & for\ \dot{\sigma} > 1.3\ Mpa \end{cases} \qquad \textit{Equation 4.20}$$

Based on the discussion in previous chapters, the values of parameters in these two functions are listed in Table 4-1.

Reference ice crushing strength σ_0 is taken as maximum value in the stress rate dependent strength curve 3 MPa. For wide structure, diameter D=6 m is used for ice crushing strength calculation. The ice thickness h is assumed to be 0.4 m and monopile structure radius r= 3 m. Based on the results of linearization, the slopes and intercepts for different stress rate regime are obtained with $a_1 = 3.352$, $b_1 = 2.193$, $a_2 = -2.8347$, $b_2 = 3.783$.

Table 4-1 Parmeters for Määttänen-Blenkarn model

σ_0(MPa)	D(m)	r(m)	h(m)	A_0=2rh	a_1	b_1	a_2	b_2
3	6	3	0.4	2.4	3.352	2.193	-2.8347	3.783

4.3 Results of Määttänen-Blenkarn model

Time domain simulations for ice speed 0.015 m/s, 0.02 m/s, 0.03m/s, 0.04 m/s, 0.08 m/s, 0.13 m/s, 0.2 m/s, 0.3 m/s and 0.4 m/s were processed based on Maataanen-Blenkarn model. The time varying structure reaction force, structure displacement and structure velocity were exported and the plots for steady state time signals are attached in Appendix 3.

In this session, general statistical results will be analyzed first. In order to analyze ice-structure interaction process, the time domain results for structure displacement and ice loads will be investigated in detail. The response spectrums and load spectrums will be further discussed.

4.3.1 Statistical overview

In order to have a global view of the ice loads and structure response, preliminary statistical analysis is done for ice load, structure velocity and displacements and results are listed in Table 4-2.

Table 4-2 Statistics for results of M-B model

Ice speed (m/s)	Ice force (MN)			Velocity (m/s)			Displacement (m)		
	Mean	Standard Deviation	max	Mean	Standard Deviation	Max	Mean	Standard deviation	max
0.015	5.2037	0.496	6.7434	-7.40E-06	0.011	0.020	0.036	1.41E-04	0.037
0.02	12.387	1.191	14.428	-6.85E-05	0.015	0.029	0.037	6.29E-04	0.038
0.03	12.459	2.750	16.718	-9.90E-05	0.027	0.039	0.037	0.001	0.040
0.04	13.686	3.041	18.300	-1.55E-04	0.046	0.049	0.037	0.002	0.041
0.08	17.058	2.917	21.936	-1.21E-03	0.105	0.095	0.037	0.004	0.047
0.13	17.920	0.838	19.935	2.06E-04	0.124	0.155	0.041	0.006	0.048
0.2	15.203	0.496	6.7434	-4.48E-04	0.130	0.230	0.048	0.004	0.055
0.3	12.387	1.191	14.428	1.20E-04	0.0351	0.066	0.052	0.001	0.054
0.4	12.355	0.105	12.445	4.72E-11	4.38E-09	1.09E-08	0.049	2.11E-09	0.049

A first look at the numbers reveals that the ice loads and structure response will climb up with increasing ice speeds and reach their peaks at around 0.13 m/s, after which the force and response tend to decrease and sustain the same values after reaching 0.4 m/s.

In order to check the relation between ice speed, structure reaction force and response, the concept of relative standard deviation is used, which helps to describe the variability of time signals. A larger relative standard deviation represents larger fluctuation amplitudes compared with mean value. Considering that the mean values of structure velocity are so small and almost approaches 0, the application of relative standard deviation might not be feasible. Here, only diagrams for structure loads and structure displacements are presented in Figure 4-9 and Figure 4-10.

As can be found from the plots, the mean values are almost constant for ice speeds smaller than 0.1 m/s and larger than 0.3 m/s and increase of mean value can be seen between. Larger oscillations around mean value could happen for ice speed between 0.1 m/s and 0.3 m/s.

The largest structure vibration might occur around 0.13m/s, corresponding to the peak for relative standard deviation for structure response. The peak for structure force relative standard deviation also lies around 0.13 m/s.

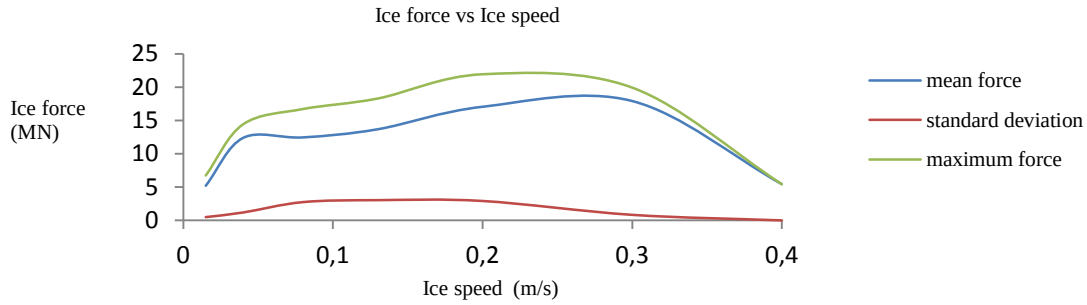

Figure 4-9 Loads vs Ice velocity

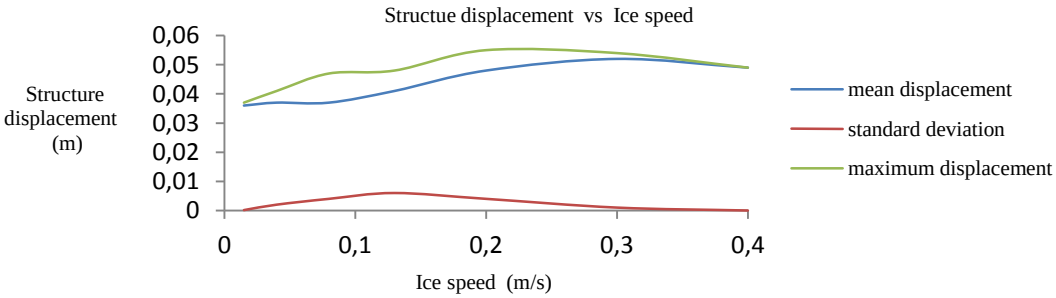

Figure 4-10 Structure displacement vs ice velocity

Seeing that ice speed ranging from 0.02 m/s to 0.4 m/s is just within regime that ice crushing strength is very sensitive to strain rate, it can be concluded that the larger standard deviation of within this range results from the stress rate dependent ice crushing strength.

4.3.2 Displacement time series for different ice velocities

Due to the strain rate dependency of ice crushing strength, when structure moves forward, the relative speed between ice and structure decreases and the strain rate of ice decreases. When the structure moves backward, the strain rate increases. It is supposed that this alternation of loading rate makes dynamic ice forces transmit from one mode to another. The same is shown in the

displacement signals during simulation, the response of wind turbine for various ice velocities illustrates different properties.

For low ice velocities (Vice<0.02 m/s), the ice loading period is much longer than the structure eigen period, the response is considered to be quasi-static. Saw-tooth shape of structure response can be obtained (Figure 4-11).

Specifically, for ice speed Vice= 0.02 m/s, some wiggles can be captured during the increase of structure displacement. The saw tooth shape response can be characterized as quasi-static structure response. Due to the slow ice approaching speed, the global ice force will grow up to its peak value. The peak load is followed by an instantaneous drop of the contact force, which seems to be associated with an ice pulverization event in the attendant zone between intact ice and the crushed layer. (Kärnä T. a., 1989). During the loading phase and a nearly static equilibrium exists between the internal and external forces acting on the structure at the events of maximum ice force. After the pulverized rubbles are pushed away, the new intact ice approaches structure and a new cycle of loading will commence. Thus, this response can also be defined as quasi-static vibration. (Kärnä T. K., 1999)

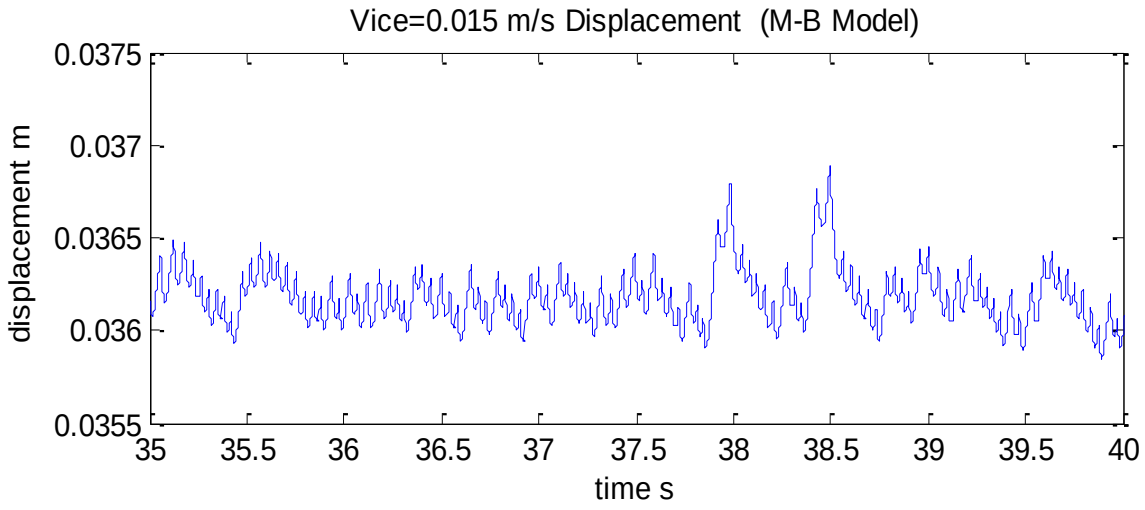

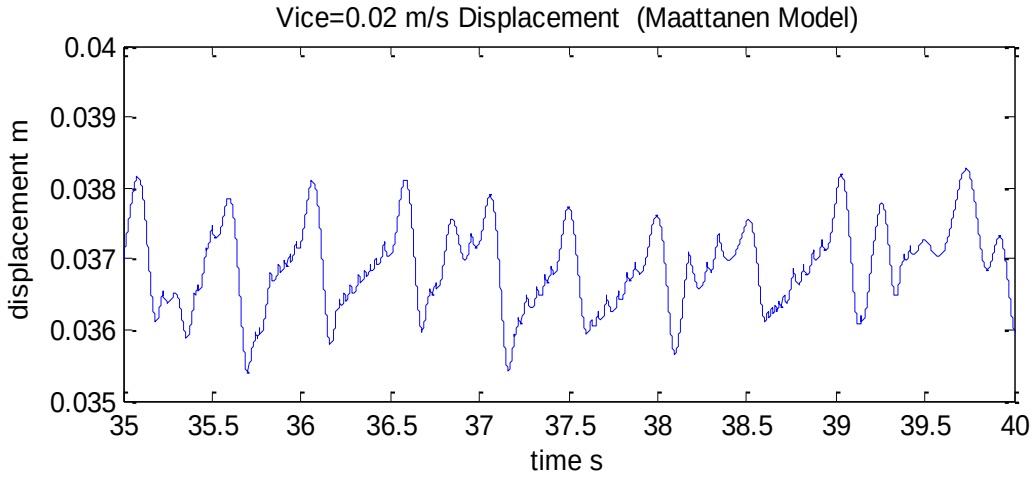

Figure 4-11 Displacement for ice velocity 0.015 m/s &0.02 m/s

When the ice speed reaches 0.03 m/s, the time signal for structure displacement becomes regular overtime and the high frequency oscillations at the tail of loading cycles disappears (Figure 4-12). It is assumed that the ice-structure interaction enters into ductile – brittle transition regime.

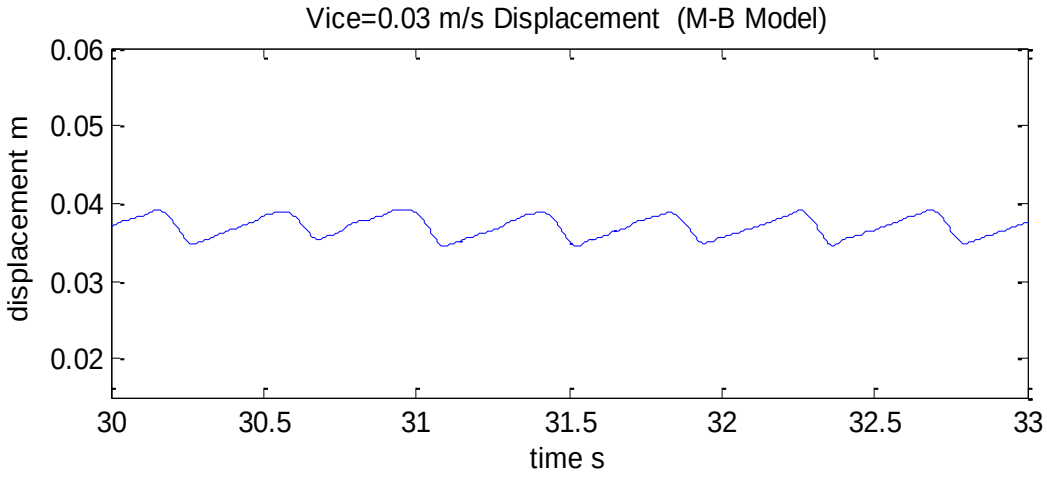

Figure 4-12 Displacement for ice velocity 0.03 m/s

When ice speed equals 0.13 m/s, the shape of time signal becomes rather smooth and has sinusoidal shape with the amplitude almost constant over time (Figure 4-13). This type of response can be identified as frequency-lock-in phenomenon. The ice force spectrum in Figure 4-14 reveals that the peak of ice load spectrum locates at 5 Hz, which is close to one of structure eigen frequencies. As is expected the structure vibrates at one of its eigen frequency and the

dominant frequency of fluctuating ice force is locked in it. The effect of ice force will be magnified by the dynamics of structure and the largest magnitude of structure response could be found. (Qianjin Yue F. G., 2009). After checking out the velocity signals, it could be found that the velocity amplitude of the structure at the water line is approximately the same as the velocity of ice, which attests to the characteristic of frequency locked in phenomenon that structure and ice moving at similar speed. (Kärnä T. T. R., 1990)

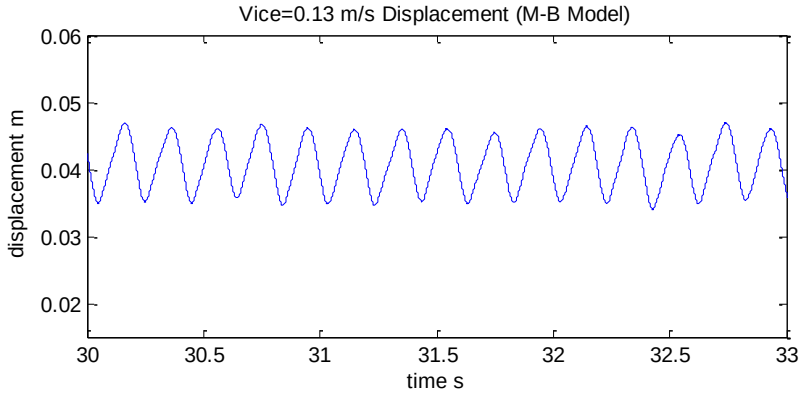

Figure 4-13 Displacements for ice velocity 0.13 m/s

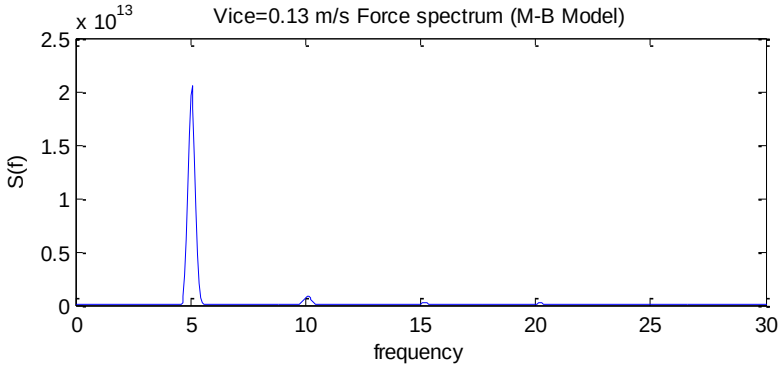

Figure 4-14 Force spectrum for Vice=0.13 m/s

It is indicated in structure response for ice speed 0.3 m/s (Figure 4-15), the mean structure response increases to a higher value but the fluctuation magnitude decreases. After a spin up period, the initial effect will disappear and structure will vibrate with regular signal shape. An equilibrium is reached between the strain rate dependent ice loads and structure response.

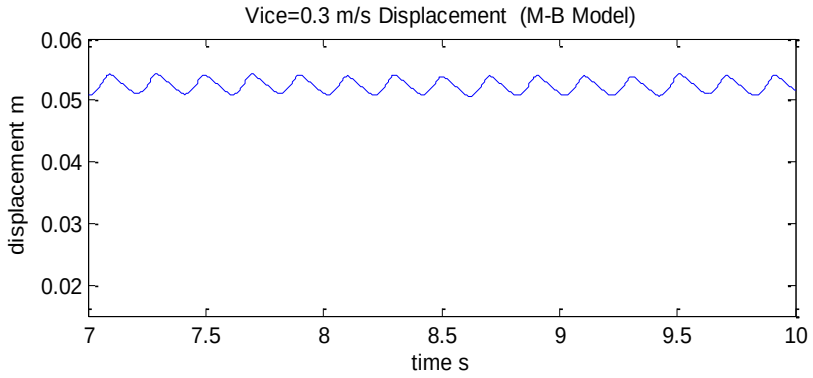

Figure 4-15 Displacement for ice speed 0.3 m/s

When the ice speed reaches 0.4 m/s, the structure oscillation is rather small that can be ignored compared with ice velocity. The negative damping will switch to a positive constant value in this case and the ice loads will also become constant. Due to positive damping coefficient, the structure response will decay over time to a constant displacement value. It is noticeable that the stress rate of this process still locates in ductile-brittle transient region but the model is not sensitive enough to the structure response. In reality, ice speed 0.4 m/s is assumed to be high enough and supposed to be within brittle crushing regime, thus, here the simulation result for 0.4 m/s is assumed to be not reliable.

4.3.3 Response spectrum

In order to see the energy distribution of structure vibration over frequencies, Fourier transform is performed on time domain structure displacement signals. In Figure 4-16 Response spectrum for ice speed 0.015 m/s, 0.04 m/s, 0.13 m/, 0.3 m/s and 0.4 m/s are listed.

It could be seen from the results that for very low ice speed like 0.015 m/s, low frequency component will dominant the structure response. The low ice speeds define the low frequency ice actions and the structure will also be excited at lower eigen frequencies. If the ice velocity is low enough with frequency around 0.3 Hz, resonance is expected to occur, but the ice loads could be rather small and the ice loading process is too slow that structure response is almost quasi-static.

As with increasing ice speed, frequency peak will also shift to the right, with 0.04 m/s around 3 Hz and 0.13m/s around 5 Hz. This might be related to high frequency excitation induced by higher ice velocities and the structure will also be excited at high frequency.

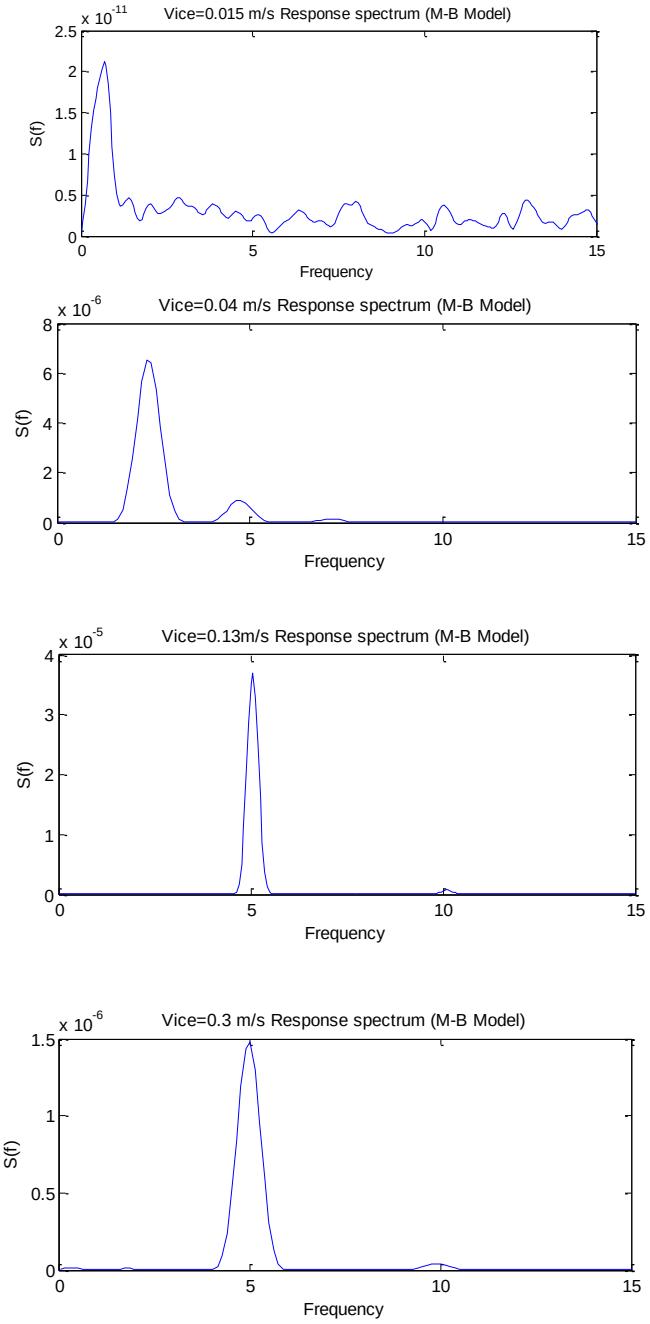

Figure 4-16 Response spectrum for ice speed 0.015 m/s, 0.04 m/s, 0.13 m/, 0.3 m/s and 0.4 m/s

It is worthy of mentioning that the spectrum peak value for ice velocity 0.13 m/s is the highest which can be explained by frequency lock in phenomenon. Compared with ice velocity 0.015 m/s, the ice loads for this velocity have been rather large and the resonance between external ice

loads and high structure eigen frequency will amplify structure response, thus, largest structure vibration can be expected.

Some secondary peaks can be observed for ice speed between 0.02 m/s to 0.4 m/s. Secondary protrusions might result from stress rate dependent ice crushing strength. As is shown in Figure 4-2 , this stress rate-crushing strength relation will have great influence on low and intermediate ice speeds. This influence might induce the high frequency oscillations. This could explain why the high frequency part of spectrum has no bumps for ice speed larger than 0.4 m/s. And for very low ice speeds (Vice<0.02 m/s), it could be explained by the extremely low strain rate which make the changing ice strength not sensitive enough and the response is quasi-static. Therefore, the secondary peaks are small enough to be ignored. Physically, these secondary peaks can be explained by the ice splitting failure, which creates periodic impulsive loads on the structure.

4.3.4 Ice loading time series

The Määttänen-Blenkarn model is established based on stress rate- strength relation. The stress rate dependent ice crushing strength is implemented on the structure through a structure-response-independent ice load and an extra damping coefficient. Thus, the measured ice force time signals during simulation are only the structure response independent part of ice loads. Post processing is needed in order to get the actual total ice force, which is based on equation

$$F_{ice}(t) = F_{measured}(t) + damping(t) \times V_{structure}(\mathrm{t})$$

After summing up two parts of ice loads, the final ice loading time series are obtained and results are shown in Figure 4-17.

Generally, mean value of ice force is increasing with increasing ice speed, but the fluctuation amplitude would be different. As is analyzed above, resonance is expected to happen around ice speed 0.13 m/s. According to load signals, the largest load fluctuation amplitude can be observed for ice speed 0.13 m/s. High frequency oscillations can be seen for all ice speeds, which could result from the relaxation effect when the ice loads climb up to peak backing moving ice .

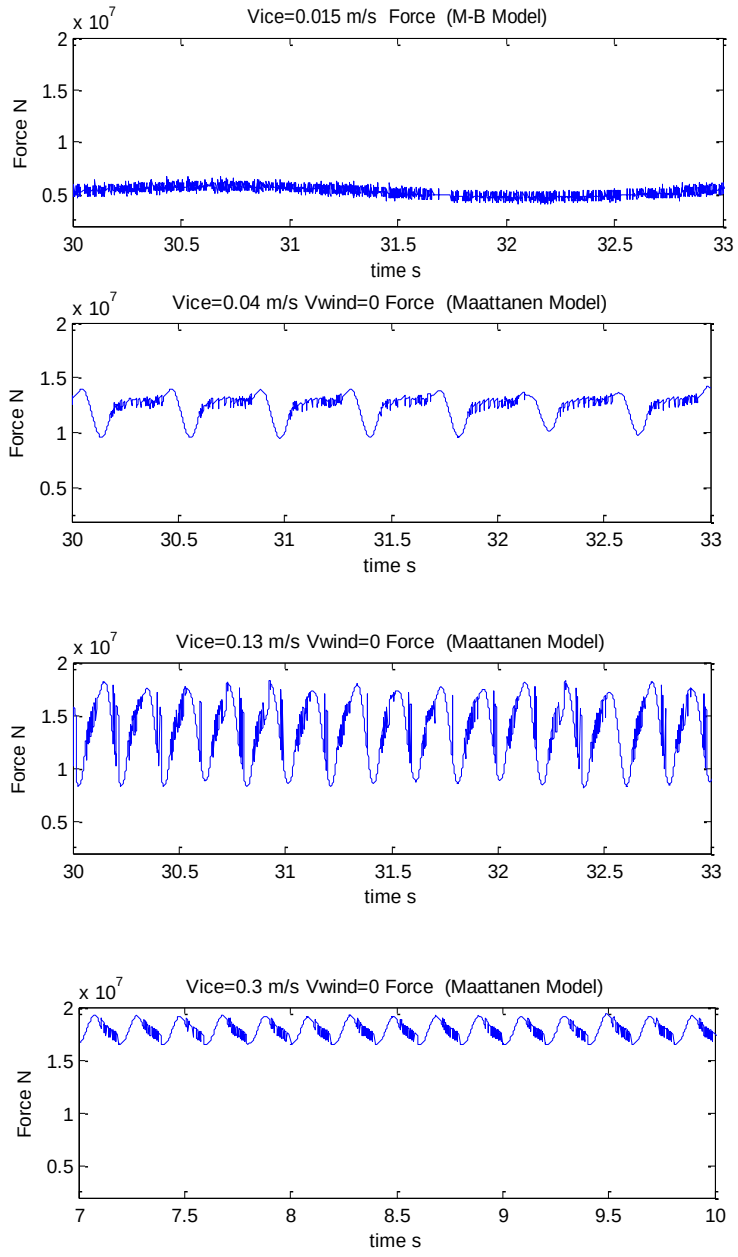

Figure 4-17 Ice force for speed 0.015 m/s, 0.04 m/ , 0.13 m/s and 0.3 m/s

4.3.5 Ice loads spectrum

Fourier transform is used on ice loads time series and spectrums for various ice velocities are shown in *Figure 4-18*.

These ice loads spectrums seem to resemble the shape of response spectrum. But the spectrum peaks are more obvious compared with response spectrum, due to the filter effect of structure mechanical properties. Some of the high frequency signals will be depressed and the low

frequency part, especially when close to structure natural frequency, the signals might be amplified. That might explain why the peak of protrusions seems to weigh more on force spectrum than on response spectrum.

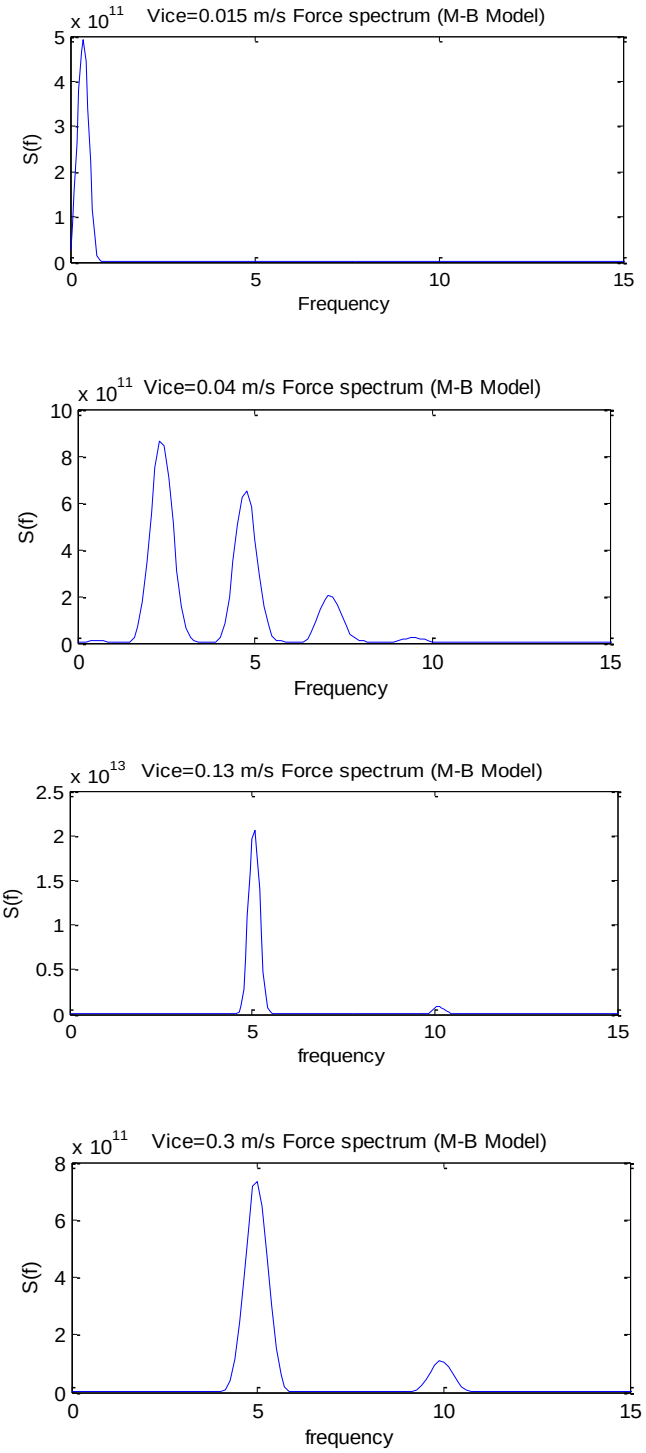

Figure 4-18 Ice load spectrum

In spite of these discrepancies between load spectrum and response spectrum, the similarities are still quite obvious, such as the position of primary peaks and the existence of secondary bumps. The same as response spectrum, the secondary bumps can hardly be observed for low ice speeds (Vice< 0.02 m/s) and high ice speeds (Vice>0.4 m/s). It can be explained that the shapes of these secondary peaks are related to ice crushing regime and structure response mode.

4.3.6 Frequency lock in phenomenon

Most serious structure vibration might happen under frequency lock in phenomenon. Resonance occurs when dominant ice loading frequency approaches structure eigen frequency. The structure vibrates at structure eigen frequency and the dominant frequency of fluctuating ice force is locked in it. The effect of ice force will be magnified by the dynamics of structure and the largest magnitude of structure response could be found. (Qianjin Yue F. G., 2009).

As is analyzed in 4.3.2, the frequency lock in phenomenon happens around ice speed 0.13 m/s. As is shown in Figure 4-13, time signal for structure displacement has sinusoidal shape with the amplitude almost constant over time. This type of response can be identified as frequency-lock-in phenomenon.

After checking out the velocity signals, it could be found that the velocity amplitude of the structure at the water line is approximately the same as the velocity of ice, which attests to the characteristic of frequency locked in phenomenon that structure and ice moving at similar speed. (Kärnä T. T. R., 1990)

The structure response spectrum in Figure 4-16 reveals that the structure is excited around 5 Hz, corresponding to the peak in load spectrum (Figure 4-18) around 5 Hz. One possible explanation could be that large ice speed induces this high frequency peak ice loads. Under this high frequency ice loads, the structure is excited at this high frequency. It can also be seen from the response spectrum that the peak around 5 Hz has absolute dominating effect, almost all the energy are concentrated here. This also explains the regular sinusoidal response shape.

4.4 Limitations

4.4.1 Regional limitation

The core of Määttänen-Blenkarn model lies in the relation between stress rate and ice crushing strength (Equation 4.1). This formula is calibrated from the measurement data from Cook Inlet (H.R.Peyton, 1968; Blenkarn, 1970).

Some key parameters for this curve, like the initial stress, peak stress and constant value for high stress rate, might vary over different regions due to varying ice properties. For example, the ice crushing strength for Bohai Bay calculated from empirical formula is around 6.9 MPa, but the maximum ice crushing strength in the stress rate- strength curve is about 3 MPa only which make the results of two models not comparable.

Apart from this, the value of these parameters will influence slopes of stress rate- crushing strength curve, which will determine negative damping coefficients. The existence of negative damping might trigger intermittent crushing and frequency lock in. Thus, it is expected that the definition of parameters in stress rate – strength curve could influence simulation results and the value of these parameters should be adjusted when used in another area.

4.4.2 Definition of strain rate

As is shown in the stress rate – strength curve, ice strength is very sensitive to low stress rate especially for stress rate smaller than 1.3 MPa/s. Thus, more attention should be paid on the values of parameters in stress rate formula.

The definition of stress rate is given as Equation 4.5 by Määttänen. There might still be some doubts upon the values for reference strength σ_0 and diameter D. To be conservative, maximum value in the stress rate- strength curve (3 MPa) is chosen as the reference ice crushing stress σ_0, which is not necessarily the case. The diameter D is chosen as the structure diameter based on fully contact assumption, which might not be reliable neither.

4.4.3 Linearized Määttänen- Blenkarn model assumption

The stress rate – strength curve is nonlinear as is shown in Figure 4-4. For simplicity, the curve is divided into 3 segments and linearized curve is used for the model. Noticing that structure

response is very sensitive to negative damping which is determined by slope of stress rate-strength curve, inaccuracy could be induced by sharpening the curve.

4.4.4 Structure natural frequency

As is emphasized in Määttänen-Blenkarn model, the interaction between ice and structure will change ice crushing strength and further influence structure response in next time step, which is the so-called feedback mechanism.

Noting that the structure mechanical properties could greatly influence this dynamic ice-structure interaction process, the results of simulation on a different structure might be different from previous field observations. Due to the difference in structure natural frequency and stiffness, it is possible that the velocity boundaries for different ice crushing regimes might shift for structures of different sizes and types.

Table 4-3 Structure diameter vs first eigen frequency (Andrew Palmera, 2010)

First author	Full or model scale	Structure and location	Type of ice	Structure diameter (m)	Lowest frequency (Hz)
Jefferies	FS	Molikpaq, Beaufort	Sea	89	1.3
Yue at al. (2001)	FS	JZ9-3,Bohai	Sea	1.76	2.32
Yue at al. (2001)	FS	JZ20-2 MSW, Bohai	Sea	1.2	1.37
Bjerkas	FS	Nordstromsgrund, Baltic	Baltic sea (low-salinity)	7.5	2.34
Montogomery	FS	Athabaska river, AB	Fresh	2.32	8.9
Guo and Yue (2009)	MS	(Laboratory)	Fresh	0.2	2.3
Guo and Yue (2009)	MS	(Laboratory)	Fresh	0.12	2.3
Sodhi (1991)	MS	(Laboratory)	Fresh	0.05	7.1 to 14.3
Maatanen	MS	(Laboratory)	Urea ice	0.1	7.5 to 24
Singh	MS	(Laboratory)	EG/AD/S ice	0.06	17.6

As is known, the definition of ice structure interaction regime is based upon the frequency of external ice excitation and the natural frequency of structure. When the ice loads entered into frequency locked in regime, resonance could occur due to the external ice loads approaching eigen frequency of structure. But eigen frequency could vary for different structures, which is related to structure dimensions and material properties. Also, for the same structure with different foundation properties and water depths, the structure stiffness will also change.

The influence of structure diameter scaling effect was analyzed by Andrew (2010) by summarizing data measurements from different researchers. Structures of various diameters and first natural frequency are compared and listed in Table 4-3. The large difference of natural frequencies for different structure diameters is very obvious.

On the other hand, investigation reveals that the regime for locked in type of vibrations is not just related to ice velocity but also strongly depends ice thickness, which means the ratio between ice thickness and structure diameter is also worthy of testing. Thus, theoretically it is difficult to predict the boundaries for ice crushing modes.

According to the simulation results, the frequency lock in phenomenon can be expected for ice speed around 0.13 m/s for the monopile structure fixed at sea bottom with diameter 6 m and water depth 20 m.

Chapter 5
Comparison of M-B model and Spectral Model

In Chapter 3 and Chapter 4, spectral model and Määttänen-Blenkarn model are deployed for ice induced vibrations simulation on an OWT monopile structure.

As is introduced above, the two models are based on different approaches to formulate ice loads. For spectral model, ice loading time series are generated based on empirical spectrum derived from field measurements directly, without considering the influence of different ice properties and structure feedback effect. While, in Määttänen-Blenkarn model, the ice force will be calculated at each time step based on structure response at previous time step and instant ice properties.

Therefore, it is understandable that different ice crushing modes can be captured by Määttänen-Blenkarn model but not for spectral model. The ice–structure interaction process is described in detail by Määttänen-Blenkarn model and differences in structure response for different ice velocities can be observed. And the simulation results of spectral model might share similar characteristics.

5.1 Ice loads

The maximum ice forces for different ice speeds are collected from both models and listed in Table 5-1. Discrepancies can be observed in the maximum value of ice loads between two models. The ice force of spectral model is much larger than that of Määttänen-Blenkarn model and little variation over ice speed can be observed for spectral model. These phenomena can be ascribed to several reasons.

Table 5-1 Comparison of max ice force for M-B model and Spectral model

Ice speed (m/s)	max ice crushing force (MN)	
	M-B model	Spectral model
0.04	14.42	66.68
0.13	18.30	67.67
0.2	21.93	63.59
0.3	19.93	68.54

First, the different mechanisms used by two models might lead to the deviation of simulation results. Time varying ice loads were applied for both simulation models, but the formulations of input ice loads are based on different methods. For spectral model, ice loads consist of mean ice load calculated manually through empirical formulas and the time varying component is generated from spectrum. Thus, the applied ice loading time series from spectral model has prescribed values. While, for Määttänen–Blenkarn model, there will be iteration on ice loads calculation on each time step. The ice load exerted on structure at next time step is determined by output from previous time step. In this way, instantaneous loads and responses can be expected in Määttänen-Blenkarn model.

As is analyzed in previous chapters, regional limitations might induce the gap between the results of two models. The mean ice stress for Bohai Sea is about 6.8 MPa as is calculated from GL Guideline. But as is shown in Figure 4-2, the max ice crushing strength might just be 3 MPa, which is for stress rate 0.3 MPa/s. In view of higher ice speed, which could be located in the constant ice crushing strength regime with stress rate higher than 1.3 MPa/s, the corresponding ice crushing strength will reach a constant value 1 MPa, which is much lower than the mean crushing stress for Bohai Sea 6.9 MPa. Noting that the valid ice speed range for spectral model lies in 0.04m/s to 0.35 m/s, among which high ice speeds are included which might lead to ice brittle crushing mode with relatively low ice crushing strength. In this situation, the difference of mean ice force between two models could be even larger.

In conclusion, Määttänen-Blenkarn model is process based model, which considers ice-structure interaction process. Various ice crushing modes can be observed under Määttänen-Blenkarn model. But not for spectral model, similar response pattern for various ice speeds can be

observed from spectral model simulations, which is mainly continuous ice crushing mode for high ice speed.

5.2 Structure response

After comparing statistical results from 2 models in Table 3-1 and Table 4-2 , it can be concluded that the structure response of spectral model is much larger then response of M-B model. For structure displacement, larger standard deviation can be observed for spectral model and the maximum structure displacement is almost 4 times that of M-B model. Little difference in displacement can be found for different ice speeds in spectral model, except for slight increase in fluctuation amplitude. But for Määttänen-Blenkarn model, structure response is rather sensitive to ice speeds and largest structural response can be expected at ice speed 0.13 m/s. The large displacement for spectral model compared with M-B model might be a direct result of large ice loads. As is discussed in previous session, mean ice crushing strength of spectral model is much larger than maximum ice crushing strength of Määttänen-Blenkarn model due to regional ice properties.

As is indicated in 4.3.2 Displacement time series for different ice velocitiesthe results of Määttänen-Blenkarn model clearly illustrate the different structure response properties for different ice speeds, like quasi-static structure response, steady state structure response and frequency lock in phenomenon, which results from stress rate dependent ice crushing strength. Instead of investigating the ice–structure interaction, spectral model just deploys a prescribed ice load time series and constant mean ice load. Therefore, it is impossible to discover ice-structure interaction process in spectral model because the structure feedback influence on ice loads is not considered. Thus, the structure displacement time signals from spectral model in 3.7.2 share similar characteristics for different ice speeds.

5.3 Spectrums

In order to further analyze differences of structure response in frequency domain, response spectrums for structure displacement under different ice velocities are compared in Figure 5-1.

In accordance with previous discussions, for lower ice speeds, the structure tends to be excited at lower eign frequencies and the peak of response spectrum locates at low frequency range. For

higher ice velocities the peak of spectrum will shift to high frequency ranges due to the high frequency ice loading.

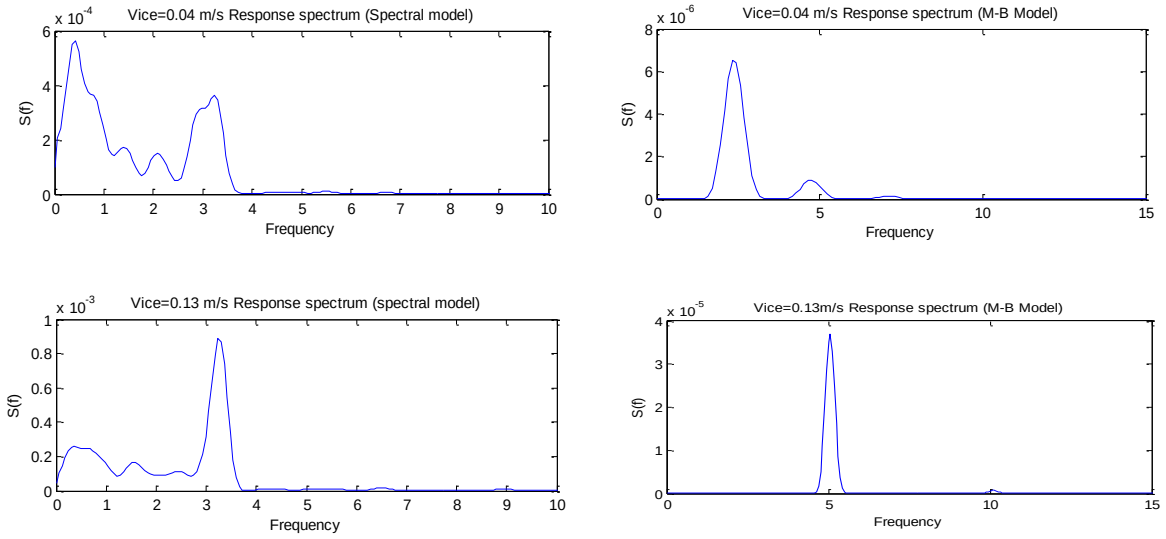

Figure 5-1 Response spectrum of spectral model (left) and M-B model (right)

As is summarized above, the results from M-B model illustrates different structure vibration mode but response spectrums for spectral model seem to have similar characteristics. This can be explained by the shape of response spectrums.

Comparing the response spectrum of different ice speeds, it could be found that for M-B model the energy is mainly focused at the peak of spectrum accompanied by some small secondary peaks. It is these secondary peaks that define structure vibration modes. For Vice =0.13 m/s , the peak frequency has absolute dominating effect that the secondary peaks are small enough to be neglected, this explains why the structure response time signals for frequency lock in vibration is rather regular.

For spectral model, energy contributions from low frequency regime can be observed. Due to the existence of these low frequency components, the irregular structure response pattern seems to be the same for all ice speeds which is believed to be within continuous ice brittle crushing regime.

Ice force spectrums of both models for ice speed 0.04 m/s and 0.13 m/s are shown in Figure 5-2. For M-B model, the load spectrums have similar shape with structure response spectrums.

Primary peaks have dominating effects and some secondary peaks can be seen. Response spectrum also shows that the structure vibrates at corresponding peak frequencies.

Different from M-B model, energy distribution covers the whole low frequency regime in force spectrums of spectral model. Main difference for different ice velocities lies in low frequency regime from 0 to 2.5 Hz. The shape of load spectrum is quite different from that of response spectrum for spectral model. A comparison of force and response spectrum shows that structure is excited at 3.3 Hz and lower eigen frequencies.

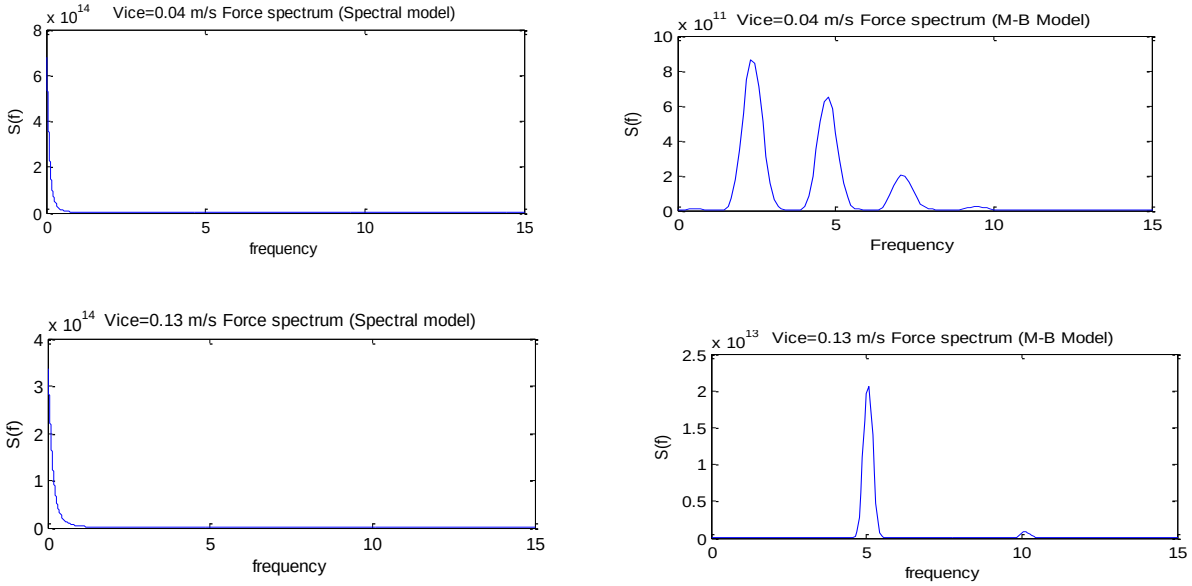

Figure 5-2 Structural force spectrums for spectral model (left) and M-B model (right)

Ice force spectrums are shown in Figure 5-2. For M-B model, the spectrums for structure reaction force have similar characteristics with structure response. Primary peaks have dominating effects and some secondary peaks can be seen from spectrums. As with force spectrums of spectral model, main difference for different ice velocities lies in low frequency regime from 0 to 2.5 Hz. Load spectrum shape is quite different from that of response spectrum for spectral model. A comparison of force and response spectrum shows that structure will be excited at 3.3 Hz and lower eigen frequencies.

Chapter 6

Discussion on ice models

Based on the results in Chapter 3 & 4 and the analysis in Chapter 5, a brief conclusion for both models is given in 6.1. The limitations and drawbacks of existing model are summarized in 6.2. Finally, some further discussions and potential improvements on current models are offered in 6.3.

6.1 Conclusions

In current thesis work, the theory of spectral model is studied and implemented on OWT monopile structure through FEDEM. Time domain simulations are performed for different ice velocities. Simulation results are analyzed and compared in detail. The sensitivity of existing spectral model to different ice velocities is discussed in 3.7 and the limitations and drawbacks of spectral model are summarized in 3.6 Limitations.

As is concluded in Chapter 3, the spectral model is based upon infield measurements and mainly feasible for high ice speeds in brittle crushing regime. The simulation results illustrate that structure response is not very sensitive to ice speeds. For ice speeds ranging from 0.04 m/s to 0.35 m/s, the structure will always be excited at 3.3 Hz and lower eigen frequencies. The differences of ice load spectrum for various ice speeds can be observed in low frequency region especial when frequency smaller than 0.25 Hz. It is notable that compared with other large size offshore structures, OWT monopile structure has relatively small natural frequency and the example structure used in this thesis has the first eigen frequency of 0.32 Hz. For structures with

even smaller eign frequency, the influence of changing shape of ice spectrum could be more significant and large changes on structure response can be expected.

Considering that the spectral model is established from measurements directly without analyzing the details of ice-structure interaction process, process- based Määttänen-Blenkarn Model is also applied on the same OWT monopile structure in Chapter 4 and the results of two models are compared and the validity of two models are discussed in Chapter 5.

The simulation results of Määttänen-Blenkarn model show that the structure response is highly sensitive to changing ice speeds due to the stress rate dependent ice crushing strength. Structure vibrations will have different characteristics under different ice speeds and self-excited phenomenon can be observed due to the added negative damping. For low ice speeds smaller than 0.02 m/s quasi-static structure response can be discovered. Steady state vibrations can be found for higher ice velocities, structure could be excited at higher frequencies. The maximum oscillation amplitude occurs around ice speed 0.13 m/s and the effect of ice force is magnified by the dynamics of structure, which is defined as frequency lock in phenomenon.

Compared with the results of Määttänen-Blenkarn model and spectral model, it is obvious that the structure response of M-B model is more complex and characteristics for different ice failure modes can be distinguished from each other. The responses of spectral model with different ice speeds seem to share similar characteristics.

After investigating the response spectrum of two models, some differences could be found in the response spectrums of two models. Differences lie in the energy distribution over frequency ranges and location of spectrum peaks. According to the analysis in 4.4.3 it is the location and value of these peaks that define structure vibration modes. Thus, theoretically it is possible to calibrate spectral model through the results of M-B model to enable spectral model to simulate low to intermediate ice velocities.

It is worth mentioning that the thesis focuses on OWT monopile structure with relatively low natural frequency. It is assumed that for frequency components larger than 2.5 Hz, the influence on structure response can be really small that could be ignored. Resonance between structure first eigen frequency and ice loads is expected to happen at low ice speed with low loading frequency. But according to ice mechanical property, low ice speed means low ice crushing

strength and the ice load could be rather small. Together with slow ice loading process, the structure response is almost quasi-static.

6.2 Limitations

The limitations of both models are analyzed in detail in Chapter 3 & 4 separately.

Regional limitation is one of the common problems for both models. The ice properties can be quite different in different regions. Määttänen-Blenkarn model is mainly based on the measurements from Cook Inlet and spectral model from Bohai Bay. The different sources of data define the difficulty to compare simulation results quantitatively. The mean ice crushing strength in Bohai Bay is calculated to be 6.9 MPa and the maximum ice crushing strength in stress rate-strain curve is 3 MPa. The large gap between the ice loads values is supposed to be under expectation.

Scaling effect and structure types might also induce discrepancies between the results of models. The empirical equations of spectral model are generated from a small monopod structure in Bohai Bay with diameter round 1.6m, which is smaller than the diameter of the example monopile structure. The structure and ice might not fully contact each other and the ice force itself has scaling effect that the ice force tends to get smaller for larger structure. On the other hand, the natural frequency of structure might also change for structures with different sizes and types. Seeing that for M-B model ice-structure interaction process is very sensitive to structure eigen frequencies, inconsistencies of results could happen if not considering structure type and size effect.

A comparison of spectral model and M-B model reveals that without considering the feedback mechanism of structure response, the spectral model cannot simulate distinguished structure vibration modes. Because in spectral model, prescribed ice load time series generated from ice spectrum is applied directly and structure response is not able to be considered in the ice force at next time step.

For Määttänen-Blenkarn model, it is found that the definition of parameters has direct influence on behavior of structure vibrations. The boundary of various structure oscillation modes will shift when the values of these parameters change. The changing ice crushing strength is very

sensitive to stress rate calculation. More investigation should be made when determining the values of stress rate parameters.

6.3 Further discussions

6.3.1 Spectral models for low& intermediate ice speeds

In this thesis, response spectrums for spectral model and M-B model are compared and analyzed in detail. Results show that spectral model is only valid for high ice velocities in ice brittle crushing regime. M-B model is feasible for different ice velocity ranges and can simulated different ice crushing modes. It is the location of the secondary peaks and the peak values for load spectrum that defines different structure oscillation modes.

In order to apply spectral model in low & intermediate ice speeds, it is necessary to make modifications on existing spectral model. It is possible to make a collection of spectrums from M-B model of different ice speeds and summarize the distribution pattern of these secondary peaks. By applying curve-fitting tools, it might be possible to generalize empirical formula to calculate spectrum for ice loads in ductile and ductile-brittle transient regime.

In this way, the structure response of spectral model could resemble that of M-B model. But it is notable that the applied ice loads are still prescribed ice force time series and still no ice-structure interaction process is modeled. Another problem is also introduced that the new spectral model cannot be justified on a second structure as the structure properties get involved in empirical spectrum formulation from M-B model.

But considering that for OWT monopile structures, the influence of structure properties could be small or the influences are predictable. It would be very promising to investigate the influence of structure properties on response spectrum in M-B model like structure diameter, height and natural frequency.

6.3.2 Ice thickness and aspect ratio

This thesis work emphasizes the influence of ice velocities on dynamic ice loads and structure response only and the influence of ice thickness on ice force are not considered assuming constant ice thickness 0.5 m in both models.

A key reason for this simplification is that the ice forces are measured as point load on individual panels in spectral model and there is no detail information on the stress distribution over ice thickness. Also, ice loads are modeled as point load working on monopile, thus, constant stress distribution over ice cross section is assumed and summed up directly.

As is emphasized, the ice scaling effect will have large influence on ice failure behavior and ice crushing loads and structure response will be influenced consequently. It is possible that the ice thickness and aspect ratio will influence the secondary peaks in the load spectrums of M-B model and also the structure vibration mode.

6.3.3 Coupling with environmental loads and soil properties

It has been introduce in 1.1.5 Simulation tools for OWT coupled simulation tools are used for structure model building. In order to simplify the situation and focus on ice loading effect, all the current simulations are applied on stand still turbines, which means no wind loads and hydro loads are considered at this moment. It will be meaningful to check the joint influence of all the environmental loads on operating turbines. In Chapter 7, the coupling effect of wind loads and ice loads will be investigated.

Apart from this, the soil properties which could have large influence on structure natural frequency should also be considered. In existing model, the turbine is assumed to be fixed on the sea bottom.

Due to the complex operating condition of OWT structure in temperate and arctic area, a comprehensive ice-wind- hydro-structure-soil interaction numerical model could be established to investigate the structure operating behavior in the future.

6.3.4 Application on jacket support structure

It is notable that the current study is only valid for monopile substructure with rather large diameter and low natural frequency. When it comes to jacket support structure, the situation tend to be more complex.

For jacket structure the contact area for ice loading could be much smaller and the total ice force might also be smaller with constant ice crushing strength. Seeing that jacket structure is multi-leg structure, ice sheet might contact one leg first and then contact the legs left. The whole process

might depend on ice speed, distance between legs and the direction of ice movement which defines phase difference of ice loads on different legs. The interaction of ice action on different legs is in need of deep discussion.

On the other hand, the natural frequency of jacket structure could be more than 1.2 Hz, larger than that of monopile structure. As is known from M-B model, structure response modes are determined by ice-structure interaction in which ice velocity and structure natural frequency are key parameters. The natural frequency of monopile structure is rather low and resonance at first eigen frequency could only happen when ice speed is very low with low loading frequency. But ice loading value for low ice speeds is too small that the resonance at first eign frequency cannot be seen at all. For jacket structure with larger natural frequency, resonance between intermediate ice velocity with larger ice loads and first eigen frequency could happen. Thus, more serious structure vibrations could be expected for an OWT jacket structure.

Chapter 7

Coupling model of wind and ice

In order to investigate the joint influence of ice and other environmental loads, time domain simulations on coupling model are performed. In order to consider the structure feedback effect, Määttänen-Blenkarn model will be deployed for the coupling mode. Considering that the Määttänen -Blenkarn model is mainly for ice covered calm water surface, there might be almost no wave loads. And compared with dominating wind loads for wind turbines, the current loads could be relatively small. Thus, for simplicity this thesis work will focus on the coupling effect of wind force and ice loads only.

Based on previous conclusions, the worst ice loading effect can be observed on Määttänen-Blenkarn model with ice velocity 0.13 m/s which correspond to frequency lock in phenomenon. The joint effect of ice velocity 0.13 m/s and different wind speeds will be investigated and analyzed with priority and different ice velocities will be tested later.

The rated wind speed for NREL 5MW wind turbine is 11.4 m/s. In order to see the coupling effect of ice loads and various wind speeds, wind speeds 0 m/s, 6m/s, 10 m/s, 14 m/s and 18 m/s are chosen for simulation. In order to avoid initial effect and ensure the stable state has been reached with full ice-wind-structure interaction process covered, the total simulation time is set to 150 seconds.

7.1 OWT structure response to wind loads only

For the sake of comparison, simulations with OWT structure subject to wind loads only are run first. Structure responses for different wind speeds are given in Figure 7-1, it can be found in

structure response time series that for large wind speeds, the structure will have some oscillations in the beginning with structure displacement increasing to its peak. After the drop of the peak value, stable state can be reached and the displacement is getting constant over time. But for lower wind speed Vwind=6m/s, structure displacement will just steadily increase to a constant value after a transitional period.

A close look at turbine pitching action reveals that blades will start to pitch after the rotational speed of rotor increases to a fixed value. The pitching action leads to an increase of structure displacement which is especially obvious for larger wind speed. The displacement time signals also reveal that the peak displacement during transitional period varies a lot over wind velocities, but the variation for steady state displacement under different ice velocities is very small.

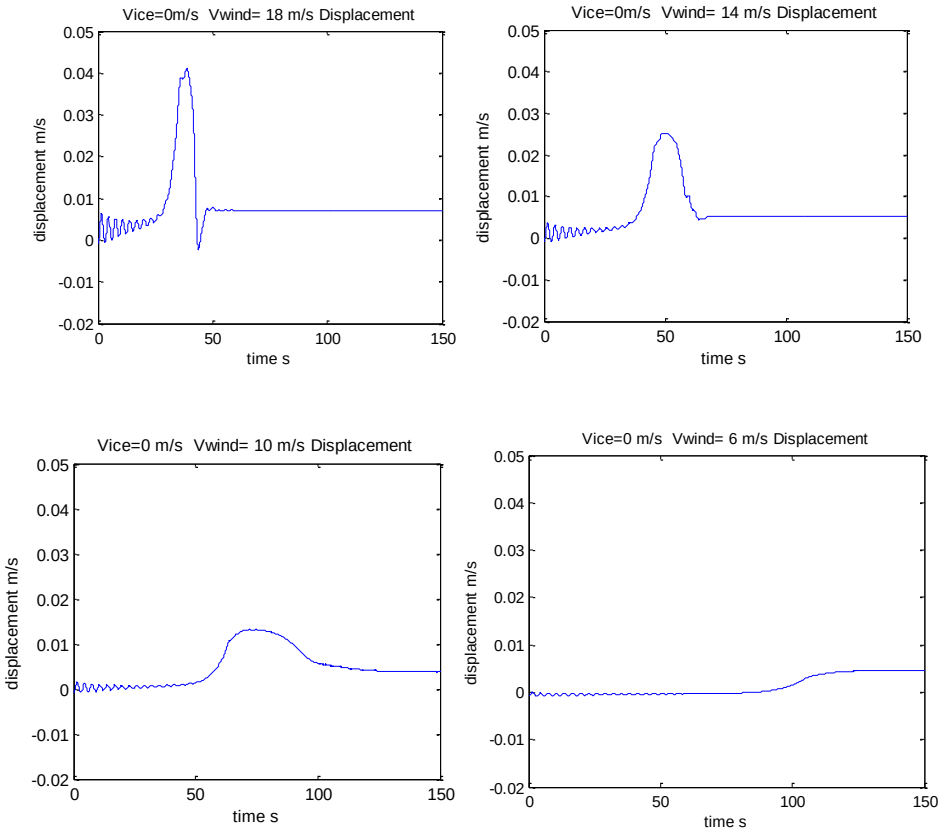

Figure 7-1 Structure response with various wind speeds and no ice

The structure responses for time domain simulation with different wind velocities are collected in Table 7-1. Significant values for structure responses and stresses are listed and compared. As can be seen from the results, it is easy to come to the conclusion that structure displacement will

increase as with growing wind speed and the time to reach peak value and stable state will be greatly shortened under large wind speeds.

Table 7-1 Structure response for wind loads only

Vice(m/s)	Vwind (m/s)	Spin up time (s)	Max displacement (m)	Steady state mean displacement (m)	Standard deviation
0	6	150	0.00463	0.00410	0.00078
	10	130	0.01316	0.00424	0.00057
	14	70	0.02512	0.00518	0.00001
	18	50	0.04109	0.00709	0.00001

7.2 Joint effect of wind and ice loads

As is mentioned above, frequency lock in phenomenon can be observed for ice speed 0.13 m/s under Määttänen-Blenkarn model which represents the most serious structure vibration condition. More attention is paid on the combination of ice loads of this speed and different wind loads under which largest damage and structure response is expected.

In Figure 7-2, structure displacement time series under ice velocity 0.13 m/s and different wind speeds are given. Compared with results in Figure 7-1, the values of displacement are much larger and more high frequency oscillations can be observed. The steady state displacement without ice loads is no more than 0.01 m and when ice loads considered the mean displacement for steady state grows up to more than 0.04m. It may well come to the conclusion that the ice loads have dominant influence in wind- ice- structure interaction.

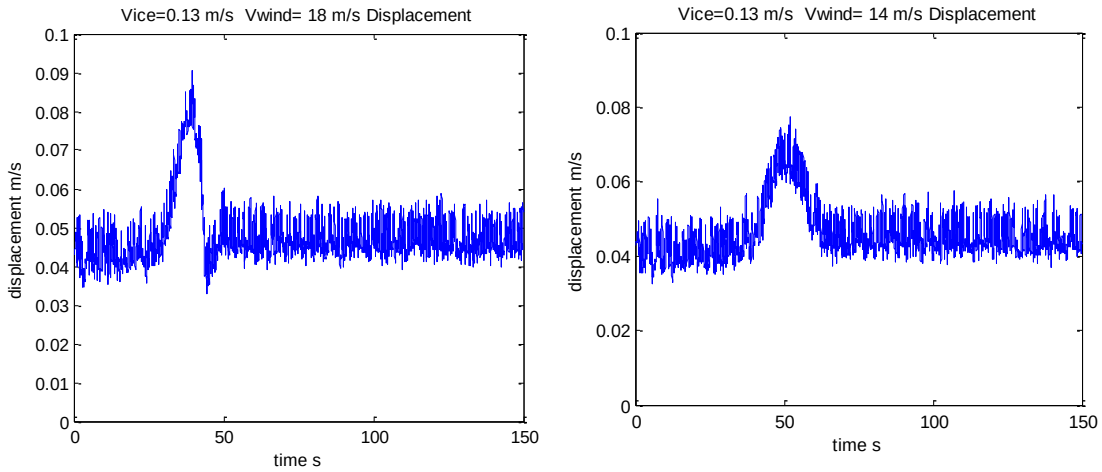

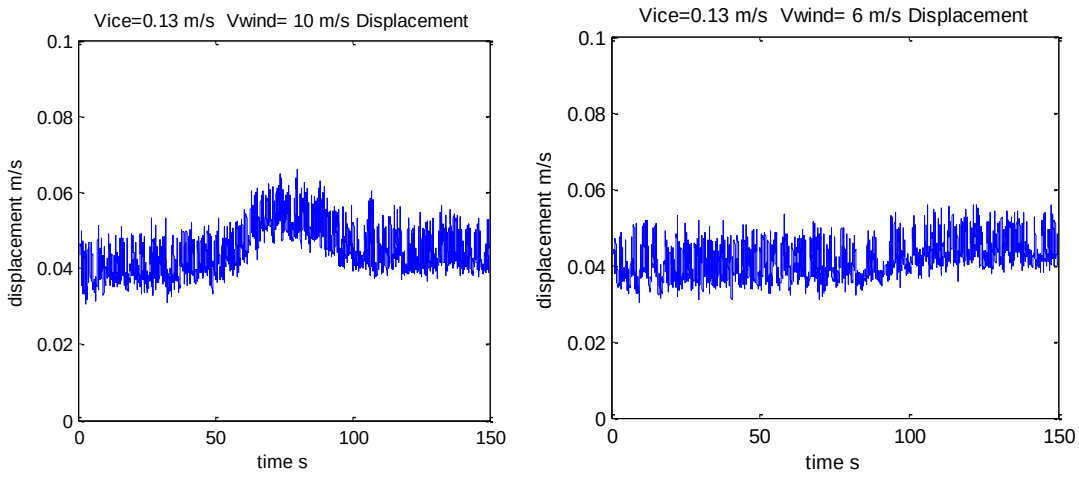

Figure 7-2 Structure response with ice velocity 0.13 m/s and different wind velocities

Information on structure response for ice velocity 0.13 m/s and different ice speeds are recorded in Table 7-2. The predominating effect of ice loads is obvious compared with structure responses without ice loads. Maximum structure displacement during pitching action and mean structure displacement at steady state have the tendency to increase with increasing wind speeds. It is notable that oscillations can be found during steady state due to ice loading and no oscillation can be observed for wind loads only. The results also show that the existence of ice loads does not have large influence on time consumed to reach steady states.

Table 7-2 Structure response for ice speed 0.13 m/s

Vice(m/s)	Vwind (m/s)	Spin up time (s)	Max displacement (m)	Steady stat mean displacement (m)	Standard deviation
0.13	6	150	0.05571	0.04440	0.00373
	10	130	0.06581	0.04398	0.00393
	14	70	0.07728	0.04474	0.00362
	18	50	0.09037	0.04702	0.00363

The time domain simulation results are collected for other ice speeds 0.08 m/s, 0.2 m/s and 0.3 m/s and listed in Appendix 4 . Table 7-3 shows that the magnitude of structure displacement will be larger for high ice speeds but the largest standard deviation of structure displacement will be at ice velocity 0.13 m/s. Thus, larger structure vibration can be expected for ice velocity 0.13 m/s which might be induced by frequency lock in effect. It is also confirmed that time needed to

reach steady state is only related to wind speed only and the influence of ice loads is so small that can be omitted.

Table 7-3 Structure response for ice speeds 0.08 m/s, 0.2 m/s and 0.3 m/s

Vice(m/s)	Vwind (m/s)	Spin up time (s)	Max displacement (m)	Steady stat mean displacement (m)	Standard deviation
0.08	6	150	0.04296	0.02937	0.00323
	10	130	0.04602	0.02900	0.00338
	14	70	0.05500	0.02980	0.00325
	18	50	0.07159	0.03129	0.00293
0.2	6	150	0.06335	0.05277	0.00349
	10	130	0.07029	0.05251	0.00352
	14	70	0.08147	0.05352	0.00362
	18	50	0.09598	0.05556	0.00357
0.3	6	150	0.06327	0.05803	0.00264
	10	130	0.07104	0.05738	0.00111
	14	70	0.08177	0.05832	0.00097
	18	50	0.09591	0.06026	0.00098

7.3 Conclusions

The results of wind–ice coupling model clearly illustrate that ice loads have dominating influence on structure response. This is due to the large ice loads compared with wind loads. The wind load for largest wind speed tested in the model 18m/s is around 0.5 MN, which is rather small compared with ice loads.

For low wind speeds, no pitching action will happen during the growth of rotor rotational speed. The structure displacement will increase gradually to a constant value. For large wind speeds, when rotor rotational speed increases to 12.1 rpm, the blades start to pitch and a displacement peak can be obtained. It is noticeable that because of the existence of ice force the peak for displacement will be increased. Especially for low wind speed, the structure response under wind load only could be rather small compared with that under joint wind and ice loads. The steady state displacement of wind and ice coupling model will have similar magnitude of response induced by ice only due to the dominating ice loads. It is worthy of mentioning that the joint

effect of wind and ice loads during blade pitching action will lead to large structure displacement.

7.4 Limitations

The model at this stage focused on the joint effect of wind and ice loads only. The simplicity of the model introduces some limitations.

7.4.1 Constant wind speed assumption

Constant wind speed assumption is made for simplicity and no turbulence is considered in this model. For offshore wind turbines, the influence of turbulence could be quite large especially during operation. The existing results show that maximum structure displacement could happen during blade pitching action. The introduction of turbulence will lead to even tougher situation. Thus, there will be very large inaccuracy induced by this constant wind speed assumption.

7.4.2 No current load considered

The influence of current is not considered either. It is notable that the influence of current could be smaller for jacket structure due to the small diameters but for monopile structure current loads could be larger which also depends on the location and water depth. It is assumed in this thesis that for water depth of 20 m the current loads are small compared with wind loads and current load has not been considered in the environmental loads coupling simulations by now.

Chapter 8

Fatigue analysis

In order to explore the importance of ice loads consideration during OWT monopile structure design, fatigue analysis will be performed to see the damage induced by ice loads. Considering that this thesis emphasizes OWT support structure design and ice loads work on support structure, the fatigue analysis will be performed on substructure only and the fatigue damage on blades will not be investigated at this stage.

Noticing that for ice infested area the wave loads are supposed to be rather small that could be ignored and the fatigue from wind loads only can also be neglected due to the constant steady state force, this chapter will focus on fatigue damage estimation for joint ice and wind loads and compare with fatigue induced by ice loads only to see the influence of joint wind and ice loading effect.

8.1 Fatigue calculation in time domain

There are currently two methods for fatigue load estimation. One is conventional time domain methods based on Miner's rule and the other one is Dirlik's spectral method. The fatigue calculation in this work is based on the time domain method.

8.1.1 Miner's Rule

It is assumed that each cycle of constant stress range amplitude causes a particular amount of damage *S*, and that damage increases linearly with the number of stress cycles applied *N* until it reaches a prescribed failure level. The damage induced in any single cycle is proportional to the stress range amplitude to the power of *m*, where *m* is a material parameter. (Ragan & Manuel,

2007) A second material parameter K represents the damage level the material can withstand before failure. The relation between failure level and number of cycles at failure can be expressed as

$$N_F S^m = K \qquad \textit{Equation 8.1}$$

By putting Equation 8.1 into log-log plot, linear S-N curve can be obtained and the equation can be rewritten as

$$\log S = (\log K - \log N_F)/m \qquad \textit{Equation 8.2}$$

For a random number of cycles *N* and stress range *S* the resulting damage level *D* can be expressed as

$$D = \frac{NS^m}{K} \qquad \textit{Equation 8.3}$$

Where the damage level *D* is a number between 0 and 1 and failure is reached when D=1.

8.1.2 Rainflow counting for variable stress cycle amplitudes

Rainflow cycle-counting algorithm is deployed to count variable, amplitude stress cycles. The numbers of cycles for various stress ranges will be rainflow counted and it is assumed that the damage level caused by these stress ranges can be superimposed upon one another linearly. After obtaining stress range S_i and the number of cycles *N* from the Rainflow-Counting Algorithm, the total damage can be obtained from Miner's sum

$$\mathrm{D} = \frac{\sum_{i=1}^{N} S_i^m}{K} \qquad \textit{Equation 8.4}$$

8.1.3 Equivalent fatigue load

Equivalent fatigue load (EFL) is also defined as damage equivalent load (DEL). (Freebury & Musial, 2000)As is indicated in the name, it is a constant amplitude stress range which can induce the same amount damage after the same number of cycles of the original varying amplitude stress time series. The damage equivalent load can be expressed as

$$EFL = (\sum_{i=1}^{N} \frac{S^m}{N})^{1/m} \quad \textit{Equation 8.5}$$

Using the concept of damage equivalent load, the total damage level can be modified to be

$$\mathrm{D} = \frac{N(EFL)^m}{K} \quad \textit{Equation 8.6}$$

For convenience for comparison, 1000-cycle equivalent fatigue load EFL_{1000} will be used to normalize the damage level

$$\mathrm{EFL}_{1000} = (\frac{DK}{1000})^{1/m} \quad \textit{Equation 8.7}$$

8.1.4 Total stress calculation

The stress used for fatigue analysis is a superposition of normal stress induced by axial force and normal stress induced by bending moment.

Normal stress component σ_{Nn} contributed by axial force F_N can be calculated by

$$\sigma_{Nn} = \frac{F_N}{A} = \frac{F_N}{\pi D t} \quad \textit{Equation 8.8}$$

The moment *M* induced normal stress σ_{Mn} can be obtained through formula

$$\sigma_{Mn} = \frac{M}{I} = \frac{M}{\frac{\pi}{64}(D^4 - d^4)} \quad \textit{Equation 8.9}$$

A direct summation of two stress components will lead to total normal stress to be used for fatigue analysis. Considering that the ice loads act on monopile at waterline and the maximum bending moment locates at sea bottom, the total stress at mudline is expected to have the largest value and fatigue analysis will also be based on the data from this point.

8.2 Fatigue analysis on OWT monopile structure

As is emphasized above, this thesis aims at estimating the significance of ice loads on OWT support structure design. Time domain simulations of 630 seconds with time step 0.01 s will be run. The extra 30 seconds are used to avoid initial effects. Seeing that ice acts on substructure and largest total stress is expected to be at mudline, time signals for axial force and bending moment at sea bottom will be collected.

Post processing for total stress calculation, rainflow counting and fatigue damage level calculation will be done through Matlab.

Slightly different from the theoretical formulas introduced above, based on the empirical formula provided in DNV guideline, the characteristic S-N curve is taken as

$$log_{10}^{N} = log_{10}^{a} - m * log_{10}(\Delta\sigma \left(\frac{t}{t_{ref}}\right)^{k}) \qquad \textit{Equation 8.10}$$

Parameters recommended in DNV-OS-J101 will be adopted. Intercept of logN axis is taken as $log_{10}^{a} = 11.764$ and negative slope of S-N curve is m=3. t_{ref} is defined as reference thickness which is $25mm$ and k =0.2 is thickness exponent. (DNV, 2010)

After rainflow counting for each stress range $\Delta\sigma$ is processed and cumulative fatigue damage is calculated by Miner's sum

$$D_c = \sum_{i=1}^{I} \frac{n_i}{N_i}$$

8.3 Results

8.3.1 Fatigue damage induced by ice loads only

Without considering wind loads, time domain simulations for ice speed 0.08 m/s, 0.13 m/s, 0.2 m/s and 0.3 m/s are run for 630 seconds. The time results for the first 30 seconds are cut to avoid initial effect.

After fatigue calculation based on simulation results for 10 min, the damage level caused by ice loads are listed in Table 8-1. For larger ice speed, values of stresses could be larger but stress

ranges might not be as large as those of intermediate ice speeds. Seeing that the damage is determined by magnitude of stress fluctuation and number of cycles, it is understandable that for intermediate ice speeds with large stress fluctuations might have larger fatigue damage.

Table 8-1 Fatigue damage by ice loads

Vice(m/s)	Standard deviation of stress	Maximum stress (MPa)	Mean stress (Mpa)	EFL_{1000}(MPa)	Damage level
0.08	0.2566	2.7101	1.5454	0.516926	1.51E-10
0.13	0.3319	3.4173	2.5374	0.444292	2.38E-10
0.2	0.3574	3.9705	3.0022	0.418491	1.26E-10
0.3	0.1004	3.8848	3.3669	0.110603	2.33E-12

8.3.2 Fatigue damage induced by wind loads only

In order to have a better view of dominating influence of ice loads, fatigue analysis for structure under wind speeds 6 m/s, 10 m/s ,14 m/s and 18 m/s is provided. Damages of 600 seconds wind loads are shown in Table 8-2.

Table 8-2 Fatigue damage by wind loads

Vwind(m/s)	Standard deviation of stress	Maximum stress (MPa)	Mean stress (Mpa)	EFL_{1000}(MPa)	Damage level
6	0.00500	0.05130	0.04450	0.002547	2.85E-17
10	0.00530	0.13030	0.04800	0.004289	1.36E-16
14	0.00074	0.27060	0.05620	0.014668	5.43E-15
18	0.00150	0.54310	0.07850	0.028854	4.14E-14

Apparently, the wind loads are rather small compared with ice loads. The largest stress induced by wind force under wind speed 18 m/s is just around 0.5 MPa. The fatigue damages are so small because of the constant wind speed with no turbulence assumption that the stress will rise to a constant value with little stress range and fatigue damage.

8.3.3 Fatigue damage under joint ice and wind loads

Combining wind and ice action, the coupling effect of ice and wind loads are investigated. The damage caused by ice speeds 0.08 m/s, 0.13 m/s ,0.2 m/s and 0.3 m/s combining wind speeds 6 m/s ,10 m/s ,14 m/s and 18 m/s are tested separately.

As can be seen from Table 8-3, the joint effect of wind and lower ice speeds might have larger damage. For high ice and wind speeds, the damage could be very small.

This is understandable that when both ice speed and wind speed are high, the spin up time could be very short and structure response would quickly reach a constant value and enter into steady state. The Määttänen-Blenkarn model used for ice loads considers structure response induced by both ice loads and wind loads. Large structure reaction force could be expected for low to intermediate ice speeds within the Määttänen-Blenkarn model sensitive domain. For Vice=0.13 m/s, frequency lock in phenomenon could happen which explains the large stress range and fatigue damage.

Table 8-3 Fatigue damage for joint ice and wind effect

Vice(m/s)	Vwind(m/s)	Standard deviation of stress	Maximum stress (MPa)	Mean stress (Mpa)	EFL_{1000}(MPa)	Damage level
0.08	6	0.25600	2.77960	1.58910	0.444292	1.51E-10
	10	0.25780	2.9781	1.5876	0.419726	1.27E-10
	14	0.25600	2.86840	1.59320	0.444488	1.51E-10
	18	0.25790	2.83010	1.61400	0.43856	1.45E-10
0.13	6	0.33190	3.41730	2.53740	0.518025	2.39E-10
	10	0.33620	3.47290	2.53270	0.518947	2.41E-10
	14	0.33090	3.49080	2.52760	0.516142	2.37E-10
	18	0.33580	3.68830	2.56100	0.521991	2.45E-10
0.2	6	0.34310	3.93980	3.07080	0.398006	1.09E-10
	10	0.34070	3.91580	3.06150	0.401747	1.12E-10
	14	0.34050	4.06030	3.07690	0.385845	9.89E-11
	18	0.34570	4.15150	3.10100	0.396078	1.07E-10
0.3	6	0.14570	3.85100	3.39870	0.120758	3.03E-12
	10	0.10040	3.88480	3.36690	0.110603	2.33E-12
	14	0.10080	3.80490	3.38090	0.098748	1.66E-12
	18	0.10270	3.97620	3.40090	0.100409	1.74E-12

8.4 Conclusions

In this chapter, the fatigue damage effect of ice loads, wind loads and joint ice and wind loads on OWT monopile structure are investigated. Results illustrate that the fatigue damage resulting from ice loads are much larger than that induced by wind loads due to the large ice load magnitude and oscillation.

The existence of wind will add to the structure damaged caused by ice loads. The M-B model deployed considers ice-structure interaction and the wind force will contribute to larger structure displacement. Thus, the ice loads could be amplified under wind-ice coupling model. Especially

in ductile-brittle transient regime with intermediate ice speed, where resonance frequency lock in phenomenon could happen, larger stress range and fatigue damage could be expected.

It is worthy of mentioning that the value of ice loads might change for different regions and the dominance of ice loads could also change for areas with lighter ice problems. Also, existing analysis is for monopile structure only with rather large diameter. For jacket structure with small ice-structure contact area the dominance of ice loads will be open to doubt.

Also, current loads and wind turbulence are not considered in existing fatigue analysis which are believed to have influence on simulation results. Especially for wind turbulence, more stress variation could be detect if turbulence can be applied and more fatigue damage can be expected.

Chapter 9

Discussions about ice loads on OWT

9.1 Summary

In this thesis work, OC3 based OWT monopile structure model was built on FEDEM first. Empirical data based spectral model for ice loads analysis was studied and applied. In order to assess the performance of existing spectral model, Määttänen-Blenkarn model was also investigated and used on the same structure. The results of two models are compared in detail and shortcomings and possible improvements of two models are analyzed. The results show that Määttänen-Blenkarn model will offer a more accurate simulation results by considering structure feedback mechanism.

After the analysis of two models, the coupling effect of joint wind and wave loads were studied. Structure responses for ice loads only, wind only and ice-wind coupling model are compared and the influence of ice loads on structure response was analyzed. It was concluded that the ice loads will have dominating effect on structure response due to the large load value and structure displacement will be amplified under joint wind-ice load especially during blade pitching action. Fatigue analysis was also performed for 10 minutes time domain simulation results. Large stress values could be expected for combination of large wind and ice speeds but largest stress range and fatigue damage locates at intermediate speeds around 0.13 m/s.

9.2 Recommendations on OWT structure design

The simulation results based on the simplified model demonstrate that ice loads will have very large influence on structure response and structure damage compared with wind loads. Thus, for offshore wind turbine design in ice infested area, it is necessary to consider the effect of ice loads.

But it is notable that the current study is only valid for monopile substructure with rather large diameter and low natural frequency. The resonance between low ice velocities and structure first eigen frequency is difficult to capture, because the ice crushing strength for low ice velocity is rather small and the slow ice loading process makes structure response quasi-static. For jacket structure, the natural frequency is larger than monopile structure and resonance between structure first eigen frequency and intermediate ice velocity is expected under which larger vibration could happen. But it is also notable that the contact area for ice load could be much smaller and phase lag exists for ice loading on different legs. Thus, it is difficult to predict the ice induced vibrations of jacket structure.

The current ice models used are from Bohai Bay (Spectral model) and Cook Inlet (M-B model). The differences of ice loads obtained from two models are quite obvious due to the different ice properties of two regions. It is reasonable that for some temperate areas ice loads could be much lower and the influence of ice loads could also be smaller.

For the simulation of ice-structure interaction, Määttänen-Blenkarn model seems to give more accurate results through considering structure feedback mechanism. More attention should be paid to the definition of parameters on stress rate –crushing strength curve, because the slope will determine negative damping value which will have very large influence on structure response. Theoretically, if the turning points on stress rate- crushing strength curve could be calibrated by local ice loads data, Määttänen-Blenkarn model should be applicable to all ice velocity ranges and everywhere.

The existing spectral model is obtained from in field measurement data and is only valid for high ice velocities. The ice loads generated by load spectrum directly and prescribed ice loads are applied on structure directly with no structure feedback effect considered. Considering that for low to intermediate ice velocities, the structure response will have influence on ice failure

strength. Thus, the existing spectral model is not feasible for low to intermediate ice velocities. A possible method to extend the valid velocity range of spectral model is to use the results from M-B model to formulate load spectrum for spectral model in low to intermediate ice velocity range. But structure properties are involved in the M-B load spectrum formulation which make the obtained ice load spectrum cannot be used on a second structure. Therefore, even though the spectral model is rather simple and straight forward to apply, all these limitations define the difficulty in validation of spectral model for all ice speed ranges in practice.

Bibliography

Andrew Palmera, Y. Q. (2010). Ice-induced vibrations and scaling. *Cold Regions Science and Technology*, 189–192.

Bendat, J. S. (2000). Random Data Analysis and Measurement Procedures. *Wiley, New York.*

Blenkarn, K. A. (1970). Measurement and Analysis of Ice Forces on Cook Inlet Structures. *Second Annual Offshore Technology Conference*.

DNV. (2010). OFFSHORE STANDARD DNV-OS-J101:DESIGN OF OFFSHORE WIND TURBINE STRUCTURES.

Engelbrektson, A. (1977). Dynamic ice loads on lighthouse structures. *Proc. 4th Int. Conf. on Port and Ocean Eng. under Arctic Conditions, St. John's, Canada, vol. 2 (1977)*, pp. 654–864.

Eranti, E. (1992). Dynamic Ice Structure Interaction—Theory and Applications. *VTT Publication 90, Technical Research Centre of Finland, Espoo, Finland*.

Freebury, & Musial. (2000). *Determining Equivalent Damage Loading for Full-Scale Wind Turbine Blade Fatigue Tests.*

GL. (2005). *Guideline for the Construction of Fixed Offshore Installations in Ice Infested Waters.*

H.R.Peyton. (1968). Sea ice forces .Ice pressures against structures. *H.R. Peyton, 19 Technical Memorandum, 92 National Research Council of Canada, Ottawa, Canada*, pp.117–123.

International Organization of Standarisation. (2010). *ISO19906: Petroleum and natural gas industries – Arctic offshore structures.*

J. Jonkman, S. B. (February 2009). Definition of a 5-MW Reference Wind Turbine for Offshore System Development.

Jochmann, P. a. (2001). Ice Force Measurements at Lighthouse Norströmsgrund—Winter 2000. *Hamburgische Schiffbau-Versuchsanstalt, Hamburg, LOLEIF Rep. No. 9. Contract No MAS3-CT-97-0098*.

Kärnä T., Q. Y. (2007). A Spectral Model for Forces Due to Ice Crushing. *Transactions of the ASME*, Vol. 129.

Kärnä T., T. R. (1990). A straightforward technique for analysing structural response to dynamic ice action. *OMAE'90. Proc. 9th Int. Conf Offshore Mechanics and Arctic Engineering*, 135-142.

Kärnä, T. (1992). A Procedure for Dynamic Soil-Structure-Ice Interaction. *Proceedings 2nd International Offshore Polar Engineering Conference, San Francisco, June 14–19, Vol. 2*, pp. 769–771.

Kärnä, T. a. (1989). Dynamic Response of Narrow Structures to Ice Crushing. *Cold Regions Sci. Technol., 17*, pp. 173–187.

Kärnä, T. a. (2004). A spectral model for dynamic ice actions. *EU FP5 EESD project No EVG1-CT-2002-00024: Measurements on Structures in Ice (STRICE).*

Kärnä, T. K. (1999). A Numerical Model for Dynamic Ice-Structure Interaction. *Comput. Struct., 72*, pp. 645–658.

Kärnä, T. Q. (2006). A Model of the Global Ice Force on Vertical Structures. *Proceedings 18th International Symposium on Ice, Sapporo, Japan, August 28–September 1*, Vol. 3 .

Kolari, K. K. (2004). Ice Failure Analysis Using Strain-Softening Viscoplastic Material Mode. *Porceedings European Congress Compt. Meth. Appl. Sci. Eng., Jyvaskyla, Finland, 24–2*.

Lin, Y. K. (1967). Probabilistic Theory of Structural Dynamics. *McGraw–Hill, New York.*

Løset, S. (2006). *Actions from ice on arctic offshore and coastal structures.*

Määttänen, M. (1978). On conditions for the rise of self-excited ice induced autonomous oscillations in slender marine pile structures. *Ph.D., University of Oulo*.

Määttänen, M. (1998). *Numerical model for ice-induced vibration load lock-in and synchronization.* New York. 923-930.: 14th International Symposium on Ice.

Määttänen, M. R. (1977). Ice Structure Interaction Studied on a Lighthouse in the Gulf of Bothnia Using Response Spectrum and Power Spectral Density Function Analyse. *Proceedings 4th International Conference Port Ocean Engineering Arct. Cond., St.John's, Newfoundland, Canada, September 26–30*, pp. 321–334.

Matlock, H. D. (1969). A Model for the Prediction of Ice Structure Interaction. *First Annual Offshore Technology Conference*.

Musial, J. J. (2010). lOffshore Code Comparison Collaboration (OC3) for IEA Task 23 Offshore Wind Technology and Deployment.

Newland, D. E. (1975). Random Vibrations and Spectral Analysis. *Longman, London*.

Ou, J. D. (1996). The Stochastic Process Model of Ice Acting on Upright Column of Marine Platform and Determination of Model Parameters. *Proceedings IAHR Ice Symposium ,Beijing*, pp.302-311.

Popko, W. (2014). COMPARISON OF FULL-SCALE AND NUMERICAL MODEL DYNAMIC. *International Conference on Ocean,Offshore and Arctic Engineering*.

Popko, W., Vorpahl, F., Zuga, A., Kohlmeier, M., Jonkman, J., Robertson, A., . . . Kaufer. (2012). Offshore Code Comparison Collaboration Continuation (OC4), Phase I -- Results of Coupled Simulations of an Offshore Wind Turbine with Jacket Support Structure. *Proceedings of the 22nd International Offshore and Polar Engineering Conference (ISOPE), International Society of Offshore and Polar Engineers*, pp. 337-346.

Q. Yue, X. Z. (2001). Measurements and analysis of ice induced steady state vibration . *Prod 16th Int. Conf. Port Ocean Eng. under Arctic. Cond., Ottawa, Canada (2001)*.

Qianjin Yue, F. G. (2009). Dynamic ice forces of slender vertical structures due to ice crushing. *Cold regions science and technology*.

Qianjin Yue, X. B. (2002). Dynamic ice forces caused by crushing failure. *Ice in the Envrionment : Porceedings of the 16th IAHR international symposium*, 134-141.

R., K. T. (1989). Dynamic response of narrow structures to ice crushing. *Cold Regions Science and Technology 17(1989)* , pp. 173-187.

Ragan, P., & Manuel, L. (2007). Comparing Estimates of Wind Turbine Fatigue Loads Comparing using Time-Domain and Spectral Methods.

Reddy, D. V. (1977). Reddy, D. V., CheemaRelationship Between Response Spectrum and Power Spectral Density Analysis of Ice-Structure Analysis. *Reddy, D. V., Cheema, P. S., and Sundarajan, C., 1977, "Relationship Between Response Spectrum and Power Spectral Density Anal Proceedings 4th International Conference Port Ocean Engineering Arct. Cond.*

Reddy, D. V. (1975). Ice Force Response Spectrum Modal Analysis of Offshore Towers. *Proceedings 3rd International Conference Port Ocean Eng. Arct. Cond. , University of Alaska, 11–15August*, pp. 887–910.

Reddy, D. V. (1979). Non-stationary Response of Offshore Towers to Ice Loads. *Proceedings 6th International Conference Port Ocean Engineering Arct. Cond., Norwegian Institute of Technology, Trondheim, Norway, August 13–18*, Vol. II, pp. 1155–1171.

Schulson, E. M. (2001). Brittle failure of ice. *Engineering Fracture Mechanics,vol. 68, no. 17–18*, p. 1839–1887.

Shkhinek, K. K. (2000). Numerical Simulation of Ice Interaction With a Vertical Wall. *Proceedings 15th IAHR Ice Symposium, Gdansk, August 28–September 1, Vol. I*, pp. 231–242.

Sinding-Larsen, E. (2014). Numerical modelling of ice induced vibrations of lock-in type. *Graduation thesis*.

Sodhi, D. S. (1988). Ice Induced vibration of Structures . *IAHR Ice Symposium, Vol. 3*, pp. 625-657.

Stearns, S. D. (2003). Digital Signal Processing With Examples in MATLAB. *CRC, London*.

Sundararajan, C. a. (1973). Stochastic Analysis of Ice Structure Interaction. *Proceeding 2nd Interntational Conference Port Ocean Eng. Arctic Cond. (POAC'73), Reykjavik, Iceland, August 27–30*, pp. 345–353.

Sutherland, H. J. (1999). *Fatigue Analysis of Wind Turbines.*

T. Fischer, W. d. (2010). Upwind Design Basis-WP4: Offshore Foundations and Support Structures.

T. Laakso, H. H.-G. (2003). State-of-the-art of wind energy in cold climates.

Timoshenko, S. P. (1951). Theory of elasticity.

Toussain, M. B. (1976). Mechanisms and Theory of Indentation of Ice Plates. *Symposium on Applied Glacioloty*.

Vorpahl, F., Schwarze, H., Fischer, T. (2013). Offshore wind turbine environment, loads, simulation, and design Wiley Interdisciplinary Reviews. *Energy and Environment*, 548-570.

Yue, Q. a. (2000). Ice-Induced Jacket Structure Vibrations in Bohai Sea. *J. Cold Reg. Eng.*, pp. 81–92.

Appendix 1

Codes for ice loads generation in spectral model

```
close all
clear all
clc

%%%%%Freqency range%%%%%%

F0=0;
Fmax=15;
DeltaF=0.001;

%%%%%%Space range%%%%%%%

X0=0;
Xmax=6; % width of monopile 6m
DeltaX=0.01;
Angle=-0.5*pi:pi/(Xmax/DeltaX):0.5*pi;

%%%%%%Time range%%%%%%

tmax=300;
dt=0.01;

%%%%%%Parameters%%%%%%%

alpha=0.2;
beta=3;
rou=0.1;
h=1;
R=0:DeltaX:Xmax;    %distance between 2 locations
F=0:DeltaF:Fmax;    %frequency range
b=1.34;
ks=3.24;
v=0.3;
a=b*power(v,-0.6);

%%%%%%Parameters for nondimensional autospectrum%%%

In=0.4;
K=4;
fmax=6800000;
sigma=In/(1+K*In)*fmax;  % local force variance
miu=0.05;                % friction coefficient
```

```
%%%%%%%%%%   rxy  %%%%%%%%%%

for i=1:Fmax/DeltaF+1
    for j=1:Xmax/DeltaX+1
    kesi=R(j)/h;
    r(i,j)=(1/(1+rou+alpha*kesi))*(rou+exp(-beta*kesi*F(i)));
    end
end
figure
surf(R,F,r);
xlabel('distance')
ylabel('frequency')
zlabel('coherence function r(m,n)')
%%%%%%%%%%non dimensional Gnn(i) & local spectrum Gnn %%%%%%%%%

NONGnn=a*F./(1+ks*power(a,1.5)*power(F,2));

figure
plot(F,NONGnn)
title('NONGnn(f)')
ylabel('NONGnn(f)')
xlabel('frequency')

NONGnnmax=0;
for i=1:length(F)
    if NONGnn(i)> NONGnnmax
        NONGnnmax=NONGnn(i);
    end
end

Gnn=a*sigma^2./(1+ks*power(a,1.5)*power(F,2));

figure
plot(F,Gnn)
title('autospectral fuction Gnn(f)')
ylabel('Gnn(f)')
xlabel('frequency')


%%%%%%%%%%Gmn(f)=sqrt(Gnn(f)*Gmm(f)*rmn(f)*rmn(f))  %%%%%%%%%%

m=0:DeltaX:Xmax;
n=0:DeltaX:Xmax;

for k=1:Fmax/DeltaF+1
    for i=1:Xmax/DeltaX+1
        for j=1:Xmax/DeltaX+1
            if i==j
            Gmn(i,j)=Gnn(k);
            else e= abs(i-j);
            Gmn(i,j)= sqrt(Gnn(k)*Gnn(k)*r(k,e)*r(k,e));%assume Gnn=Gmm
            end
        end
    end
```

```
     G(k)={Gmn};
end

%%%%%%%%%Local spectrum Gloc(f) %%%%%
figure

for k=1:Fmax/DeltaF+1
    Gtemp=cell2mat(G(k));
    Gloc(:,k)=sum(Gtemp,2);
end
for i=1:Xmax/DeltaX+1
    G_temp=Gloc(i,:)*((cos(Angle(i)))^2+miu^2*(sin(Angle(i)))^2);
    Gloc(i,:)=G_temp;
    plot(F,G_temp)
    hold on
end

title('Local spectrum Gloc(f) d=6m')
ylabel('Gloc(f)')
xlabel('frequency')
save localspectrum.out Gloc -ASCII;
type localspectrum.out
dlmwrite('localspectrum.out', Gloc, ' ');

%%%%%%%%%time series formulation %%%%%%%%%%
t=0:dt:tmax;

for i=1:Xmax/DeltaX+1  %global spectrum
    if i==1
        GF=Gloc(i,:);
    else
        GF=GF+Gloc(i,:);
    end
end

figure
plot(F,GF)
title ('total load spectrum GFF(f) D=6m')
ylabel('GF(f)')
xlabel('frequency')

Amplitude=sqrt(2*GF*DeltaF);
Omega=2*pi*F;
t=0:dt:tmax;
Fi2=2*pi*rand(Fmax/DeltaF+1,1);
for i=1:tmax/dt+1
    Loadglobalspectrum(i)=sum(Amplitude.*cos(Omega*t(i)+Fi2'));
end
figure
plot(t,Loadglobalspectrum)
ylabel('Ice loads')
xlabel('time(s)')
title('time series’)

%%%%%%%%Input file for FEDEM%%%%
```

```
Output(:,1)=t;
% Output(:,2)=Globalforce;
Output(:,2)=Loadglobalspectrum;
fileID = fopen(['Iceload0.3.txt'],'w');
fprintf(fileID,'%5s \r\n ','# Ice load time series');
fprintf(fileID,'%8s %12s \r\n ','# Time [s]','Force [N]');
fprintf(fileID,'%4.3f %8.4f  \r\n', Output');
fclose(fileID);
```

Appendix 2

Results for spectral model

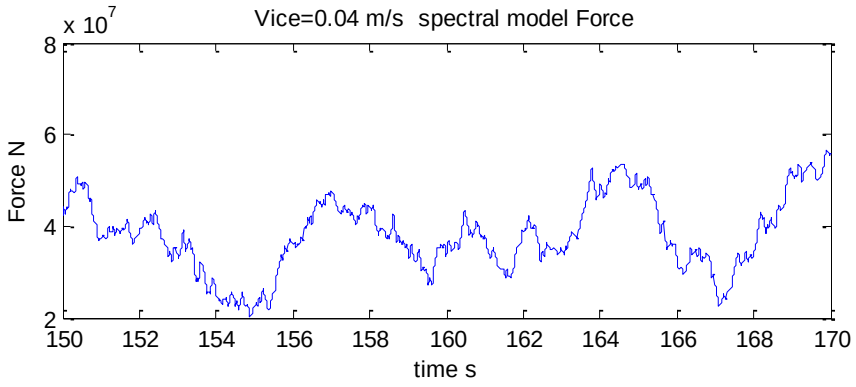

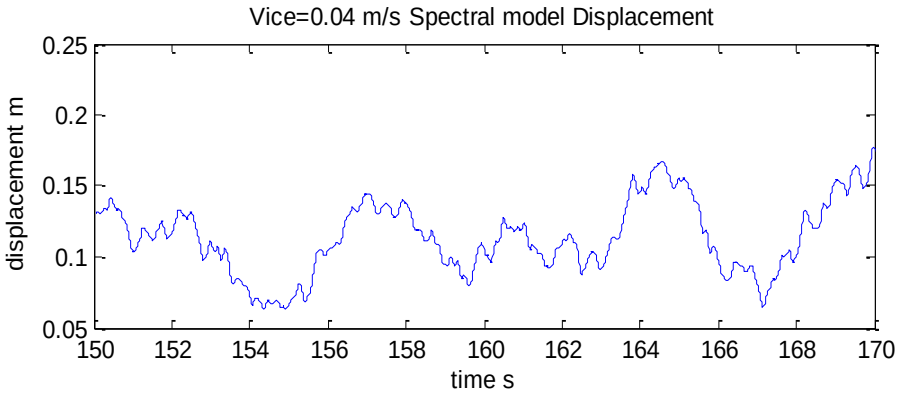

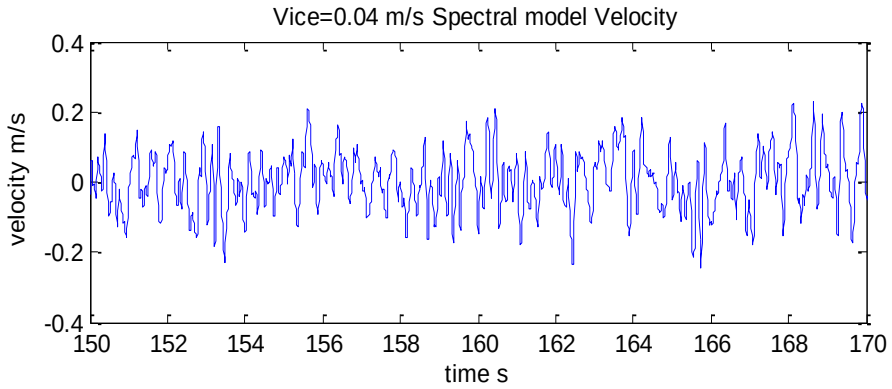

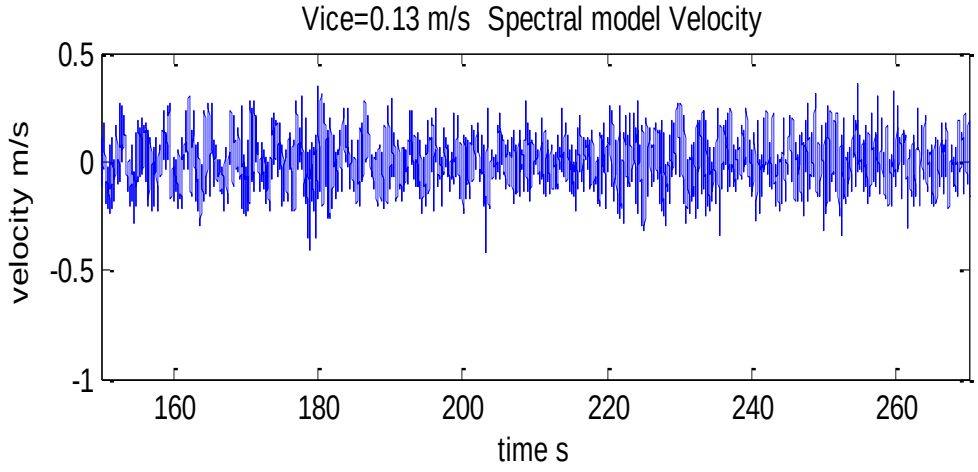
Vice=0.13 m/s Spectral model Velocity
velocity m/s
0.5
0
-0.5
-1
160
180
200
220
240
260
time s

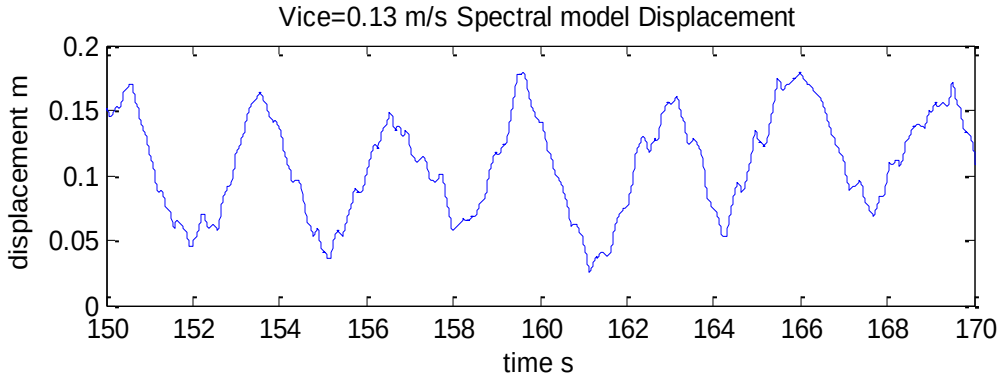
Vice=0.13 m/s Spectral model Displacement
displacement m
0.2
0.15
0.1
0.05
0
150
152
154
156
158
160
162
164
166
168
170
time s

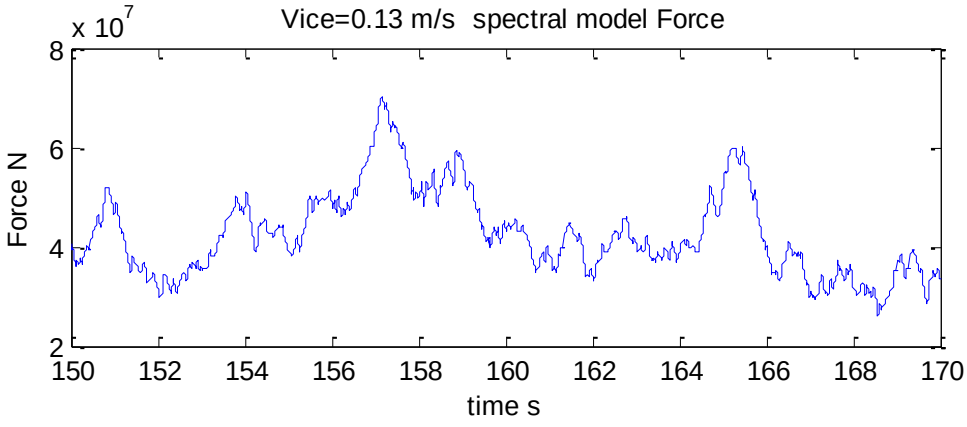
x 10^7
Vice=0.13 m/s spectral model Force
Force N
8
6
4
2
150
152
154
156
158
160
162
164
166
168
170
time s

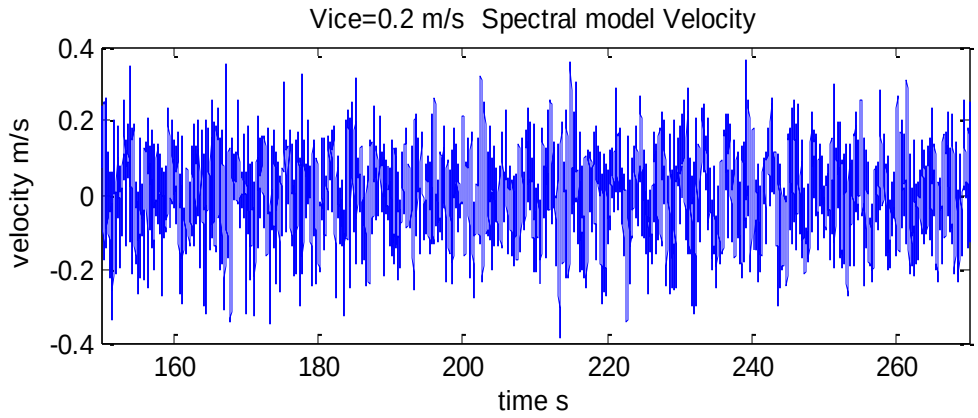
Vice=0.2 m/s Spectral model Velocity
velocity m/s
0.4
0.2
0
-0.2
-0.4
160
180
200
220
240
260
time s

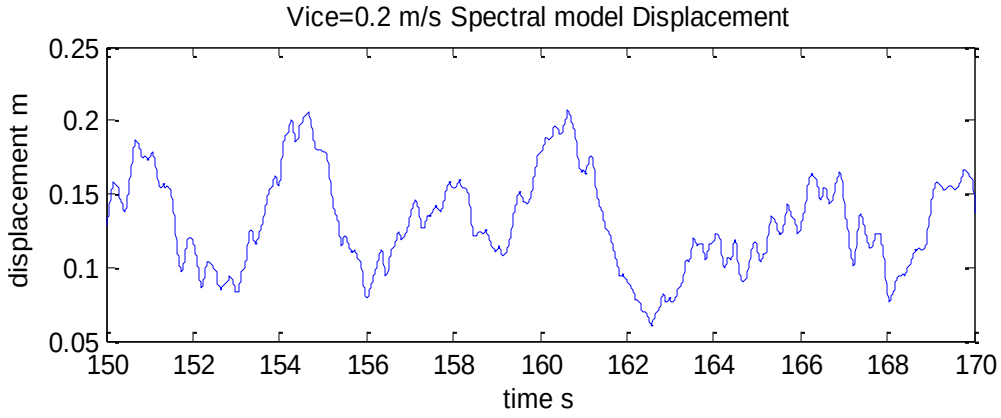
Vice=0.2 m/s Spectral model Displacement
displacement m
0.25
0.2
0.15
0.1
0.05
150
152
154
156
158
160
162
164
166
168
170
time s

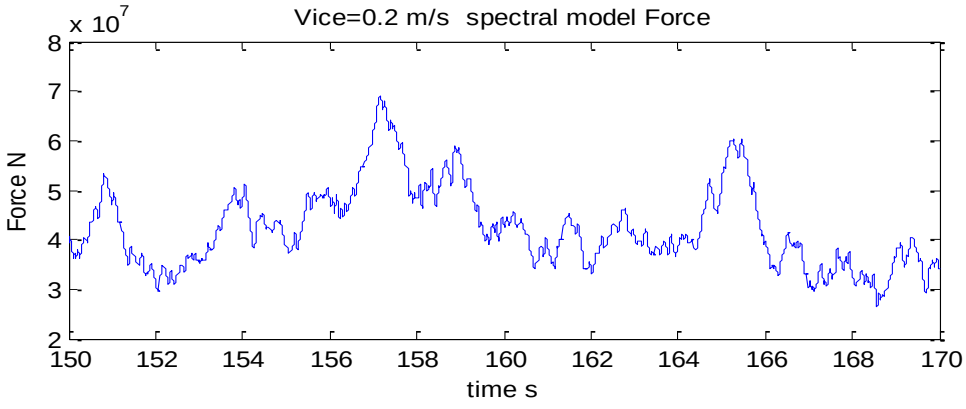
x 10^7
Vice=0.2 m/s spectral model Force
Force N
8
7
6
5
4
3
2
150
152
154
156
158
160
162
164
166
168
170
time s

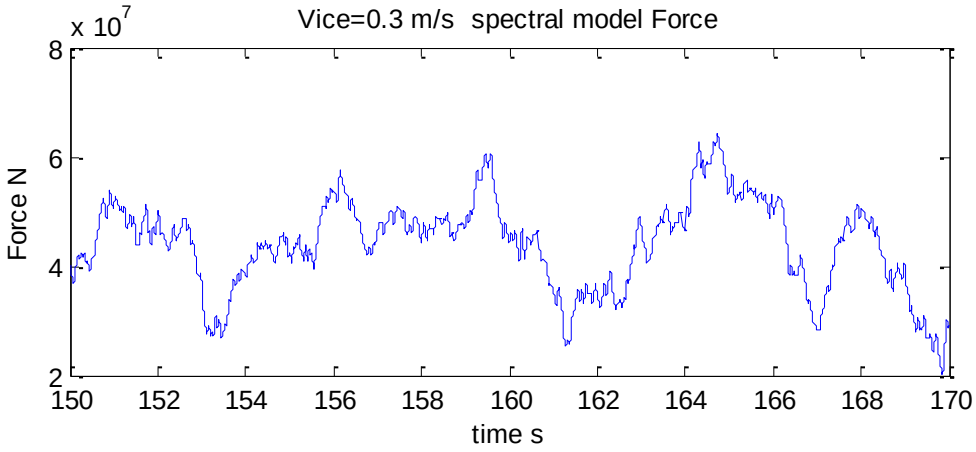
Vice=0.3 m/s spectral model Force
x 10^7
Force N
time s

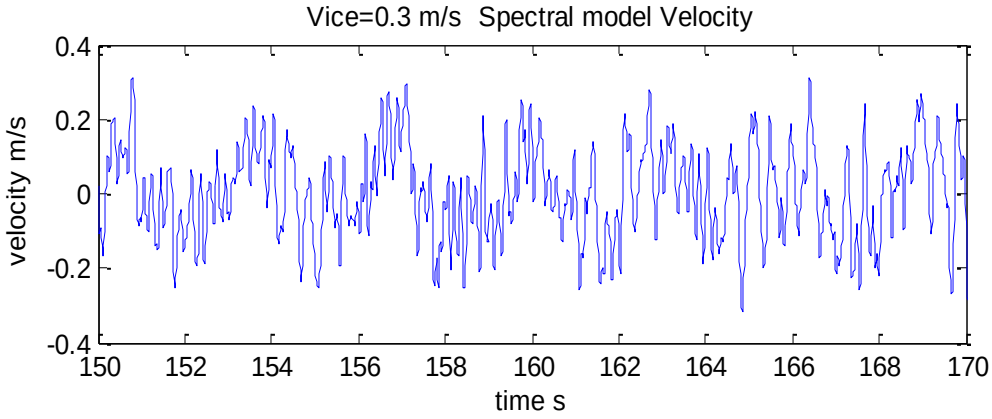
Vice=0.3 m/s Spectral model Velocity
velocity m/s
time s

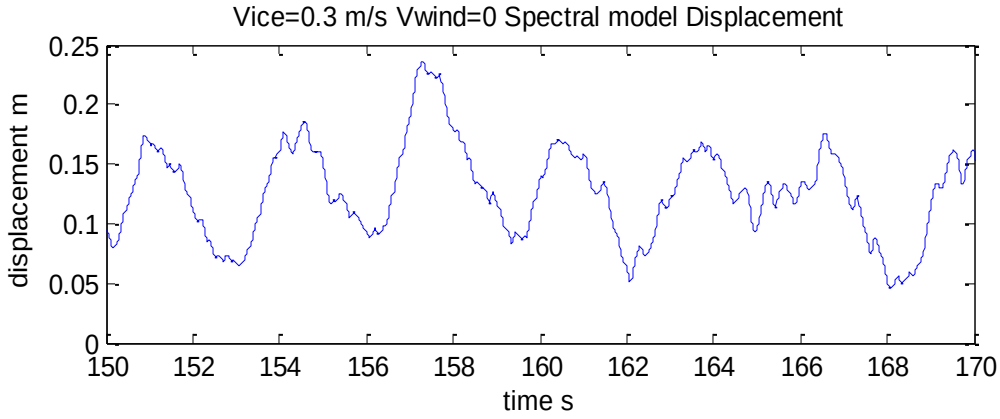
Vice=0.3 m/s Vwind=0 Spectral model Displacement
displacement m
time s

Appendix 3

Results for M-B Model

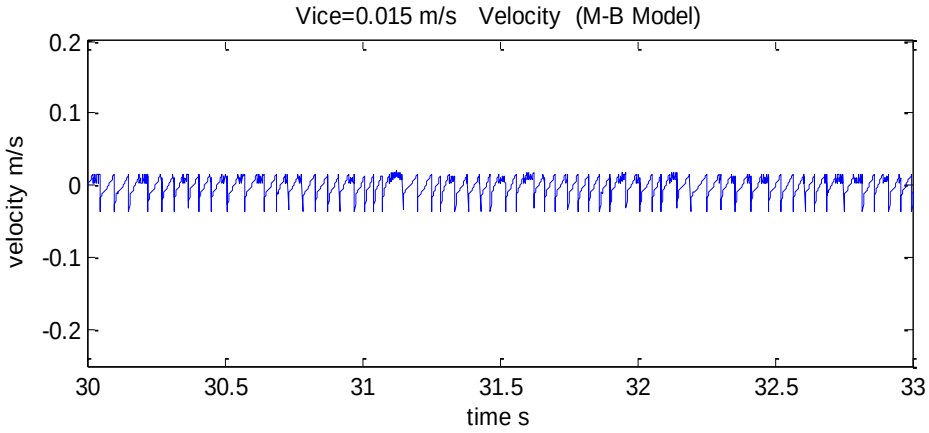

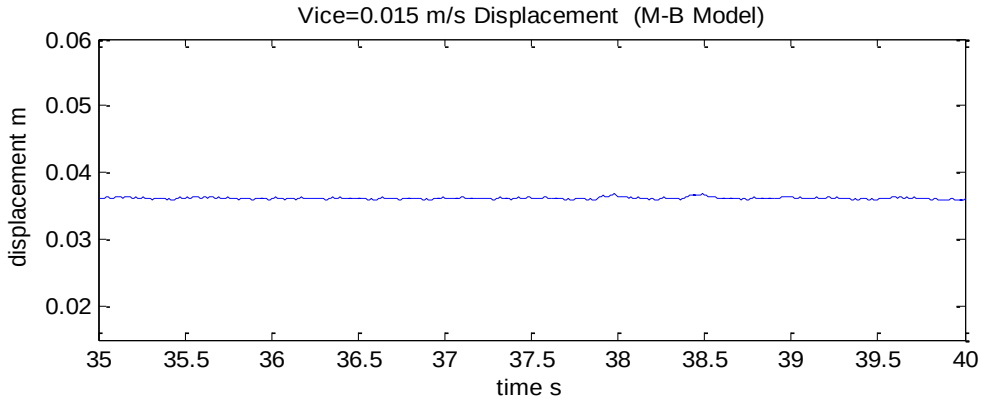

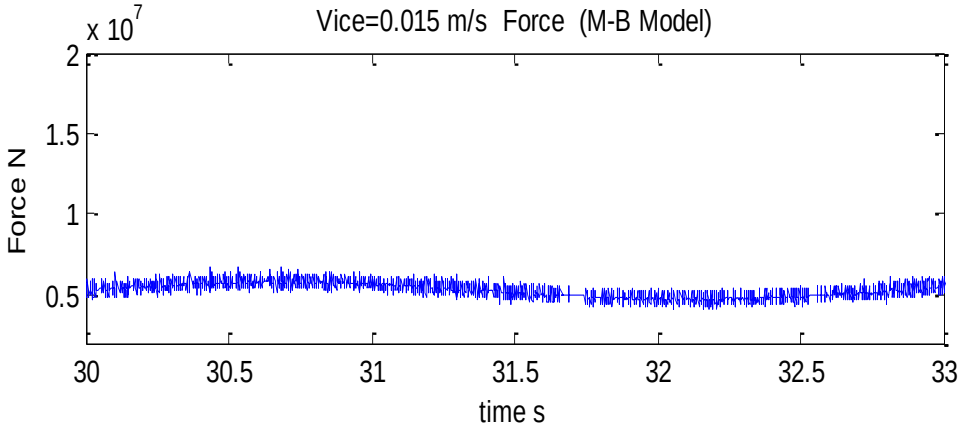

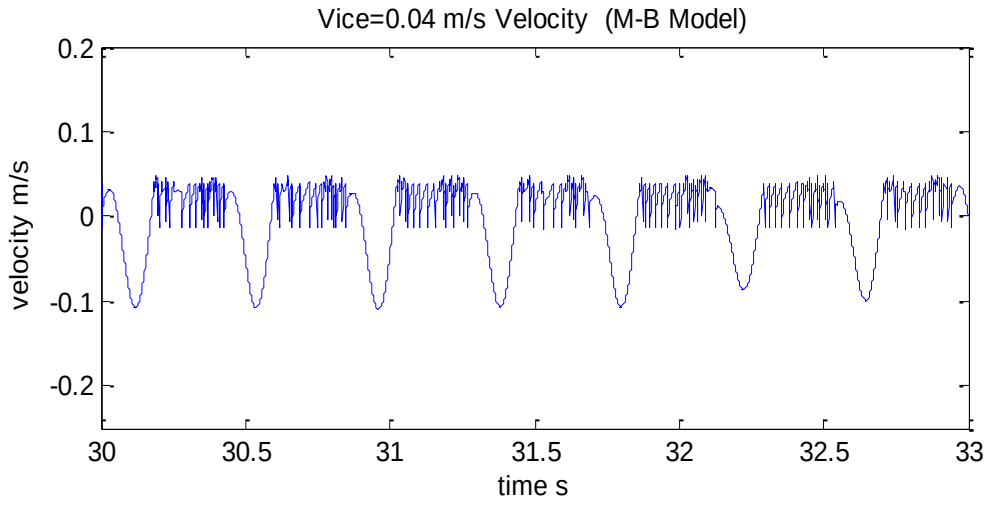
Vice=0.04 m/s Velocity (M-B Model)
velocity m/s
0.2
0.1
0
-0.1
-0.2
30
30.5
31
31.5
32
32.5
33
time s

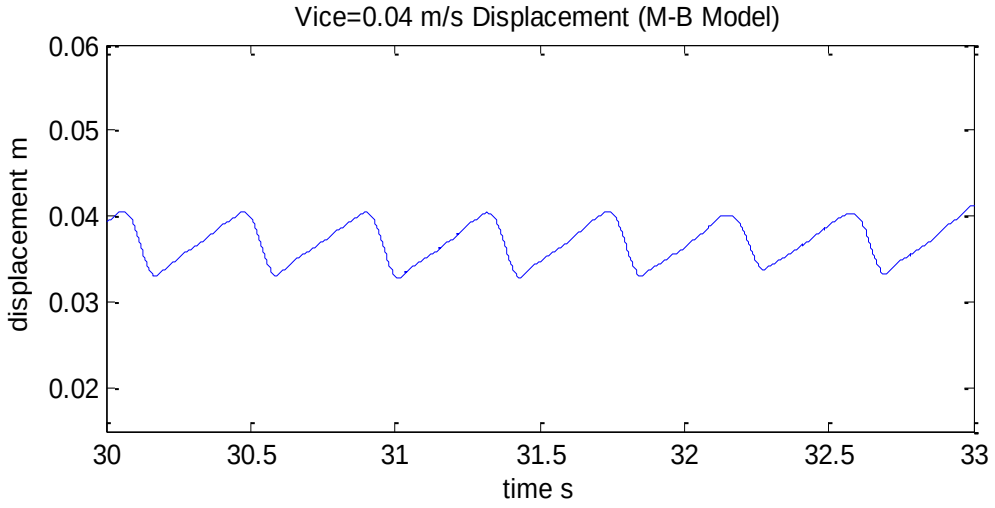
Vice=0.04 m/s Displacement (M-B Model)
displacement m
0.06
0.05
0.04
0.03
0.02
30
30.5
31
31.5
32
32.5
33
time s

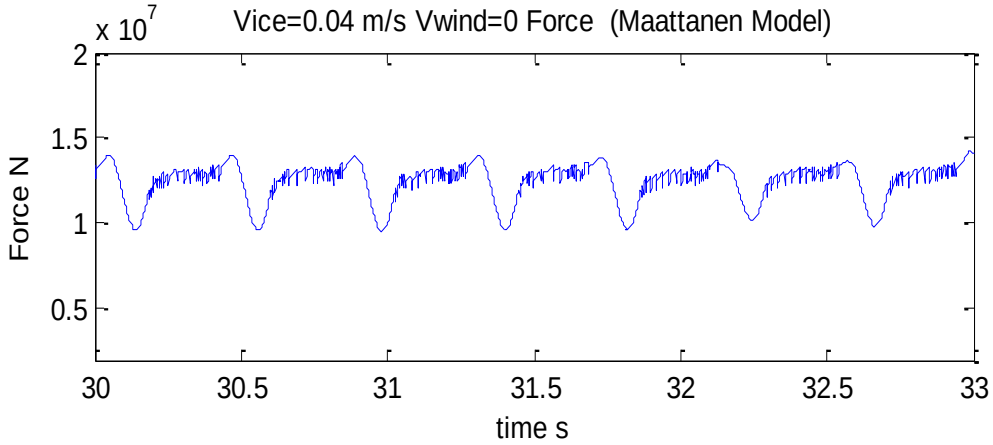
x 10^7
Vice=0.04 m/s Vwind=0 Force (Maattanen Model)
Force N
2
1.5
1
0.5
30
30.5
31
31.5
32
32.5
33
time s

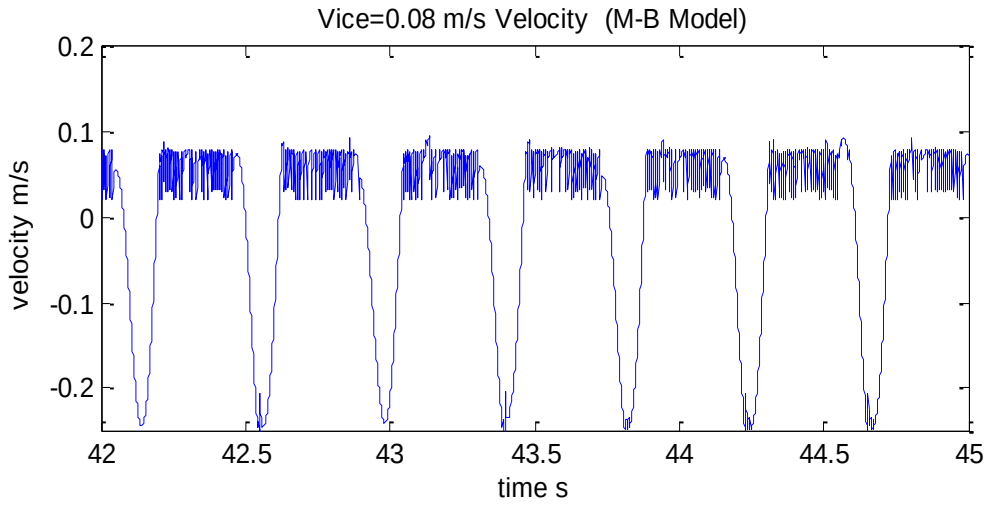
Vice=0.08 m/s Velocity (M-B Model)
velocity m/s
0.2
0.1
0
-0.1
-0.2
42
42.5
43
43.5
44
44.5
45
time s

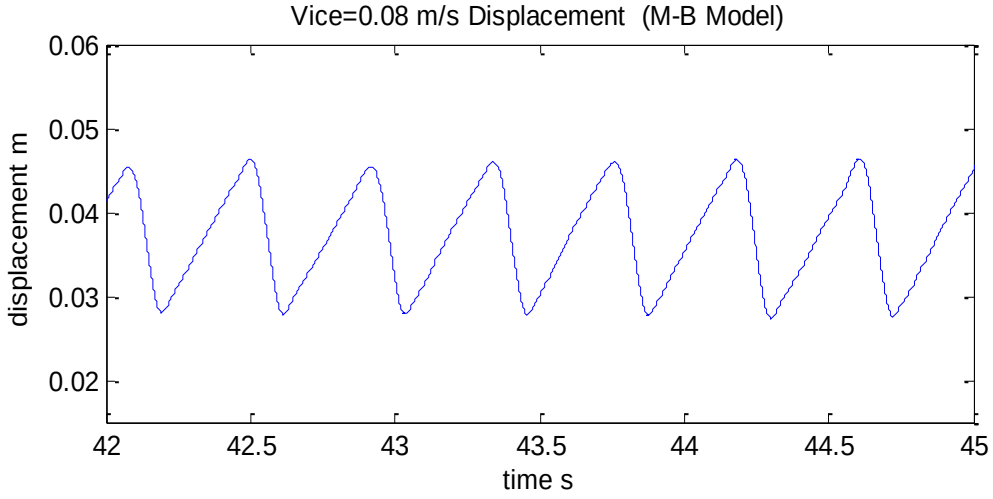
Vice=0.08 m/s Displacement (M-B Model)
displacement m
0.06
0.05
0.04
0.03
0.02
42
42.5
43
43.5
44
44.5
45
time s

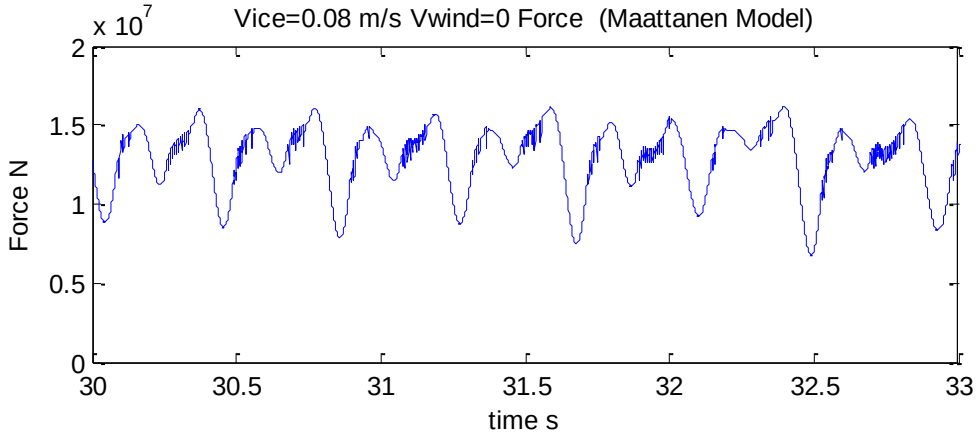
x 10^7
Vice=0.08 m/s Vwind=0 Force (Maattanen Model)
Force N
2
1.5
1
0.5
0
30
30.5
31
31.5
32
32.5
33
time s

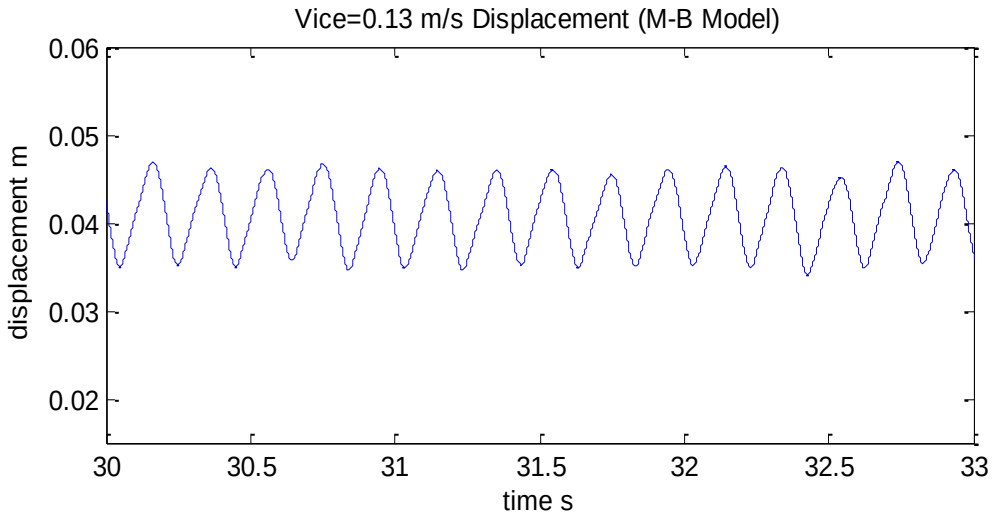
Vice=0.13 m/s Displacement (M-B Model)
displacement m
0.06
0.05
0.04
0.03
0.02
30
30.5
31
31.5
32
32.5
33
time s

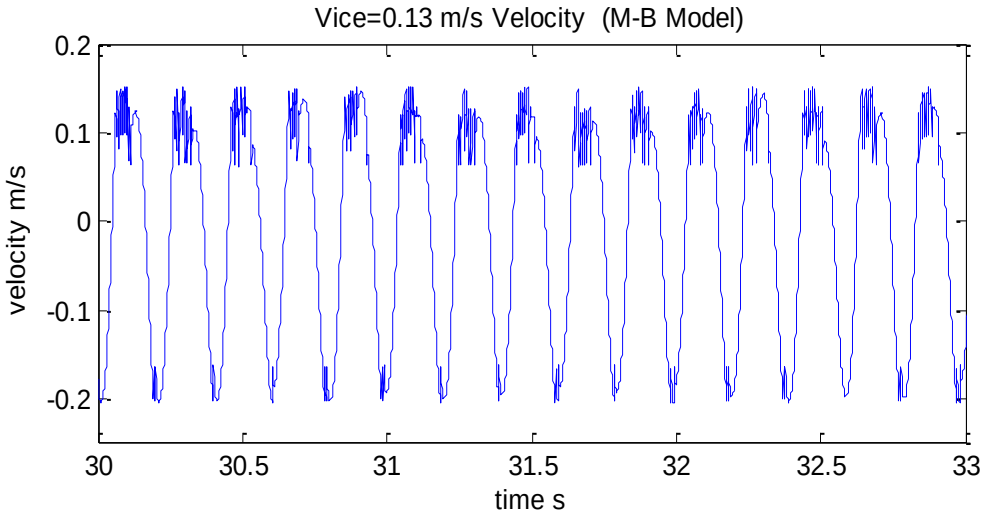
Vice=0.13 m/s Velocity (M-B Model)
velocity m/s
0.2
0.1
0
-0.1
-0.2
30
30.5
31
31.5
32
32.5
33
time s

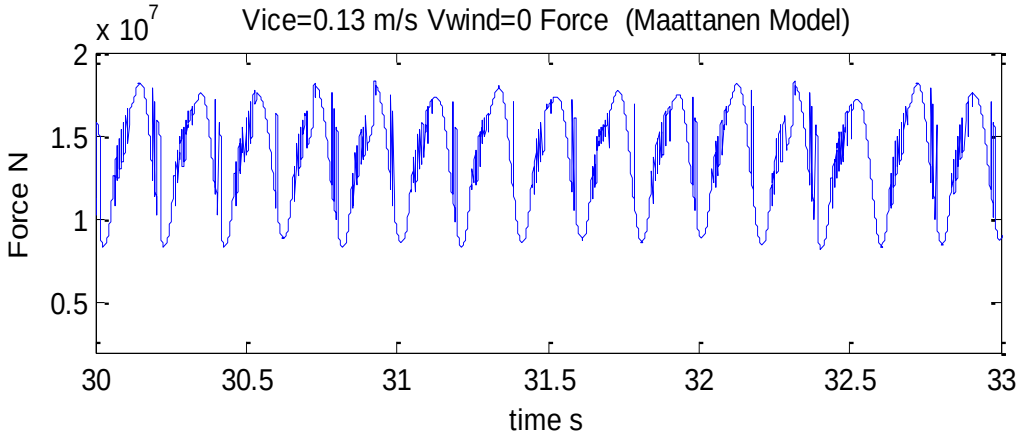
x 10^7
Vice=0.13 m/s Vwind=0 Force (Maattanen Model)
Force N
2
1.5
1
0.5
30
30.5
31
31.5
32
32.5
33
time s

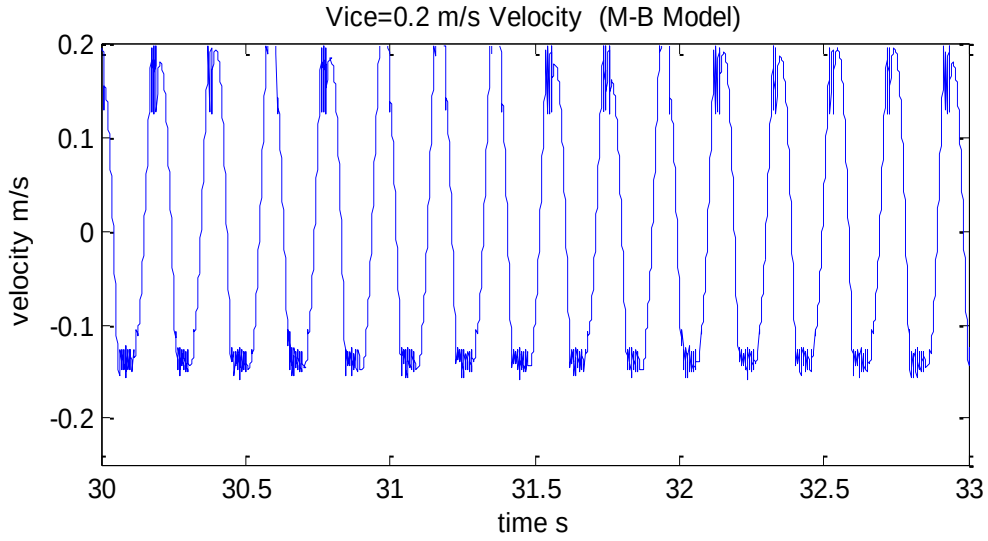
Vice=0.2 m/s Velocity (M-B Model)
velocity m/s
0.2
0.1
0
-0.1
-0.2
30
30.5
31
31.5
32
32.5
33
time s

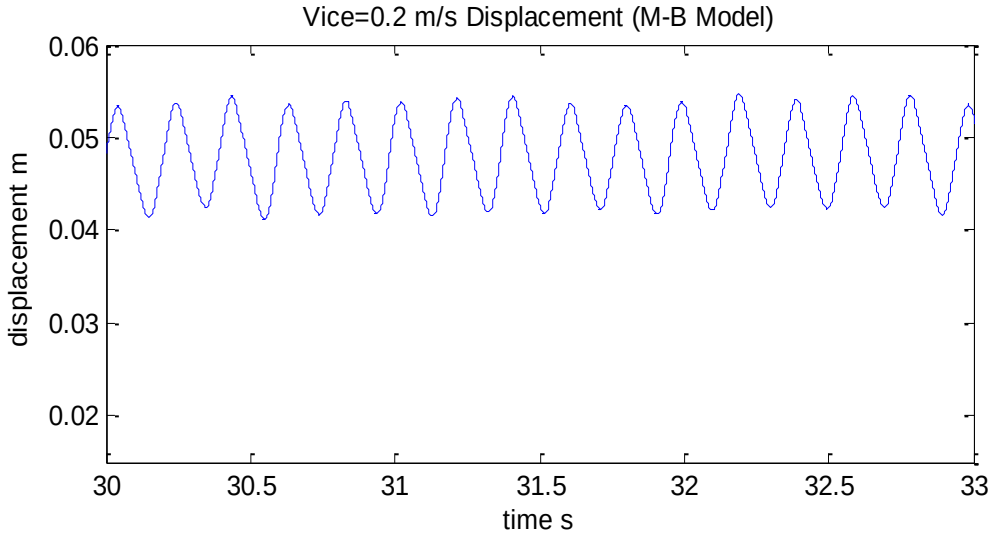
Vice=0.2 m/s Displacement (M-B Model)
displacement m
0.06
0.05
0.04
0.03
0.02
30
30.5
31
31.5
32
32.5
33
time s

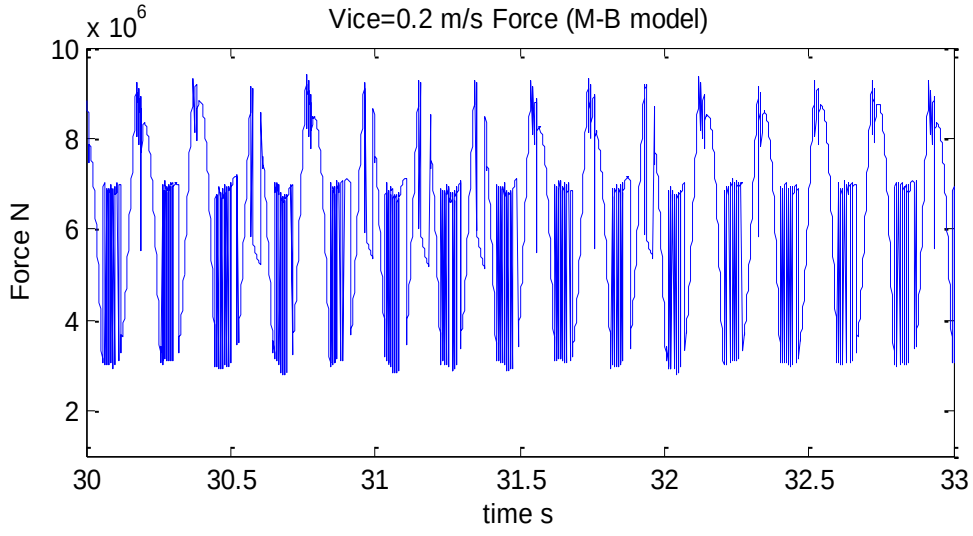
Vice=0.2 m/s Force (M-B model)
x 10^6
Force N
10
8
6
4
2
30
30.5
31
31.5
32
32.5
33
time s

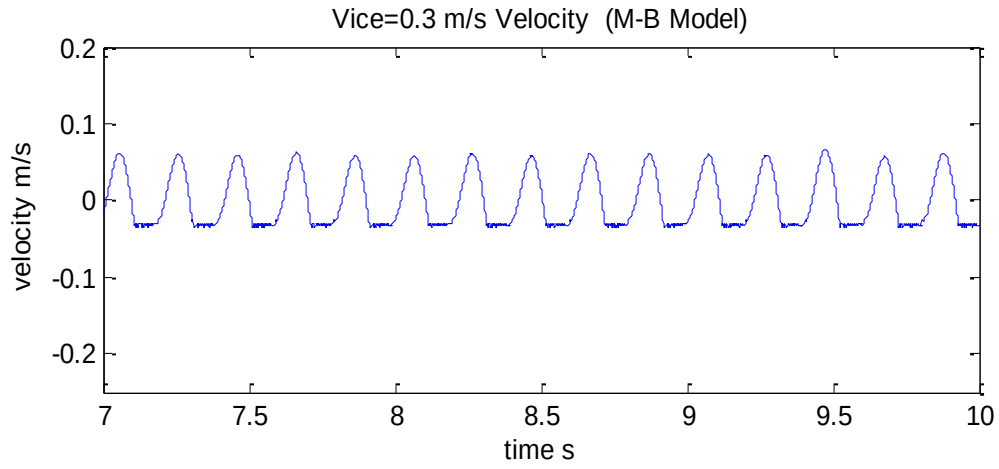
Vice=0.3 m/s Velocity (M-B Model)
velocity m/s
0.2
0.1
0
-0.1
-0.2
7
7.5
8
8.5
9
9.5
10
time s

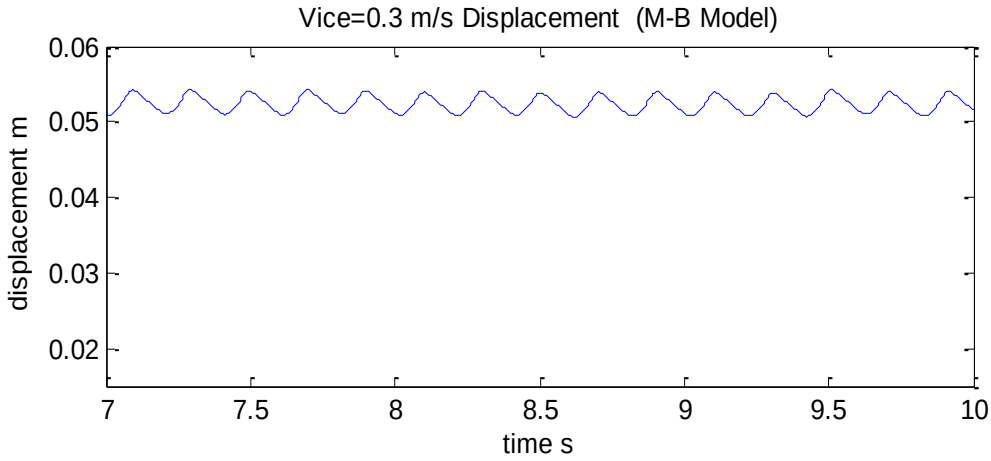
Vice=0.3 m/s Displacement (M-B Model)
displacement m
0.06
0.05
0.04
0.03
0.02
7
7.5
8
8.5
9
9.5
10
time s

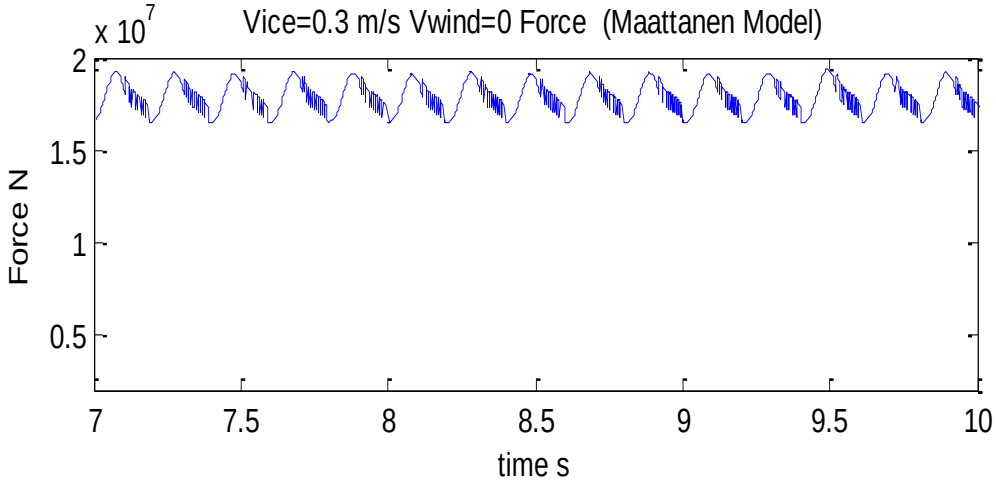
x 10^7
Vice=0.3 m/s Vwind=0 Force (Maattanen Model)
Force N
2
1.5
1
0.5
7
7.5
8
8.5
9
9.5
10
time s

Appendix 4

Structure response for ice-wind coupling model

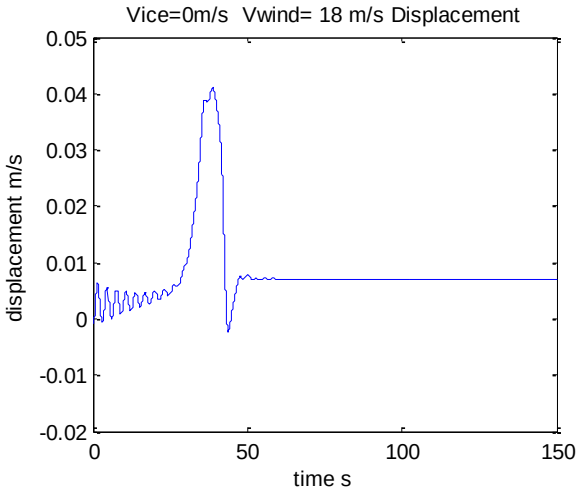

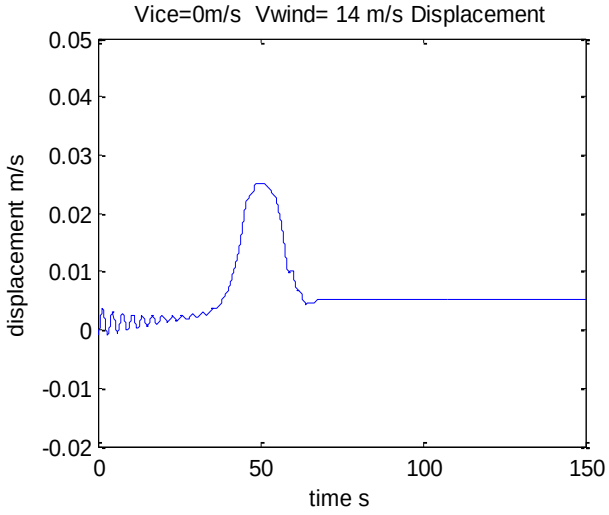

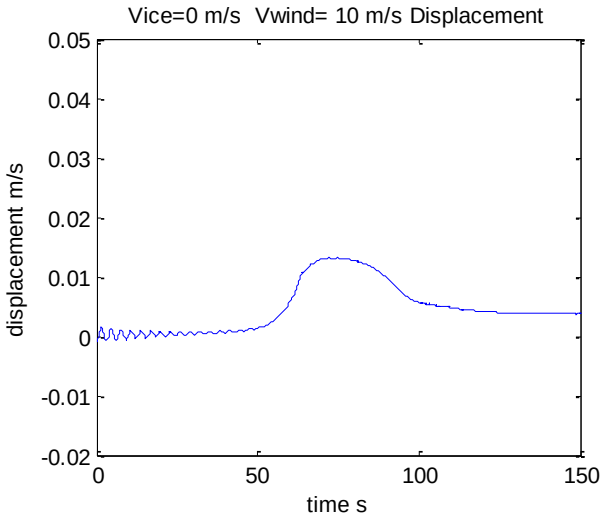

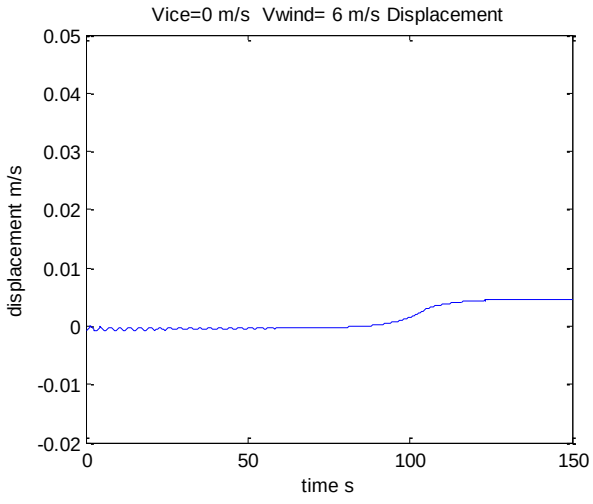

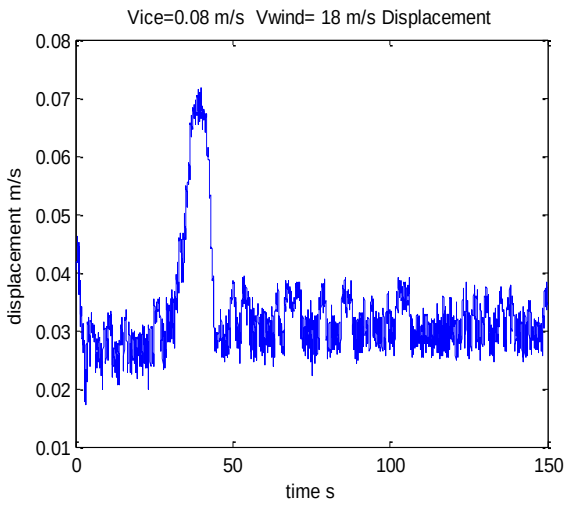
Vice=0.08 m/s Vwind= 18 m/s Displacement
displacement m/s
time s
0.08
0.07
0.06
0.05
0.04
0.03
0.02
0.01
0
50
100
150

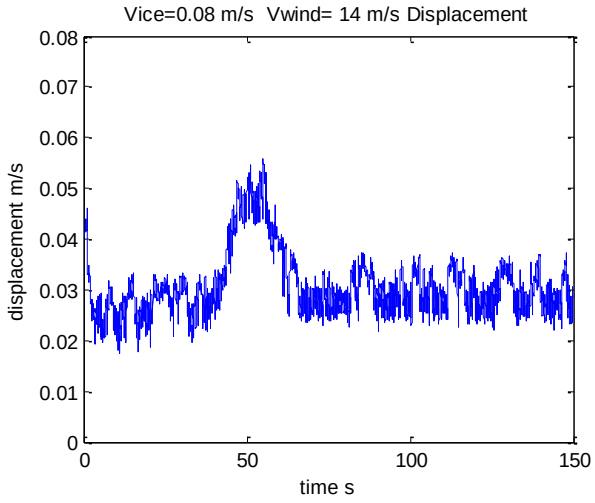
Vice=0.08 m/s Vwind= 14 m/s Displacement
displacement m/s
time s
0.08
0.07
0.06
0.05
0.04
0.03
0.02
0.01
0
50
100
150

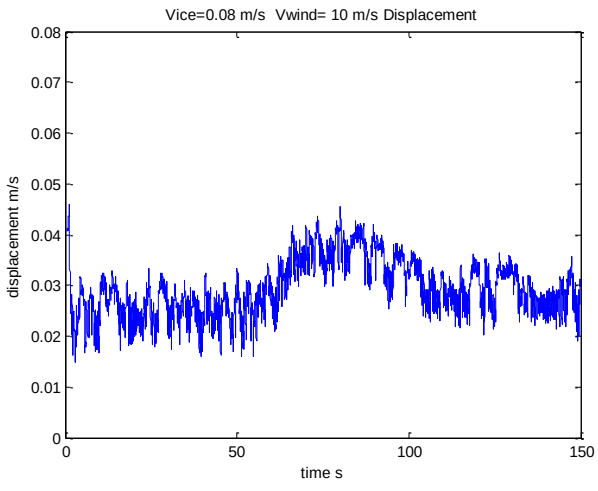
Vice=0.08 m/s Vwind= 10 m/s Displacement
displacement m/s
time s
0.08
0.07
0.06
0.05
0.04
0.03
0.02
0.01
0
50
100
150

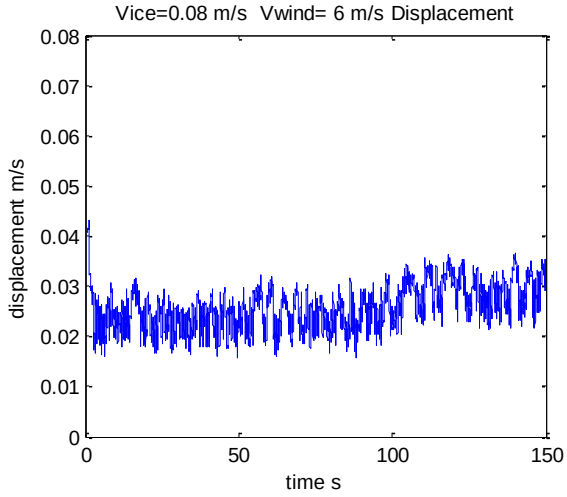
Vice=0.08 m/s Vwind= 6 m/s Displacement
displacement m/s
time s
0.08
0.07
0.06
0.05
0.04
0.03
0.02
0.01
0
50
100
150

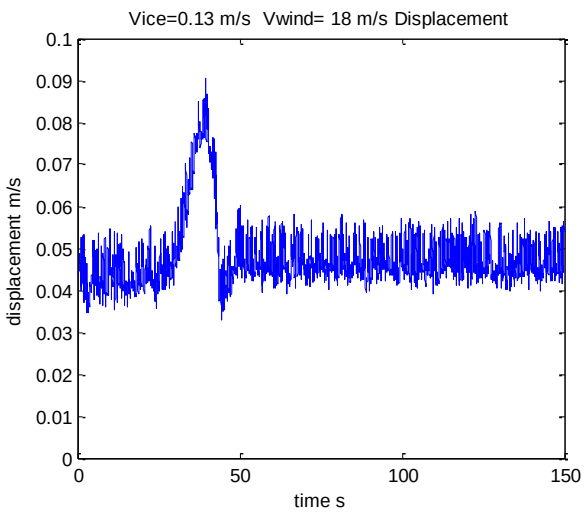
Vice=0.13 m/s Vwind= 18 m/s Displacement
displacement m/s
time s
0
0.01
0.02
0.03
0.04
0.05
0.06
0.07
0.08
0.09
0.1
0
50
100
150

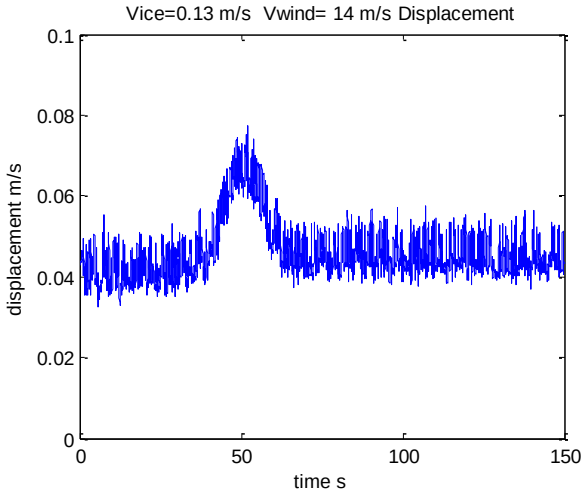
Vice=0.13 m/s Vwind= 14 m/s Displacement
displacement m/s
time s
0
0.02
0.04
0.06
0.08
0.1
0
50
100
150

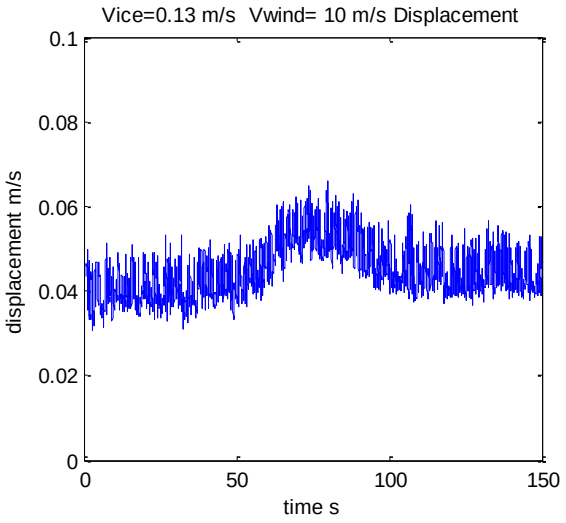
Vice=0.13 m/s Vwind= 10 m/s Displacement
displacement m/s
time s
0
0.02
0.04
0.06
0.08
0.1
0
50
100
150

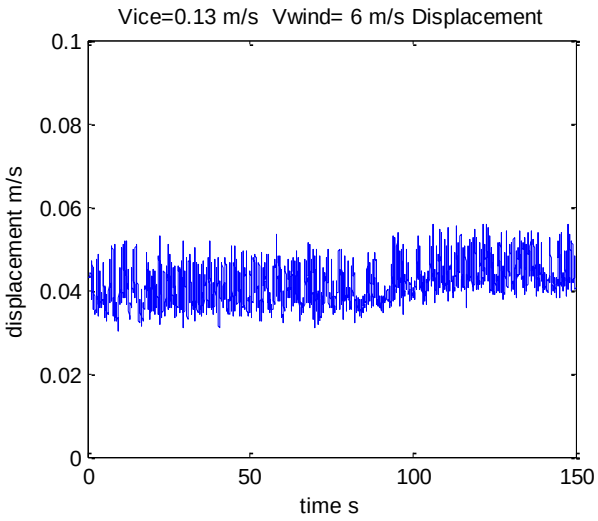
Vice=0.13 m/s Vwind= 6 m/s Displacement
displacement m/s
time s
0
0.02
0.04
0.06
0.08
0.1
0
50
100
150

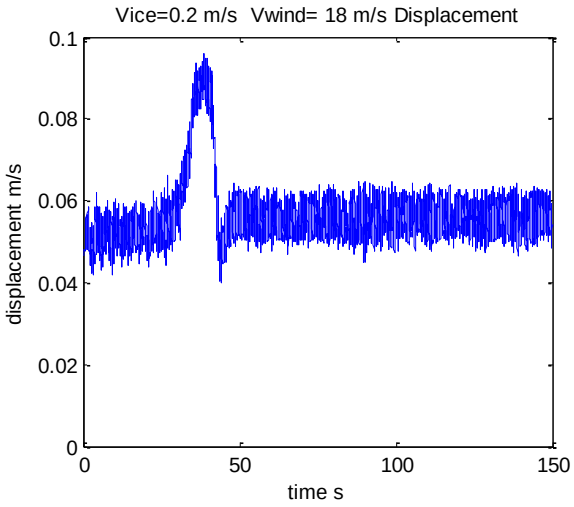
Vice=0.2 m/s Vwind= 18 m/s Displacement
displacement m/s
time s
0
0.02
0.04
0.06
0.08
0.1
0
50
100
150

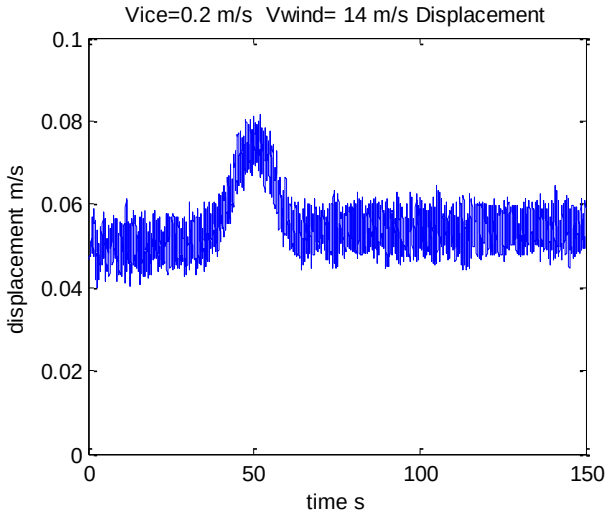
Vice=0.2 m/s Vwind= 14 m/s Displacement
displacement m/s
time s
0
0.02
0.04
0.06
0.08
0.1
0
50
100
150

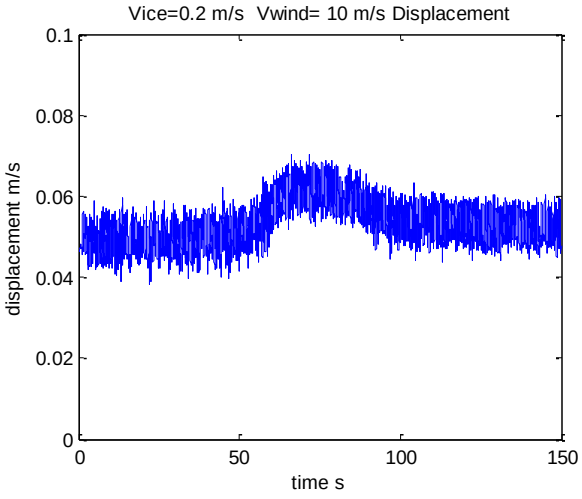
Vice=0.2 m/s Vwind= 10 m/s Displacement
displacement m/s
time s
0
0.02
0.04
0.06
0.08
0.1
0
50
100
150

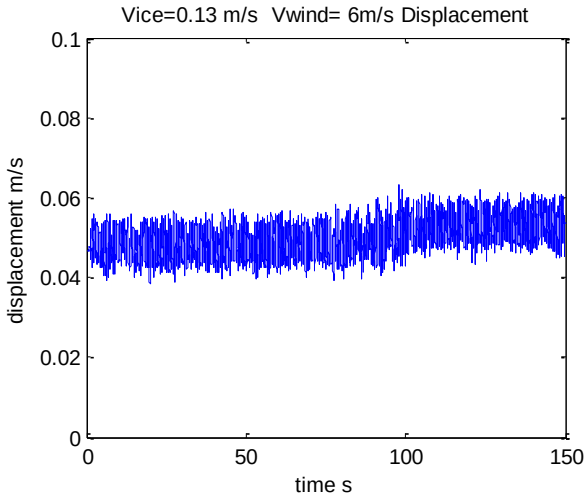
Vice=0.13 m/s Vwind= 6m/s Displacement
displacement m/s
time s
0
0.02
0.04
0.06
0.08
0.1
0
50
100
150

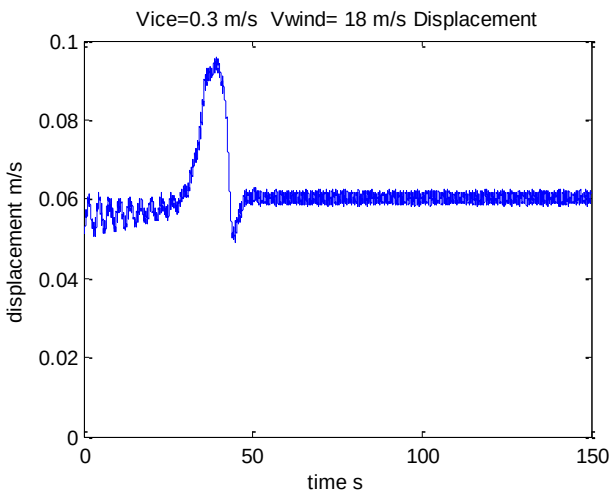
Vice=0.3 m/s Vwind= 18 m/s Displacement
displacement m/s
time s
0
0.02
0.04
0.06
0.08
0.1
0
50
100
150

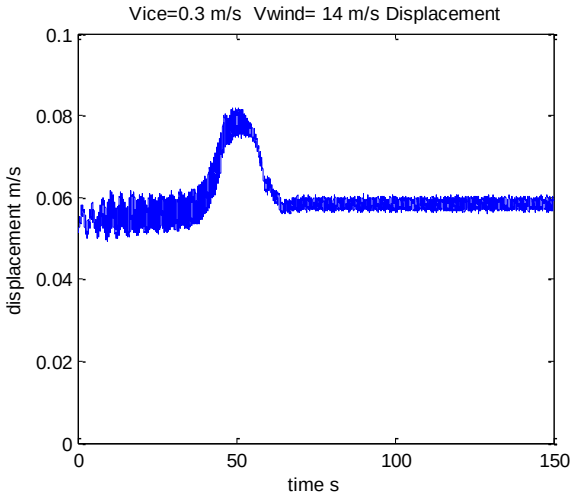
Vice=0.3 m/s Vwind= 14 m/s Displacement
displacement m/s
time s
0
0.02
0.04
0.06
0.08
0.1
0
50
100
150

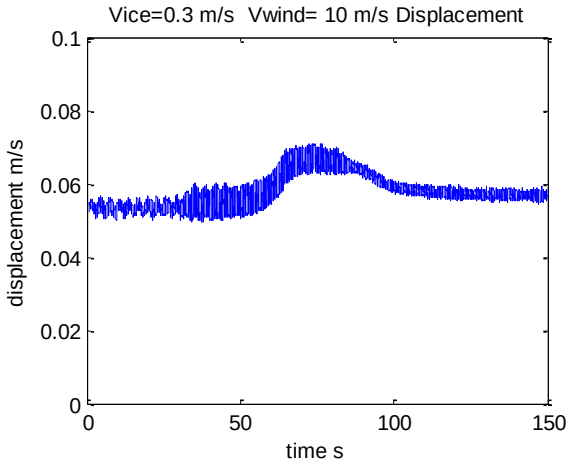
Vice=0.3 m/s Vwind= 10 m/s Displacement
displacement m/s
time s
0
0.02
0.04
0.06
0.08
0.1
0
50
100
150

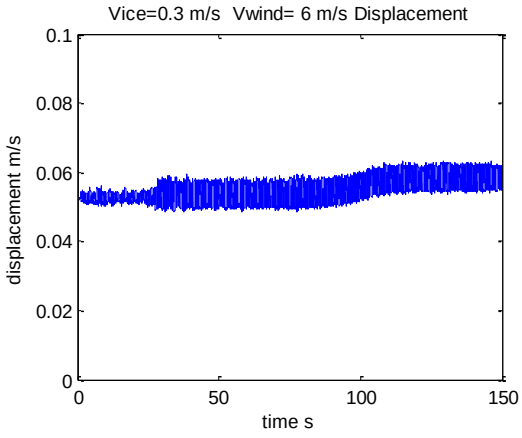
Vice=0.3 m/s Vwind= 6 m/s Displacement
displacement m/s
time s
0
0.02
0.04
0.06
0.08
0.1
0
50
100
150

Appendix 5

Codes for fatigue analysis

```
clear all
close all
clc
%%%%%%%%%%%%%%%%%%%%      Parameters    %%%%%%%%%%%%%%%%%

Diameter= 6.0;
Thickness= 0.3;
log10a=11.764;
m=3;
k=0.2;
t=33;
tref=25;

%%%%%%%%%%%%%%%%  Read output file  %%%%%%%%%%%%%%%%%%%

file_name  = ['displacement.asc.txt'];
file_id    = fopen(file_name, 'r');
file_dataDISPLACEMENT  = textscan(file_id,'%f %f '
,'headerlines',7,'delimiter',',');
fclose(file_id);
Time =cell2mat(file_dataDISPLACEMENT(:,1));
ResponseDISPLACEMENT=cell2mat(file_dataDISPLACEMENT(:,2));
figure
plot(Time,ResponseDISPLACEMENT)
title('Vice=0.13 m/s  Vwind= 18 m/s Displacement')
ylabel('displacement m/s')
xlabel('time s')

file_name  = ['forebase.asc.txt'];
file_id    = fopen(file_name, 'r');
file_dataFORCE  = textscan(file_id,'%f %f '
,'headerlines',7,'delimiter',',');
fclose(file_id);
Time =cell2mat(file_dataFORCE(:,1));
ResponseFORCE=cell2mat(file_dataFORCE(:,2))./1000000;
figure
plot(Time,ResponseFORCE)
title('Vice=0.13 m/s  Vwind= 18 m/s Force')
ylabel('Force MN')
xlabel('time s')

file_name  = ['momentbase.asc.txt'];
file_id    = fopen(file_name, 'r');
file_dataMOMENT  = textscan(file_id,'%f %f '
,'headerlines',7,'delimiter',',');
fclose(file_id);
ResponseMOMENT=cell2mat(file_dataMOMENT(:,2))./1000000;
figure
plot(Time,ResponseMOMENT)
```

```
title('Vice=0.13 m/s  Vwind= 18 m/s Moment')
ylabel('Moment MN')
xlabel('time s')

%%%%%%%%%%%%%%%%%  Stress calculation  %%%%%%%%%%%%%%%

Tau=ResponseFORCE./(pi*Diameter*Thickness);
Sigma=ResponseMOMENT./(pi/64*(Diameter^4....
               -(Diameter-2*Thickness)^4));
TotalStress=sqrt(power(Tau,2)+power(Sigma,2));  %total stress

figure
plot(Time,TotalStress)
title('Vice=0.13 m/s  Vwind= 18 m/s Total stress')
ylabel('Stress MPa')
xlabel('time s')

%%%%%%%%%%%%%%%%%%% Rainflow counting %%%%%%%%%%%%%%%%%%

rf = rainflow(TotalStress)          %Rainflow function
[Amplitude,pos]=sort(rf(1,:));      %put amplitude in ascending order
n=rf(3,pos);                        %number of each amplitude
StressRange=Amplitude.*2;           %stress range=2*amplitude


%%%%%%%%%%%%%%%%%% Fatigue life calculation %%%%%%%%%%%%%%%

N=power(10,(log10a-m*log10(StressRange.*(t/tref)^k)));

%%%%%%%%%%%%%%%%%% Cumulative damage %%%%%%%%%%%%%%%%%

Dc=sum(n./N)

%%%%%%%%%%%%%%%%%% Statistics %%%%%%%%%%%%%%%%%
meand=MeanPos(ResponseDISPLACEMENT(10000:end))
stadd=std(ResponseDISPLACEMENT(10000:end))
maxd=max(ResponseDISPLACEMENT)

meanforce=MeanPos(TotalStress(10000:end))
stadforce=std(TotalStress(10000:end))
maxforce=max(TotalStress)
```